

**Group V pro-catalysts for the polymerisation of ethylene and  
 $\epsilon$ -caprolactone**

**Lucy Clowes**

A thesis submitted in accordance with the requirements for the degree of Doctor  
of Philosophy by research at the University of East Anglia

**University of East Anglia**

**Department of Chemistry**

June 2011

© This copy of the thesis has been supplied on condition that anyone who consults it is understood to recognise that its copyright rests with the author and that no quotation from the thesis, nor any information derived therefrom, may be published without the author's prior, written consent.

## Abstract

In this study, a number of group V complexes have been synthesised and characterised. The catalytic behaviour of these pro-catalysts towards ethylene polymerisation and the ring opening polymerisation of  $\epsilon$ -caprolactone is discussed.

Reaction of  $[V(X)(OR)_3]$  ( $X = O, Np$ -tolyl,  $R = {}^nPr, {}^tBu$ ) with 5,11,17,23- ${}^tBu$ -25,27-dihydroxycalix[4]arene ( $L^1H_2$ ) led to the formation of  $[VX(OR)L]_2$   $X = O, R = {}^nPr$  (**1**);  $X = Np$ -tolyl,  $R = {}^nPr$  (**3**);  $X = Np$ -tolyl,  $R = {}^tBu$  (**4**) as the major products. In the case of  $X = O$ , the minor hydrolysis product  $\{[VO(O{}^nPr)]_2(\mu-O)L\}_2$  (**2**) has also been characterised.

Oxovanadium(V) complexes (**5** and **6**) bearing calixarenes bridged by sulfinyl ( $-SO-$ ,  $L^2H_4$ ) or sulfonyl ( $-SO_2-$ ,  $L^3H_4$ ) linkers were obtained by reacting  $[VO_2Cl_2][PPh_4]$  with  $L^2H_4$  or  $L^3H_4$ , respectively.

A series of related bridged phenoxy-imine ligands ( $L^4H_2-L^{11}H_2$ ) were treated with  $[VCl_3 \cdot 3THF]$  to afford numerous mononuclear vanadium(III) complexes (**7-10** and **13, 14**) and dinuclear vanadium(III) systems (**11** and **12**).

Niobium and tantalum pro-catalysts bearing either phenoxy-imines ( $L^{12}H$ ), phenoxy-imine/imidazole ( $L^{13}H_2$ ) or oxazole ligands ( $L^{14}H$ ) were prepared. The niobium(V) phenoxy-imine (**15**), phenoxy-imine/imidazole (**16**) and oxazole (**18**) complexes were prepared by treatment of  $L^{12}H-L^{14}H$  with  $[NbCl_5]$ . The corresponding tantalum system was produced by the same method by treatment of  $L^{13}H_2$  with  $[TaCl_5]$ . The niobium(V) oxychloride complexes (**17** and **20**) were obtained *via* complexation of  $L^{13}H_2$  and  $L^{14}H$  with  $[NbOCl_3]$ .

All the compounds studied proved to be highly active for the polymerisation of ethylene. The niobium complexes (**15-17** and **19, 20**) proved to be significantly active, greatly surpassing previously published niobium systems.

The vanadium(V) complexes (**1-4**) and vanadium(III) systems (**7-14**) showed varying degrees of efficiency for the ring opening polymerisation of  $\epsilon$ -caprolactone, indicating the need for steric considerations when designing catalysts to produce poly( $\epsilon$ -caprolactone).

## Abbreviations

### General

Å	angstrom
acac	acetylacetate
Ar	aryl
<sup>t</sup> Bu	tertiary butyl
Cp	$\eta^5$ cyclopentadienyl
DEAC	diethylaluminium chloride
DMAC	dimethylaluminium chloride
DSC	differential scanning calorimetry
Et	ethyl
ETA	ethyltrichloroacetate
GPC	gel permeation chromatography
HDPE	high density polyethylene
h	hour
LDPE	low density polyethylene
LD50	lethal dose, 50 %
LLDPE	linear low density polyethylene
MeCN	acetonitrile
M	metal
Me	methyl
min	minute
$M_n$	number average molecular weight
$M_w$	weight average molecular weight
m.p.	melting point
PDI	polydispersity index
<sup>n</sup> Pr	linear propyl
PP	polypropylene
R	alkyl
THF	tetrahydrofuran
TEA	triethylaluminium chloride
°C	degree Celsius

NMR	nuclear magnetic resonance
br	broad
$\delta$	chemical shift
d	doublet
J	coupling constant
ppm	parts per million
s	singlet
t	triplet
MS	mass spectrometry
CI	chemical ionisation
EI	electron impact
ESI	electrospray ionisation
MALDI	matrix-assisted laser desorption ionisation
TOF	turnover frequency
IR	infra-red
m	medium
s	strong
w	weak

## Contents

	page
<b>Abstract</b>	i
<b>Abbreviations</b>	ii
<b>Contents</b>	iv
<b>Acknowledgements</b>	vii
<b>Chapter 1: General Introduction</b>	
1. Introduction	2
1.1 Plastics	2
1.2 Early discoveries	3
1.3 Metallocene catalysts	4
1.4 Post-metallocenes	5
1.5 Co-catalyst/Activators	6
1.6 Vanadium Catalysts	8
1.6.1 Vanadium catalysts and re-activators	10
1.6.2 Active species	11
1.7 Niobium and tantalum catalysts	12
2. The problem with plastics	15
2.1 Poly( $\epsilon$ -caprolactone)	16
2.2 Polymerisation of cyclic esters	17
2.2.1 Polycondensation	19
2.2.2 Enzymatic polymerisation	19
2.3 Ring opening polymerisation	20
2.3.1 Anionic polymerisation	21
2.3.2 Cationic polymerisation	22
2.3.3 Coordination/insertion polymerisation	23
2.4 Vanadium complexes	25
3. Aim of the study	27
4. Thesis overview	29
<b>Chapter 2: Vanadium(V) pro-catalysts supported by 1,3-depleted calix[4]arenes</b>	
1. Introduction	38
1.1 Depleted calix[4]arenes	39
2. Results and Discussion	40
2.1 Vanadium(V) alkoxide 1,3-depleted calix[4]arenes	40
2.2 Vanadium(V) imido-alkoxide 1,3-depleted calix[4]arenes	44
2.3 Ethylene polymerisation	48
2.3.1 Temperature screening	48
2.3.2 Equivalent of co-catalyst	50
2.3.3 Industrial ethylene screening	52
2.4 $\epsilon$ -Caprolactone polymerisation	53
3. Conclusion	56
<b>Chapter 3: Oxovanadium(V) complexes bearing sulfur-bridged calix[4]arenes</b>	
1. Introduction	60
1.1 Vanadium thiacalixarenes	63
2. Results and Discussion	64
2.1 Oxovanadium(V) tetrasulfinylcalix[4]arene complex	64

2.2 Oxovanadium(V) tetrasulfonylcalix[4]arene complex	66
2.3 Ethylene polymerisation	70
2.3.1 Temperature screening	70
2.3.2 Co-catalyst concentration	73
3. Conclusion	75
<b>Chapter 4: Vanadium(III) pro-catalysts bearing phenoxy-imine ligands</b>	
1. Introduction	80
1.1 Bridged phenoxy-imine ligands	81
2. Results and Discussion	82
2.1 Ligand synthesis	82
2.2 Vanadium(III) phenoxy-imine complexes	84
2.3 Known vanadium(III) phenoxy-imine complexes	89
2.4 Ethylene polymerisation	90
2.4.1 Comparative studies	90
2.4.2 Lifetime studies	92
2.5 $\epsilon$ -Caprolactone polymerisation	93
3. Conclusion	95
<b>Chapter 5: Group V complexes bearing phenoxy-imine/imidazole and oxazole ligands</b>	
1. Introduction	100
1.1 Phenoxy-imine/imidazole and oxazole ligands	100
2. Results and Discussion	101
2.1 Niobium(V) complexes supported by phenoxy-imine ligands	101
2.2 Group V complexes supported by phenoxy-imine/imidazole ligands	103
2.3 Niobium(V) complexes supported by phenoxy-imine/oxazole ligands	108
2.4 Ethylene polymerisation	110
2.4.1 Varying co-catalyst and concentration	110
2.4.2 Temperature screening	112
2.4.3 Lifetime studies	114
3. Conclusion	115
<b>Overview</b>	119
<b>Chapter 6: Experimental section</b>	
1. General considerations	123
2. Synthesis of known compounds	124
3. Vanadium(V) complexes bearing 1,3-depleted calix[4]arenes	125
3.1 Synthesis of $[\text{VO}(\text{O}^i\text{Pr})\text{L}^1]_2$ ( <b>1</b> )	125
3.2 Synthesis of $\{[\text{VO}(\text{O}^i\text{Pr})]_2(\mu\text{-O})\text{L}^1\}_2$ ( <b>2</b> )	126
3.3 Synthesis of $[\text{V}(\text{N}^p\text{-tolyl})(\text{O}^i\text{Pr})\text{L}^1]_2$ ( <b>3</b> )	127
3.4 Synthesis of $[\text{V}(\text{N}^p\text{-tolyl})(\text{O}^t\text{Bu})\text{L}^1]_2$ ( <b>4</b> )	128
4. Oxovanadium(V) complexes bearing sulfur-bridged calix[4]arenes	129
4.1 Synthesis of anion $[\text{VOCl}_2(\text{L}^2\text{H}_2)]^-$ ( <b>5</b> )	129
4.2 Synthesis of anion $[\text{VOCl}_2(\text{L}^3\text{H}_2)]^-$ ( <b>6</b> )	130
5. Vanadium(III) complexes bearing phenoxy-imine ligands	131
5.1 Synthesis of $\text{L}^4\text{VCl}(\text{THF})$ ( <b>7</b> )	131
5.2 Synthesis of $\text{L}^5\text{VCl}(\text{THF})$ ( <b>8</b> )	131

5.3 Synthesis of $L^6VCl(THF)$ ( <b>9</b> )	132
5.4 Synthesis of $L^7VCl(THF)$ ( <b>10</b> )	132
5.5 Synthesis of $L^8[VCl_2(THF)_2]_2$ ( <b>11</b> )	133
5.6 Synthesis of $L^9[VCl_2(THF)_2]_2$ ( <b>12</b> )	133
5.7 Synthesis of $L^{10}VCl(THF)$ ( <b>13</b> )	134
5.8 Synthesis of $L^{11}VCl(THF)$ ( <b>14</b> )	134
6. Niobium(V) complex bearing a phenoxy-imine ligand	135
6.1 Synthesis of $L^{12}NbCl_4$ ( <b>15</b> )	135
7. Group V complexes bearing phenoxy-imine/imidazole type ligands	136
7.1 Synthesis of $L^{13}HNbCl_4$ ( <b>16</b> )	136
7.2 Synthesis of $L^{13}HNbOCl_2$ ( <b>17</b> )	137
7.3 Synthesis of $L^{13}HTaCl_4$ ( <b>18</b> )	137
8. Niobium(V) complexes bearing oxazole ligands	138
8.1 Synthesis of $L^{14}NbCl_4$ ( <b>19</b> )	138
8.2 Synthesis of $L^{14}NbOCl_2$ ( <b>20</b> )	139
9. Polymerisation procedure	140
9.1 Ethylene polymerisation	140
9.1.1 Schlenk line procedure	140
9.1.2 Silica-supported procedure	140
9.2 $\epsilon$ -Caprolactone procedure	140
<b>Chapter 7: Appendix</b>	<b>143</b>

## **Acknowledgements**

Firstly, I would like to thank Dr Carl Redshaw for giving me the opportunity to embark on this challenging, yet rewarding experience over the past three years. It has definitely been ‘character building’. I thank him for all the help, advice and support he has given me throughout my PhD.

I would also like to thank all the members of the Redshaw group throughout my time in the group, especially Ms Akina Yoshizawa, Dr Chris Herbert, Mr Aaron Clayton and Mr Stephen Thorpe. A special thanks to Dr Abdessamad Arbaoui, for his help, patience, knowledge and support during our time in the lab and for his continued friendship. I would particularly like to thank Mr Oliver Rowe and Mr Mark Walton for their friendship and support, which has been greatly appreciated.

I am grateful to Dr Myles Cheesman for his role as my secondary supervisor and help with EPR. I thank Dr David Hughes for his help with the majority of my crystals and his continued support in his absence from UEA. I also thank Dr Mark Elsegood for the X-ray crystallography at Loughborough University and at Daresbury Laboratories. I am grateful to Dr Colin MacDonald for all his help and advice with NMR. Thank you to the EPSRC and all the technical staff at the department of chemistry, UEA. Acknowledgements are given to Dr Steve Holding and co-workers at RAPRA, EPSRC Mass Spectrometry Service at Swansea and Dr Stephen Boyer for elemental analysis at the London Metropolitan University.

I would also like to express my gratitude to Professor Chris Pickett’s group for their friendship and use of some of their equipment. A special thank you to Dr Joseph Wright for proof reading my thesis and for his help throughout my PhD.

I am really appreciative to all my family and friends for their unconditional patience and support, you made it a lot easier than it could have been. A special thanks to Mr Matthew Thompson for helping me to be motivated.



# **Chapter 1**

## **Introduction**

## 1. Introduction

### 1.1 Plastics

From early periods of history, the most well known being the Stone Age, the Iron Age and Bronze Age, man has utilised polymeric materials such as wool, wood, natural rubber and cotton, to make implements and basic necessities to meet his needs. Since the mid 20<sup>th</sup> century, synthetic polymers have been introduced, which challenge and extend the application of their older polymeric counterparts. Without the introduction of rubbers and plastics, everyday features of modern life, such as televisions, cars and computers, would not be possible.

Although natural polymers have been well established for thousands of years, it was not until the 1930s that saw the major growth of the synthetic polymer industry. It was during this period when the properties and potential applications of polyethylene were first noticed and approval was given to start production on an industrial scale.<sup>1</sup>

One main driving force during this time was the outbreak of the Second World War. This increased the demand for durable, cheap materials that could be produced on a commercially feasible scale. One example of this is the rigid, transparent thermoplastic, known as Perspex (poly methyl methacrylate). During the Second World War, this material became invaluable for various uses, *e.g.* the glazing of military aircraft.<sup>1</sup>

Throughout the 20<sup>th</sup> century the polymer industry has continued to grow, in the 1960s the worldwide use and production of plastics increased significantly compared to twenty years prior. Today, global plastic production is estimated to be around 240 million tons per year, with approximately 60 million tons of this plastic production being just for Western Europe.<sup>2</sup> We use and produce 20 times as much plastic as we did 50 years ago. The use of plastics is growing at an approximate rate of over 5 % per year within the western world, with the expected plastic consumption in 2016 being over 400 million tons (Figure 1).<sup>3</sup> The largest area of use is within the packaging sector, which takes up to approximately 40% of the plastic consumption in the United Kingdom.<sup>4</sup>

In the 1950s the only polyethylene that was produced was low melting and was highly branched with a wide range of molecular weights. The polymerisation conditions required to produce the polymer, consisted of high temperatures (150-230 °C) and pressures (1000-3000 atm).<sup>5</sup> Taking this into account and the demand from industry, there is pressure for process efficiency and material effectiveness. These requirements necessitate the need for new catalysts with activity improvement, cost-efficiency and synthesis of innovative polymers.

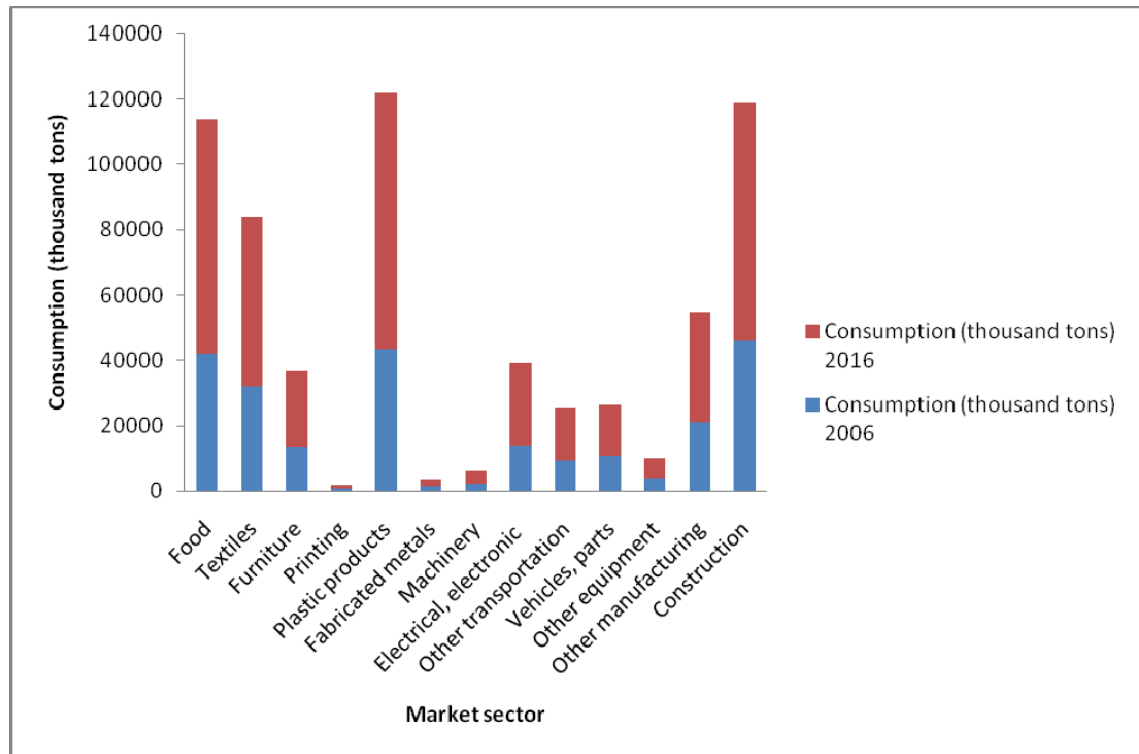


**Figure 1.** Global annual plastic consumption by market sector in 2006 and estimated consumption growth by 2016.<sup>3</sup>

## 1.2 Early discoveries

In the 1950s, Karl Ziegler reported that by reacting  $TiCl_4$  with triethylaluminium (TEA), he was able to polymerise ethylene under mild conditions.<sup>6</sup> From Ziegler's success of developing linear polyethylene, Giulio Natta was able to prepare and isolate isotactic polypropylene.<sup>7</sup> Both these discoveries were recognised for their significant importance, earning Ziegler and Natta a shared Nobel Prize in 1963.

Ziegler-Natta catalysis involves rapid polymerisation of ethylene and  $\alpha$ -olefins with the aid of catalysts based on transition element compounds, typically formed by a transition element halide or alkoxide reacting with a main group alkyl halide.<sup>6, 8</sup> Such metals include titanium, vanadium, chromium and in some cases molybdenum, cobalt, rhodium and nickel. Catalysts of this type are able to operate at low pressures (up to 30 atm) and at temperatures up to 120 °C.<sup>9</sup> These reaction conditions are vast improvements, in terms of energy input, on the high temperature and pressure conditions previously required. The Ziegler catalysis conditions are beneficially economically and safety cognisant.

Today, Ziegler-Natta catalysts are used worldwide to produce a wide range of different polymers from  $\alpha$ -olefins. Some of these polymers include high density polyethylene (HDPE) and linear low-density polyethylene (LLDPE).<sup>10</sup>

In the same decade, Hogan and Banks, for the Philips Petroleum Company (Philips Catalysts), discovered silica-supported nickel/cobalt oxide heterogeneous catalysis systems.<sup>11</sup> They were capable of co-polymerising  $\alpha$ -olefins to produce high molecular weight polymers. Field and Feller, working for the Standard Oil Company, found group VI oxide catalysts, similar to Hogan and Banks systems, had extremely high activities.<sup>12</sup> However, they possess no control over the produced polymer; the catalyst has various reaction sites allowing the polymer to grow at different rates and at various sites. This gave rise to catalyst design to enable control over the properties of the produced polymer. This research led to the discovery of metallocene-based  $\alpha$ -olefin polymerisation catalysis.

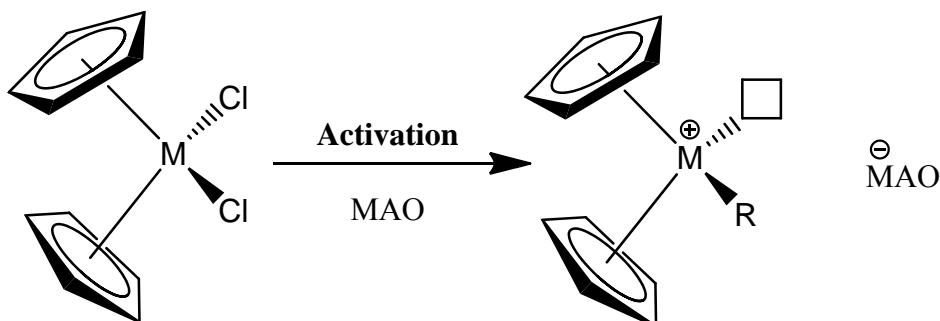
### 1.3 Metallocene catalysts

Metallocene catalysts originated from as early as 1957, when Natta reported the polymerisation of ethylene with the titanocene catalyst  $\text{Cp}_2\text{TiCl}_2$  and the co-catalyst triethylaluminium (TEA),<sup>13</sup> originally used in the Ziegler-Natta olefin polymerisation systems. Similar work was also reported at the same time by Breslow.<sup>14</sup> Both found that though the titanocene catalyst was an active complex for ethylene polymerisation, it was less active than the previous catalyst prepared from  $\text{TiCl}_4$  and TEA, because of this it was perceived as having little commercial promise.

In the mid-1970s, Sinn and Kaminsky, while studying a homogeneous titanocene dichloride polymerisation system, accidentally introduced water into a reaction system resulting in a highly active ethylene polymerisation system. After subsequent studies, it was concluded that the high activity was due to the hydrolysis of the trimethylaluminium (TMA), resulting in the formation of the co-catalyst methylaluminoxane (MAO).<sup>15</sup> Kaminsky supported this theory *via* direct synthesis of MAO and the activation of systems, such as bis(cyclopentadienyl)zirconium(IV), which showed no previous polymerisation activity, but which became highly active polymerisation catalysts with the addition of trialkylaluminium, which had previously been treated with water.<sup>15a</sup>

One advantage metallocenes have over Ziegler-Natta systems is that they only possess one defined active site in which the oligomer can bind with, rather than being multi-

sited, which is the case with the heterogeneous Ziegler-Natta systems (Scheme 1). The single site homogeneous system results in polymers with specific microstructures and narrow molecular weight distributions.<sup>16</sup>



**Scheme 1.** Activation of a metallocene with MAO. Typically; M = Zr, Ti. R = alkyl group. □ = vacant coordination site.

The ancillary ligands can affect the reactivity of the metal; the bulk of the ligand can dictate the formation of a mono-, bi- or multi-nuclear system. By altering the functional groups around the metal centre, the electronic properties and steric constraints at the metal can be tuned. For instance, when the aromatic cyclopentadienyl (Cp) is used, the delocalised electrons in the  $\pi$ -system are capable of electronically stabilising the metal centre.<sup>17</sup> It has also been noted that varying the size and functional groups on the cyclopentadienyl ligand can affect the polymer produced. For instance, Ewen and co-workers were able to show that by altering the size of the ligands on the metallocenes used within their studies, they were able to control the tacticity of the propylene polymer that was produced.<sup>18</sup>

#### 1.4 Post-metallocenes

Due to the high interest in the metallocene class of catalysts (to date there are approximately 7,500 patents filed within this field), academic research and industry stepped away from the traditional metallocenes in order to find cheap, unlicensed ligand systems/technology. Replacing either one or both of the cyclopentadienyl ligands with other systems has been the subject of investigation both academically and industrially in recent years.<sup>16, 19</sup>

The replacement of one of the Cp ligands leads to the formation of complexes referred to as ‘half sandwich’ compounds. By altering the substituents on the non-Cp ligand, the steric and electronic characteristics of the catalyst can be tuned to dictate the

characteristics of the produced polymer.<sup>20</sup> Early systems suffered from poor activities, lack of thermal stability and difficult synthesis. However, it was found that the addition of a heteroatom tethered to the Cp ligand led to improved activities.

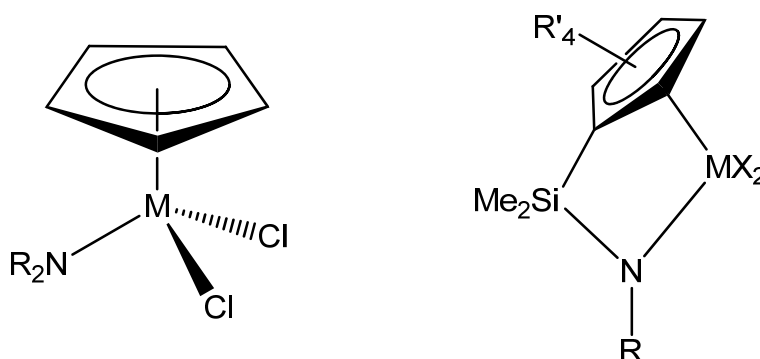


**Figure 2.** Examples of ‘half sandwich’ complex and constrained geometry pro-catalysts. Typically, M = Ti, Zr. R = alkyl, aryl. X = Cl, Me.

*ansa*-Cyclopentadienyl-amido (CpA) group IV catalysts developed by Dow and Exxon, are an example of mono-Cp complexes that have been receiving recent commercial attention (Figure 2).<sup>16</sup> This work was based on the organoscandium olefin polymerisation catalysts first introduced by Bercaw.<sup>21</sup> These types of catalyst are also examples of what can be referred to as “constrained geometry catalysts”.

One of the main features of “constrained geometry catalysts” is the open nature of the catalysts active site; this enables other olefins to be incorporated into polyethylene, such as 1-hexene and 1-octene. One other main advantage to this type of catalyst in comparison to the more traditional types of metallocene catalysts is their relative stability towards MAO and reaction temperatures of around 160 °C. They also tend to produce higher molecular weight polymers.<sup>22</sup>

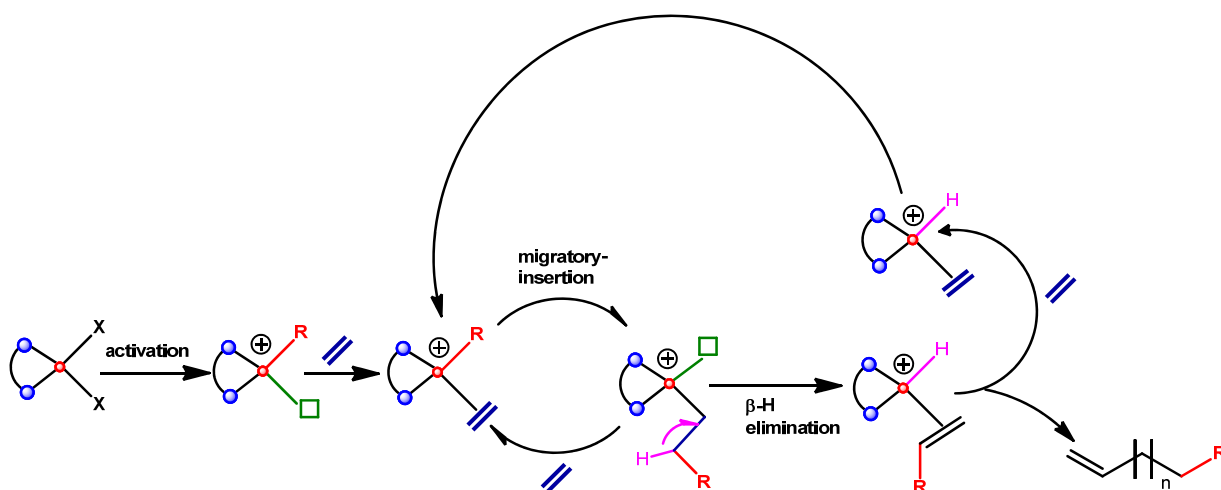
### 1.5 Co-catalyst/Activators




As mentioned previously, it became apparent in the 1970s following the work of Kaminsky *et al.* that hydrolysing TMA resulted in previously inactive species becoming highly active for ethylene polymerisation due to the formation of the co-catalyst MAO.<sup>15</sup> Since this discovery, MAO and other aluminium co-catalysts, have been used as common co-catalysts for the last 20 years.

Methylaluminoxane consists of  $[-Al(Me)-O-]_n$  subunits ( $n = 5-20$ ), and affords highly active catalysts for the polymerisation of ethylene, propylene and higher  $\alpha$ -olefins when combined with group IV metallocenes.<sup>23</sup> Although extensive research, both

academically and industrially, has been focused on identifying MAO, the exact structure of MAO is still unknown. A cage structure is now being considered as the most plausible structure for MAO.<sup>24</sup>

The active species for metallocenes consists of a 14-electron alkyl cation and a weakly coordinating anion in the form of  $[\text{Cp}_2\text{MR}]^+ [\text{A}]^-$  with M being a group IV metal and [A] MAO (Scheme 1). Alkyl aluminium reagents work by firstly alkylating the metal centre and then abstracting a methyl group providing a vacant site for ethylene to bind and for ongoing insertion reactions to occur, as shown in Scheme 2. It is thought that the aluminium metal centres of the MAO extract a methyl anion from (dimethyl)metallocenes to give a cationic active species, which is stabilised by the presence of an  $[\text{Me-MAO}]^-$  counter ion. In halogen-free systems, the alkylaluminium compound extracts a ligand off the pro-catalyst metal centre, to form a vacant site.<sup>17</sup>



**Scheme 2.** Simplified schematic representation for ethylene oligomerisation and polymerisation by a Cossee-Arlman-type mechanism. M = , R = growing polymer/oligomer chain,  = vacant coordination site,  = spectator ligand.

Catalysts can be classified using a table to quantify the activity of the pro-catalyst for polymerising  $\alpha$ -olefins (Table 1).<sup>25</sup> The category of “exceptional” has been added since publication of the initial categories due to advances in the field to represent catalysts demonstrating activities of  $>100,000$  g/mmol.h.bar. This table will be used as a reference point throughout the discussions on catalyst activities.

**Table 1.** Rating of a catalysts effectiveness based on its activity.

Rating	Activity (g/mmol.h.bar)
Very Low	< 1
Low	1–10
Moderate	10-100
High	100-1000
Very High	1000-100000
Exceptional	>100000

### 1.6 Vanadium Catalysts

In the 1960s, Natta *et al.* reported the species  $[VCl_4]$  and  $[V(acac)_3]$  at  $-78\text{ }^\circ\text{C}$  with aluminium dialkylmonohalides as the co-catalyst, as being the first active polymerisation catalysts for propylene to give syndiotactic polymer.<sup>26</sup> Vanadium complexes such as  $[V(acac)_3]$  are still commonly used commercially for the production of ethylene-propylene-diene (EPDM) elastomers.<sup>27</sup> However, to achieve these high activities it is necessary to use a large excess of organoaluminium reagent ( $Al/M = 1,000\text{--}50,000$ ). The large amount of excess aluminium residue then needs to be removed from the resulting polymer after polymerisation. Organoaluminium co-catalysts are an expensive commodity within the catalysts industry;  $2/3$  of the consumable budget within industry is used on preparation, removal and usage of organoaluminium co-catalysts.<sup>17</sup>

Vanadium catalysts are renowned for displaying lower activities compared to their group IV counterparts. This lower activity is due to the inactive low-valent vanadium complexes being formed during the alkylation process.<sup>28</sup> However, reports by various groups such as Gibson *et al.* (I)<sup>29</sup>, Fujita *et al.* (II),<sup>30</sup> Redshaw *et al.* (III)<sup>31</sup> and Nomura *et al.* (IV)<sup>32</sup> have shown that extremely high activities are achievable with vanadium catalysts.



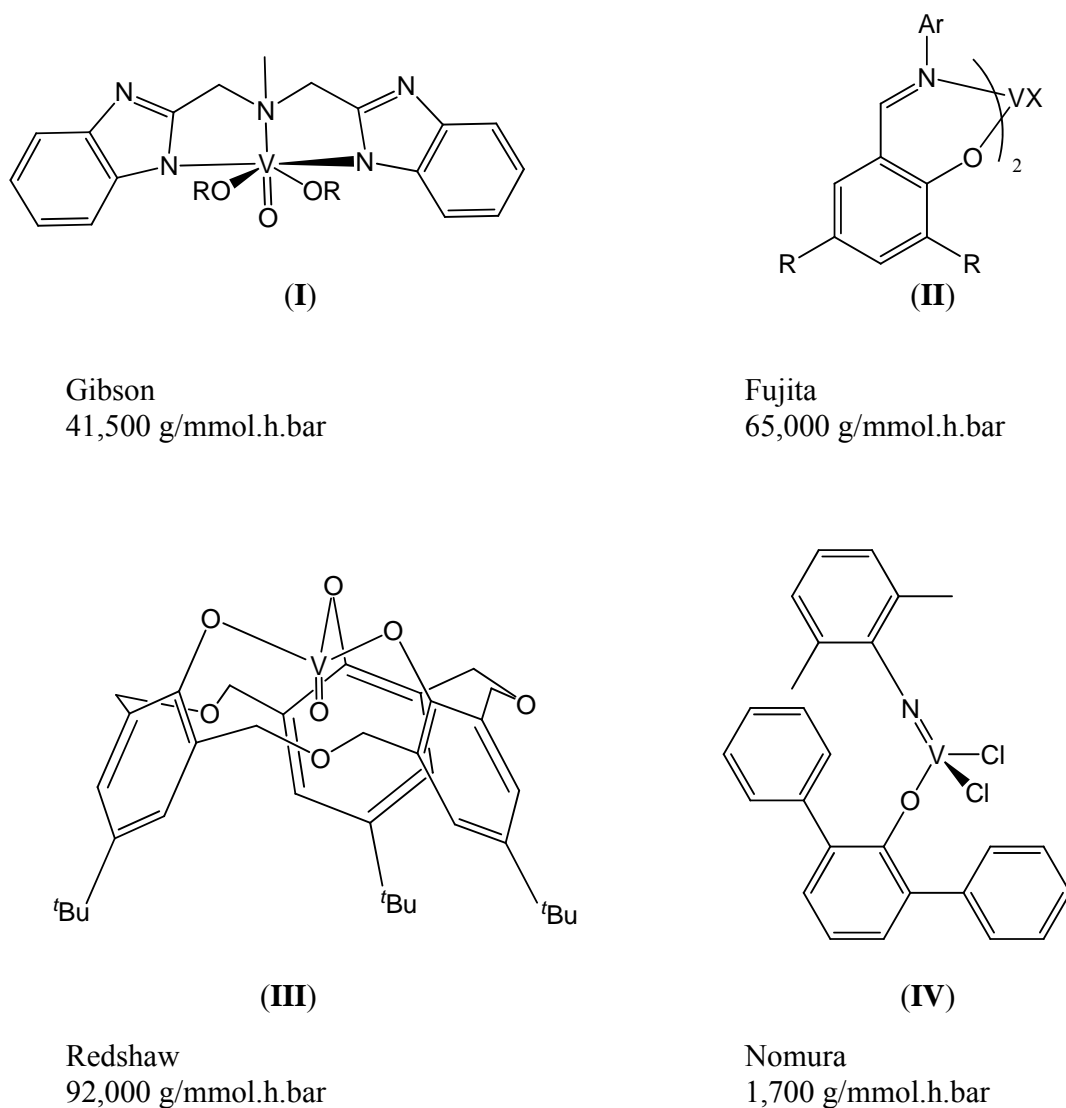


**Figure 3.** Literature examples of vanadium pro-catalysts.<sup>29, 30, 31b, 32</sup>

Gibson *et al.* have synthesised bis(benzimidazole)amine vanadium catalysts (Figure 3, **I**) with activities of around 40,000 g/mmol.h.bar.<sup>29</sup> In 2004, Fujita and co-workers reported the use of MgCl<sub>2</sub>-slurry-supported vanadyl phenoxy-imine systems (FI catalysts) (Figure 3, **II**) with alkyl aluminium co-catalyst, can reach activities in the region of 65,000 g/mmol.h.bar.<sup>30, 33</sup> Other research groups, such as Redshaw *et al.* have reported the use of oxacalix[3]arene vanadyl complexes with activities of 92,000 g/mmol.h.bar. The group have also reported exceptional activities of 166,000 g/mmol.h.bar using vanadyl complexes bearing bi- and tri-phenolate chelate ligands.<sup>31c</sup> Nomura and his group have also produced highly performing vanadium catalysts.<sup>32</sup>

### 1.6.1 Vanadium catalysts and re-activators

The main disadvantage with vanadium polymerisation catalysts is their deactivation with the reduction from an active species to inactive vanadium(II) species. One way to overcome this problem is to use a 'promoter' or 're-activator' to re-activate inactive V(II) back to the active V(III) species. Several examples of compounds that achieve this are known in the literature, however the most common method in practice is to use a halogenated hydrocarbon.<sup>34</sup>

Halogenated hydrocarbons have been used to boost the activity of vanadium-based catalysts from the 1960s. Gumboldt *et al.* discovered that the vanadium(II) species obtained by reduction from aluminium alkyl compounds were inactive for ethylene polymerisation, but became active after treatment with the halogenated hydrocarbon hexachlorocyclopentadiene (HCP).<sup>35</sup>

In 1972, Christman investigated the effects in the homogeneous polymerisation of ethylene.<sup>36</sup> He noted that for a homogeneous system to be maintained the temperature had to be kept above 105 °C. At this temperature, deactivation of the vanadium species occurs rapidly, however the continuous addition of the aluminium alkyl co-catalyst and poly-halogenated hydrocarbon re-activator ensured that polymerisation occurred.<sup>36</sup> All re-activators cause an increase in polymerisation activity, but the efficiency between the different re-activators varies. Esters of trichloroacetic acid are generally the most favoured type of re-activator. Methyl trichloroacetate (MTCA) was studied to check its efficacy on the oxidation state of vanadium. The pro-catalyst  $\text{VO}(\text{O}^t\text{Bu})_3$  was first reduced by diethylaluminium chloride (DEAC) to form a mixture of either  $\text{V}^{4+}$  and  $\text{V}^{3+}$  or  $\text{V}^{3+}$  and  $\text{V}^{2+}$ , dependent on the Al:V ratio. The MTCA resulted in the overall oxidation state to increase, demonstrating that  $\text{V}^{3+}$  and  $\text{V}^{2+}$  can both be oxidised.<sup>34</sup>

Redshaw *et al.* have achieved extremely high activities when utilising the re-activator ethyl trichloroacetate (ETA).<sup>31</sup> It is worth noting that Gamborotta's group have reported detrimental effects when using the re-oxidising agent ETA in some systems.<sup>28a, 37</sup>

As mentioned in section 1.6, Fujita of Mitsui Chemicals, supported his vanadium systems on a  $\text{MgCl}_2$  slurry to prevent reduction. Studies by Czaja found that the concentration of the inactive V(II) was significantly decreased upon supporting the catalyst on the surface of the  $\text{MgCl}_2$  slurry. The majority of the vanadium metal centres adopted the active oxidation state of V(III) in the presence of DEAC.<sup>38</sup>

### 1.6.2 Active species

It is generally thought that group V catalysts follow the Cossee-Arlman method for ethylene polymerisation (Scheme 2, Section 1.5). However, unlike the known metallocene active species, the active species for group V catalysts still remains to be elucidated. As mentioned above, experiments involving magnesium chloride supports prevent reduction to the inactive species V(II) with the remaining of the metal centres adopting a V(III) oxidation state. Fujita and Czaja's work has been supported further by Zambelli *et al.* who postulated a structural model for the active vanadium site for the polymerisation of propylene (Figure 4).<sup>39</sup> In the model, the vanadium(III) atom is penta-coordinated bearing three chlorides and the growing polymer chain. It is possible for two of the chlorines to coordinate a co-catalyst aluminium atom. The fifth site is occupied by a propylene monomer; this coordination can take place in four ways.

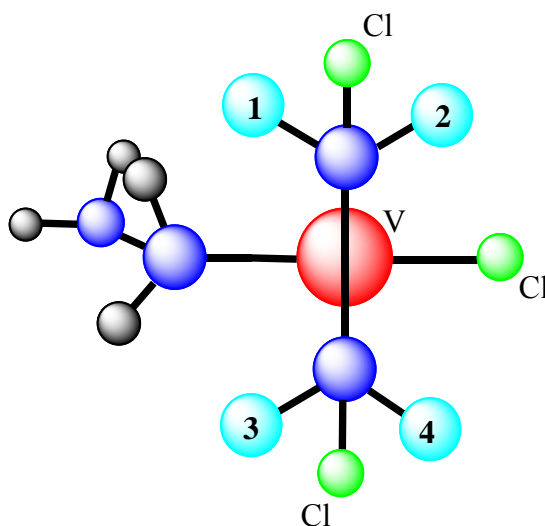


**Figure 4.** Zambelli's structural model of the vanadium(III) active site and the four possible positions of the methyl group upon coordination of propene.<sup>34</sup>

In 2003, Gambarotta reported that vanadium(II) is the inactive species by studying acac-type systems.<sup>40</sup> He stated that the deactivation was due to ligand extraction, proving this by being able to isolate  $[\text{Al}(\text{acac})_2]^+$  species. Further work led to the isolation of a vanadium-aluminium-phenoxide cluster (Figure 5). It is postulated by Gambarotta, that the vanadium active species for olefin polymerisation is similar to the  $\text{V}_2\text{Al}_4$  cluster, requiring sharing of the phenoxide/chloride/alkyl groups between the catalysts vanadium centres and the co-catalysts aluminium metal centres.<sup>40</sup>

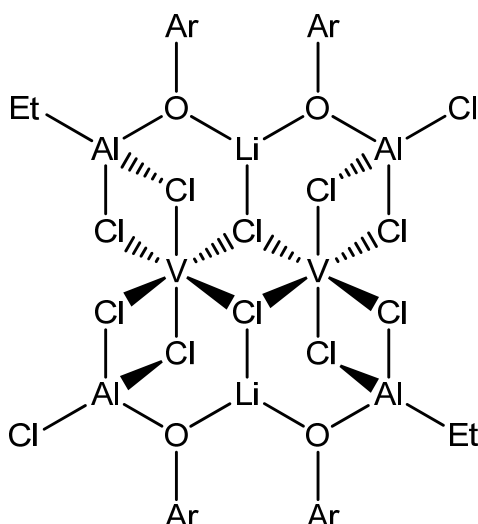


**Figure 5.** Gambarotta's postulated  $V_2Al_4$  cluster.<sup>40</sup>

### 1.7 Niobium and tantalum catalysts

Until recently, niobium systems for the polymerisation of ethylene were quite rare and generally showed low activities. Ziegler-Natta systems have been proven to give either no activities or negligible, even when supported on a MAO-modified silica support.<sup>41</sup> Half-sandwich complexes reported improved activities ( $\leq 40$  g/mmol.h.bar, *e.g.* complex **V**, Figure 6), however the screened pro-catalysts showed a lack of thermal stability with activities dramatically dropping off above 20 °C.<sup>42</sup> The general lack of activity for niobium half-sandwiched complexes redirected research towards non-metallocene compounds. Chen *et al.* also observed low activities ( $\leq 1.8$  g/mmol.h.bar) when employing various niobium benzamidinato precursors.<sup>43</sup> Amido ligands have also been utilised as potential ligands, offering alternatives to the classical Cp stabilising ligands of cationic early transition metal complexes.<sup>44</sup> However, further research by Decams and co-workers reported niobium(V) amido precursors, upon activation with MAO, were inactive towards the polymerisation of ethylene.<sup>45</sup> The highest activities were reported by Etienne, when in the presence of methyl abstracting agent such as  $B(C_6F_5)_3$  (125 g/mmol.h.bar, complex **VI**, Figure 6).<sup>46</sup>

Shiono and co-workers have recently reported the use of bis(imino)pyridine niobium systems in the presence of *t*Bu-modified MAO (MMAO), which gave activities of  $\leq 70$  g/mmol.h.bar.<sup>47</sup>

After previous successes with vanadyl phenolate systems, Redshaw *et al.* expanded their work to synthesis various niobium systems and tested them for their ability to polymerise ethylene.<sup>31c, 48</sup> One of the triphenolate systems exhibited moderate activities

in presence of DEAC and ETA (90 g/mmol.h.bar).<sup>48</sup> A niobium complex bearing a C-capped trisphenolate analogue with a pendant imine arm was shown to be inactive in the presence of various aluminium co-catalysts.<sup>49</sup> As stated in section 1.6, the vanadyl oxacalix[3]arene system showed extremely high activities, because of these exceptional results, Redshaw also extended this work by utilising the oxacalix[3]arene ligand with niobium.<sup>50</sup> It was noted that no activity was observed in the absence of an aluminium co-catalyst. The highest activities (84 g/mmol.h.bar) were observed in the presence of DMAC and ETA.

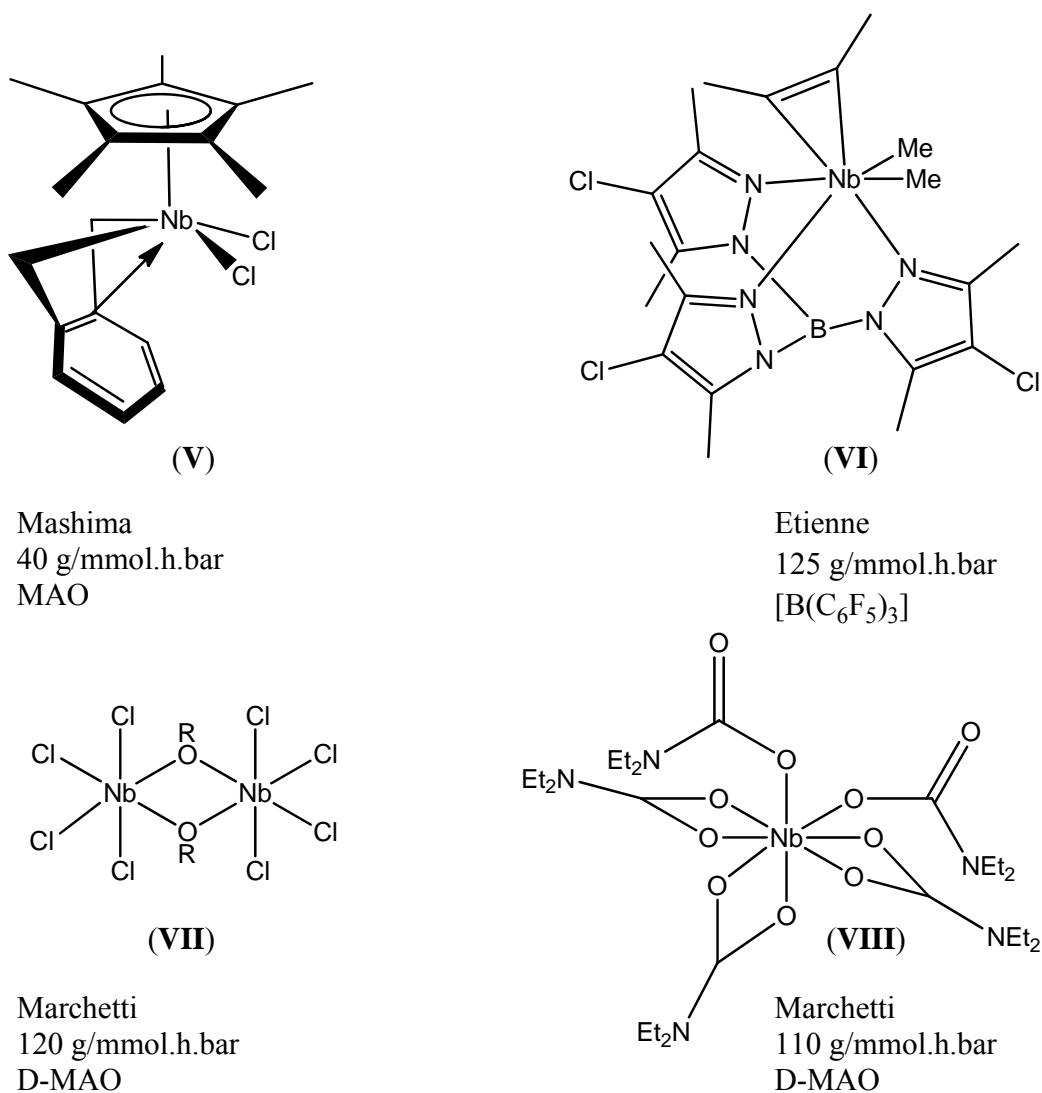
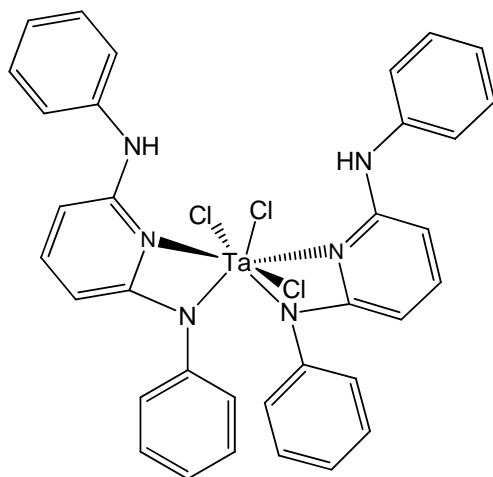


**Figure 6.** Literature examples of niobium-based pro-catalysts.<sup>42, 46, 51</sup>

However, recent reports by Marchetti and co-workers have reported activities analogues with Etienne's system (VI, Figure 6).<sup>51</sup> Niobium(V) mixed chloro-alkoxide complexes were found to be approximately 100 times ( $\leq 151$  g/mmol.h.bar) more active than some previously mentioned niobium systems (*e.g.* Chen *et al.* 1.8 g/mmol.h.bar) in the

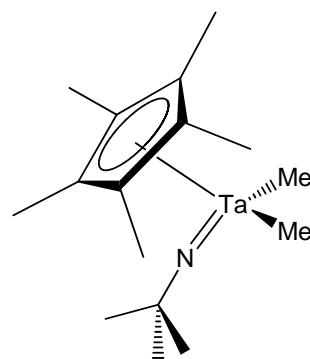
presence of various aluminium alkyl co-catalysts (*e.g.* complex **VII**, Figure 6).<sup>51a</sup> Marchetti's group have also reported niobium(V) dialkylcarbamates with similar activities ( $\leq 110$  g/mmol.h.bar, complex **VIII**, Figure 6).<sup>51b</sup> Although both niobium systems produced good activities for niobium catalysts for the polymerisation of ethylene, it is worth noting that the produced polymers had broad polydispersity indexes (5.8-24.2).

Tantalum is considerably more active than its group V counterpart. To date, the highest activity for a tantalum pro-catalyst for the polymerisation of ethylene was reported by Michiue *et al.* (25,700 g/mmol.h.bar, complex **XII**, Figure 7).<sup>52</sup> Other published systems have activities varying between 480–4,780 g/mmol.h.bar (Figure 7).<sup>53</sup> It appears that few catalysts have utilised tantalum since their catalytic activities are short-lived. This is likely to be due to the instability of the alkyl cationic active species involved in the polymerisation process.<sup>53a</sup>



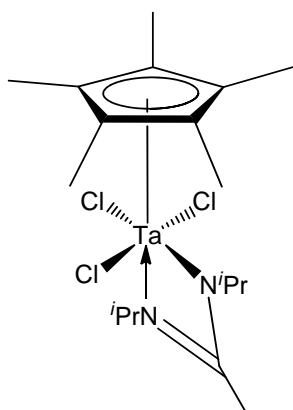
(IX)

Hakala  
4,780 g/mmol.h.bar



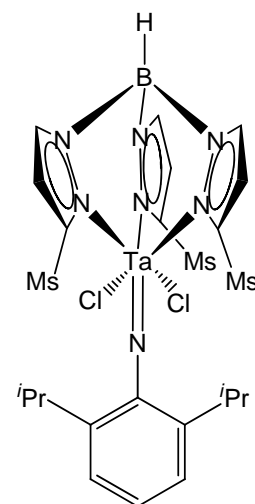
(X)

Chen  
1,186 g/mmol.h.bar



(XI)

Decker  
470 g/mmol.h.bar



(XII)

Michiue  
25,700 g/mmol.h.bar

**Figure 7.** Literature examples of tantalum-based pro-catalysts.<sup>52, 53</sup>

## 2. The problem with plastics

Polymer production is dominated by five high volume families of polyolefins; polyethylene (LDPE, LLDPE and HDPE), polypropylene (PP), poly vinylchloride (PVC), polystyrene (solid PS and expandable EPS) and polyethylene terephthalate (PET), consuming over 47 % of the western world's annual plastic consumption.<sup>2</sup> Although the world of plastics continues to grow at a rapid rate with new technologies and applications, economical considerations are becoming ever more important. For instance, such dependence on polyolefin(s) raises certain issues; (1) they are produced

from non-renewable fossil fuels, which are prone to significant price-rising (fossil fuels represent up to 80 % of polyolefin production), (2) their characteristic inertness means they suffer from a lack of biodegradability, which raises environmental issues. For instance, a polyethylene plastic bag can take up to 400 years to degrade in landfills.<sup>54</sup>

This environmental issue has been dealt with from a recycling perspective, such as utilising waste plastic materials as 'reclaimers'; millions of polyethylene bottles are recycled which can then be shredded and used as insulation in ski jackets or carpets.<sup>55</sup> Another method is to use degrading agents, such as photo-sensitizers.<sup>56</sup> Degrading agents enable the long polymeric chains to undergo degradation into shorter polymeric chains, which can then also undergo degradation by micro-organisms.<sup>54</sup> However, petroleum resources used to make the polyolefins are becoming increasingly expensive and the risk of these resources becoming scarce is viewed as inevitable. One-way to enable us to continue with the increasing polymer demand, and prevent releasing CO<sub>2</sub> from fossil fuels, is to use polymers obtained from renewable resources. Due to these reasons, there has become increasing academic and industrial interest in polymers such as polylactide and poly( $\epsilon$ -caprolactone). It is also noteworthy that Braskem and co-workers have recently patented the production of polyethylene from bioethanol obtained from sugar cane.<sup>57</sup>

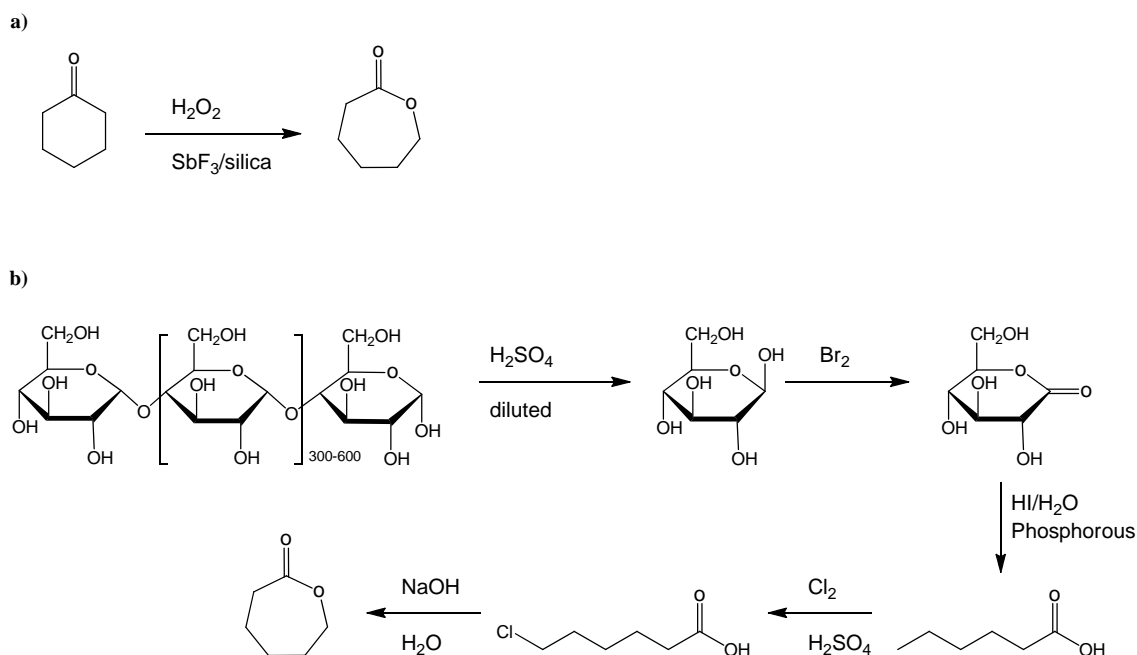
## 2.1 Poly( $\epsilon$ -caprolactone)

Polylactide, poly( $\epsilon$ -caprolactone) and related co-polymers are the most studied polymers. Their biocompatibility makes them ideal for various biomedical and pharmaceutical applications, such as scaffolds in tissue engineering,<sup>58</sup> drug delivery,<sup>59</sup> microelectronics,<sup>60</sup> adhesives<sup>61</sup> and in packaging.<sup>62</sup> The majority of the data regarding the biodegradability of poly( $\epsilon$ -caprolactone) is related to the development of the implantable contraceptive delivery system, Capronor<sup>TM</sup>. No toxic effects were observed when testing the implant and the oral LD<sub>50</sub> of poly( $\epsilon$ -caprolactone) for rats is expected to be over 2,000 mg kg<sup>-1</sup>.<sup>59</sup>

As well as their inherent biodegradability, another attractive aspect of poly(lactide) and poly( $\epsilon$ -caprolactone) is their availability from renewable resources. Lactide is already available from corn starch, with polylactide being produced by companies such as Nature Works (a joint venture between Cargill and Teijin Limited).<sup>63</sup>  $\epsilon$ -Caprolactone is mainly produced *via* the Bayer Williger oxidation of cyclohexanone with per-acids or hydrogen peroxide by companies such as Perstorp, BASF and Daicel.<sup>64</sup> However,



recent literature reports by Minami *et al.* discuss the possibility of producing  $\epsilon$ -caprolactone from starch (Scheme 3), increasing the industrial potential of poly( $\epsilon$ -caprolactone).<sup>65</sup>



**Scheme 3.** Production of  $\epsilon$ -caprolactone *via* either; a) the Bayer Williger oxidation process and b) from starch.

Its wide applicability and interesting properties (controlled degradability both *in vivo* and *in vitro*, miscibility with other polymers, biocompatibility and potential to be made from monomers derived from renewable sources) makes poly( $\epsilon$ -caprolactone) an incredibly useful polymer if its properties can be controlled and it can be produced in an inexpensive manner.<sup>66</sup>

The challenge now is to be able to produce biodegradable polymers and/or co-polymers based on polylactide or poly( $\epsilon$ -caprolactone) at low cost and with specific physical properties desired by industrial applications, to turn them into industrial competitors to their well established non-biodegradable commodity counterparts, such as polyethylene.<sup>67</sup>

## 2.2 Polymerisation of cyclic esters

More than half a century of research has been invested into studying the industrial synthesis of polyesters, such as polylactide and poly( $\epsilon$ -caprolactone).<sup>67</sup> Polyesters can be formed in a variety of ways: polycondensation,<sup>68</sup> enzymatic polymerisation,<sup>69</sup>

anionic polymerisation,<sup>59f, 70</sup> cationic polymerisation<sup>71</sup> or coordination/insertion polymerisation.<sup>72</sup>

Two problems become apparent when reviewing the literature with regard to polylactide or poly( $\epsilon$ -caprolactone) synthesis; (1) the lack of a standardised measurement of initiator/catalyst activity similar to Table 1, section 1.5 for polyethylene and (2) the deviation between the actual average molecular weight and the one obtained by gel permeation chromatography (GPC) with reference to polystyrene standards. However, Arbaoui *et al.* have recently published a review with an activity classification table, similar to that previously published by Gibson for polyethylene. Where possible, these problems have been overcome by either (1) quoting the conditions under which the initiators/catalysts have been screened and (2) the corrected values for  $M_n$  or by clarifying the measurement method (*i.e.* GPC or NMR).<sup>67</sup>

Herein, all catalyst/initiator activities regarding poly( $\epsilon$ -caprolactone) synthesis will reference back to this table.

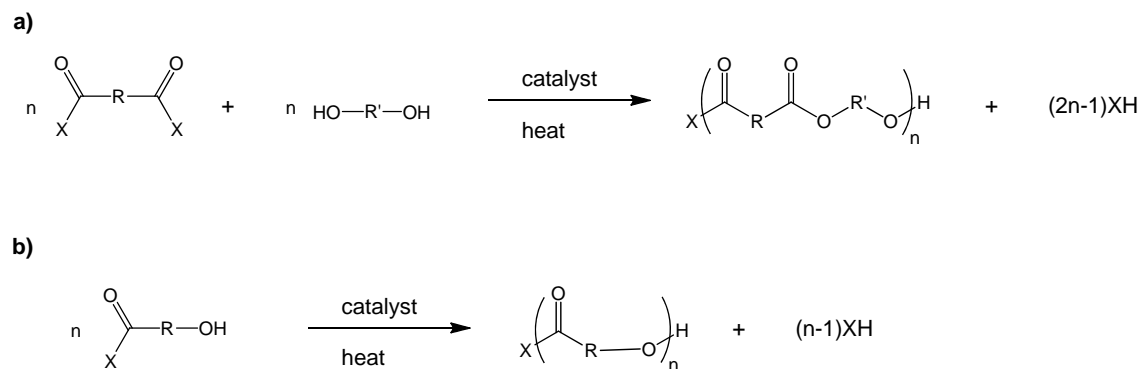
**Table 2.** Activity table for  $\epsilon$ -caprolactone polymerisation catalysts/initiators

Monomer/metal ratio	Polymerisation time <sup>a</sup>	TOF/h <sup>-1b</sup>	$M_n(\text{calculated})/\text{g mol}^{-1}$	Activity
< 100	days	< 4	< 11,400	low
	hours	0.04 to 100		poor
	minutes	> 1		moderate
100-500	days	< 21	11,400-57,000	poor
	hours	4 to 500		moderate
	minutes	> 100		good
500-1,000	days	< 42	57,000-114,100	moderate
	hours	21 to 1,000		good
	minutes	> 500		high
1,000-5,000	days	< 208	114,100-570,700	good
	hours	42 to 5,000		high
	minutes	> 1,000		very high
> 5,000	days	> 30	> 570,700	high
	hours	> 205		very high
	minutes	> 5,000		exceptional

<sup>a</sup> Polymerisation time at quantitative monomer conversion. <sup>b</sup> Indicative values only.

### 2.2.1 Polycondensation

A polycondensation reaction can be completed by reacting a diol with a diacid (*i.e.* AA + BB) or by condensing a hydroxyl acid (*i.e.* AB). In both of these cases, the reaction involves the loss of a stoichiometric amount of water from the reaction medium.



**Scheme 4.** Polycondensation *via* either a) AA + BB reaction or b) AB condensation.

Large amounts of patents describe the preparation of aliphatic polyesters from hydroxycarboxylic acids.<sup>73</sup> Braud *et al.* synthesised poly( $\epsilon$ -caprolactone) oligomers by polycondensation of 6-hydroxyhexanoic acid under vacuum, by removing the water produced in the reaction and displacing the equilibrium towards the formation of the polymer.<sup>74</sup> The synthesis was completed in the absence of a catalyst and was complete in 6 hours at 80 °C, which was gradually increased to 150 °C.

However, the polymers produced *via* polycondensation have a tendency to have broad polydispersity indexes, and need to go to high conversions to produce polymers with sufficient molecular weights. Method a) also requires precise reagent stoichiometry. The polycondensation method requires high reaction temperatures.<sup>75</sup>

### 2.2.2 Enzymatic Polymerisation

Enzymatic polymerisation was been developed as an alternative method to polycondensation. This process involves the use of biocatalysts such as lipase enzymes, which allows for the catalytic condensation of diols and diacids or the addition of cyclic esters by ring opening.<sup>69a, 72b</sup>

The use of lipase enzymes enable highly functionalised monomers to be involved in the polymerisation process without the need for protection and deprotection steps, that would be necessary in the polycondensation method. This is due to the lipases

selectively reacting with primary hydroxyl groups rather than secondary in the esterification process.<sup>75a</sup>

Another positive to using lipase enzymes in enzymatic polymerisation is that they are natural, non-toxic biocatalysts therefore making the method even more environmentally friendly. The polymerisation conditions required when using lipase enzymes for the polymerisation of lactones are rather mild.

This process does suffer from the same negative characteristics as the polycondensation method; the produced polymers tend to have broad polydispersity<sup>75a</sup> and low molecular weights.<sup>72b</sup>

6-Hydroxycaproic acid was polymerised using lipase from *Candida antarctica* under vacuum. This gave rise to polymers with an average molecular weight of 9,000 g/mol and a polydispersity under 1.5 in two days.<sup>76</sup> Lipase from *Pseudomonas* sp. at 45 °C were capable of polymerising ethyl 6-hydroxyhexanoate resulting in polymers with an average molecular weight of 5,400 g/mol and polydispersity indices under 2.26 after 20 days with 82 % conversion.<sup>77</sup>

Gross *et al.* found porcine pancreatic lipase were able to polymerise  $\epsilon$ -caprolactone, producing polymers of low molecular weights (< 3,000 g/mol by GPC) after several days.<sup>69b</sup> The enzyme *Candida Antarctica* lipase B has also been screened for its ability to polymerise  $\epsilon$ -caprolactone. Iversen and co-workers found that it was able to either form cyclic oligomers when the polymerisation was carried out in an organic solvent, or linear polymers when carried out in bulk.<sup>69c</sup> However, the molecular weight of the polymer was still low (< 5,000 g/mol).

Kobayashi *et al.* were able to produce poly( $\epsilon$ -caprolactone) with molecular weights of up to 12,000 g/mol when utilising various lipase and esterase enzymes.<sup>69d</sup> The results were achieved after 20 days using *Pseudomonas fluorescens* lipase.

### 2.3 Ring opening polymerisation

Ring opening polymerisation is an attractive method for synthesising polyesters because it enables living polymerisation to occur, which in turn provides control over the produced polymers' physical properties and polydispersity indices. The driving force behind the reaction is to relieve ring strain.<sup>75a</sup>

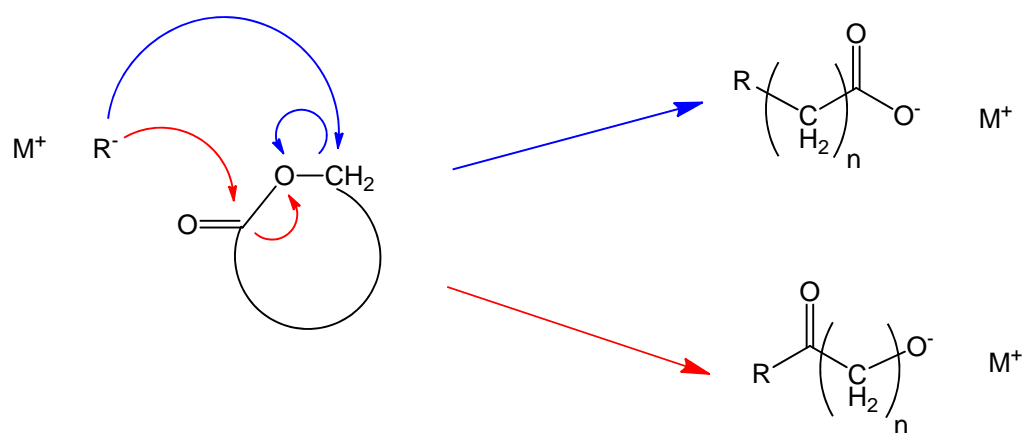
In 1934, Carothers and co-workers first reported the synthesis of poly( $\epsilon$ -caprolactone) *via* ring opening polymerisation.<sup>78</sup> However, it was not until the late 1970s that Duda *et al.* were able to produce methods to control the process.<sup>79</sup> It is generally accepted that

ring opening polymerisation occurs by either an anionic, cationic or coordination/insertion mechanism depending on the nature of the catalyst or initiator.

### 2.3.1 Anionic polymerisation

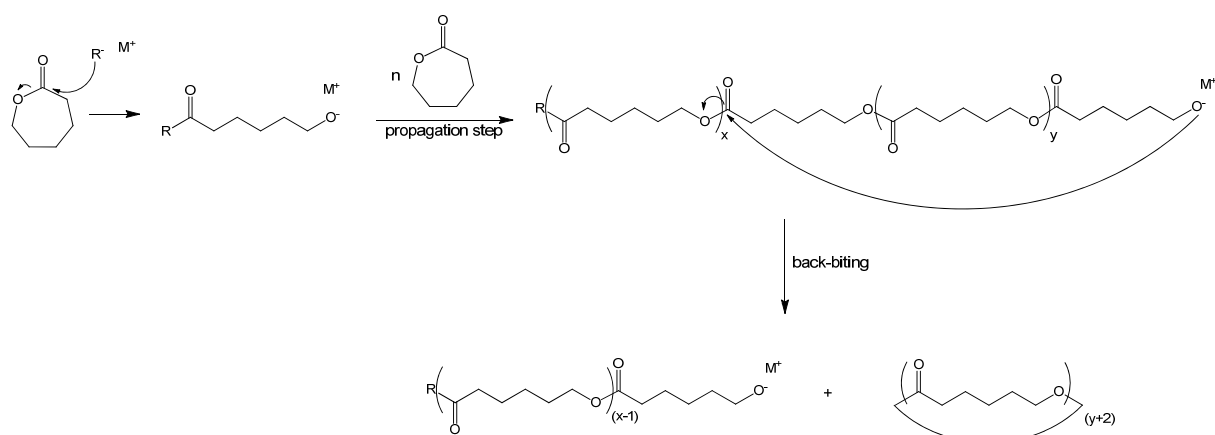
Anionic ring opening polymerisation of cyclic esters involves the formation of an anionic species (initiator) which attacks the carbonyl carbon of the monomer, forming linear polyester.

Anionic polymerisation of  $\beta$ -lactones occur through either the acyl oxygen or alkyl oxygen cleavage, forming either an alkoxide or a carboxylate growing (propagating) species, respectively (Scheme 5).



**Scheme 5.** Anionic polymerisation of cyclic ester through either; the alkyl oxygen (blue) and acyl oxygen cleavage (red).<sup>80</sup>

For large lactones, *e.g.*  $\epsilon$ -caprolactone, the nucleophilic attack occurs at the acyl oxygen producing the alkoxide as the propagating species.<sup>75b, 81</sup> The most common systems capable of initiating anionic ring opening polymerisation of  $\epsilon$ -caprolactone are amines<sup>59f, 70a</sup> and alkali metal alkoxides, such as potassium *tert*-butoxide and lithium *tert*-butoxide.<sup>70b-d</sup>



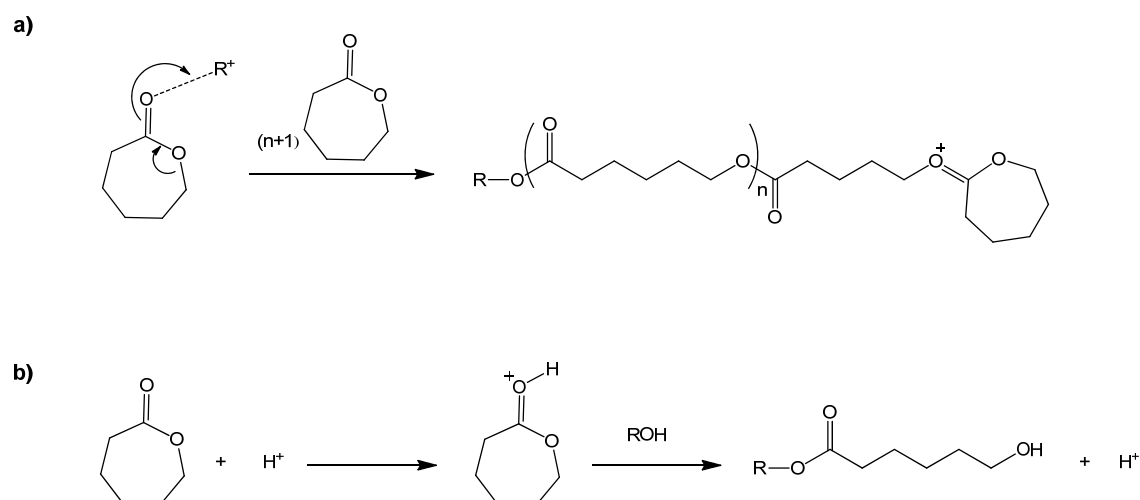
**Scheme 6.** Anionic polymerisation of ε-caprolactone, including back-biting step.

The anionic polymerisation method tends to be used for the production of low molecular weight oligomers and polymers. When alkali metal alkoxides such as potassium *tert*-butoxide are used, large quantities of cyclic oligomers are formed due to intramolecular transesterification, or “back-biting” occurring.<sup>72b, 75b</sup>

It is worth noting that high molecular weight polymers of lactones have only been synthesised *via* anionic or coordination/insertion polymerisation.<sup>72b, 82</sup>

### 2.3.2 Cationic polymerisation

Cationic ring opening polymerisation of cyclic esters can occur *via* two mechanisms; the *active chain end* and the *activated monomer* mechanisms.<sup>71a</sup> By choosing the appropriate polymerisation conditions, the mechanism which the cationic polymerisation occurs by can be tuned, *e.g.* the use of alcohol or continuous feed of monomer.



**Scheme 7.** Cationic polymerisation through either a) *active chain end* or b) *activated monomer* mechanism.

When cationic polymerisation occurs through the *active chain end* mechanism, the propagating species is a carbonium ion obtained through the cleavage of the  $\epsilon$ -caprolactones acyl-oxygen (mechanism a), Scheme 7).<sup>81</sup> In the *activated monomer* method, the cyclic ester is activated through protonation which enables another monomer or a neutral growing chain to attack (mechanism b), Scheme 7).<sup>71, 83</sup>

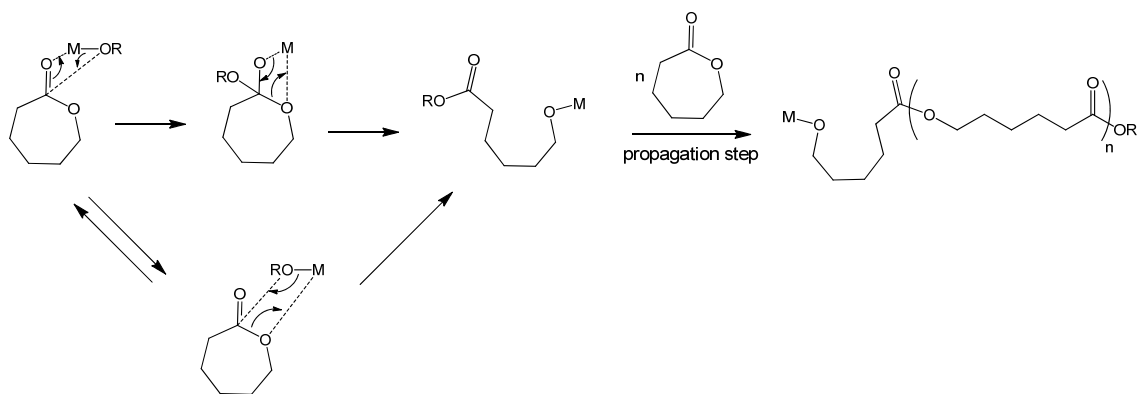
For the cationic ring opening polymerisation of  $\epsilon$ -caprolactone, numerous initiators have found to be effective, such as; protic acids,<sup>83, 84</sup> acylating agents (*e.g.*  $\text{CH}_3\text{CO}^+\text{SbF}_6^-$ ), alkylating agents (*e.g.*  $\text{CF}_3\text{SO}_3\text{CH}_3$ ) and Lewis acids (*e.g.*  $\text{FeCl}_3$ ,  $\text{BF}_3 \cdot (\text{C}_2\text{H}_5)_2\text{O}$ ).<sup>85</sup>

Strong Lewis acids are rarely used for the cationic ring opening polymerisation of poly( $\epsilon$ -caprolactone) because they tend to yield low molecular weight polymers. This is due to significant “back-biting” occurring during the polymerisation process (Scheme 6).<sup>85b</sup>

Endo and co-workers reported that when utilising hydrochloric acid diethyl etherate ( $\text{HCl} \cdot \text{Et}_2\text{O}$ ) in the presence of a protic source, such as an alcohol or water, the mixture was active for cationic polymerisation of  $\epsilon$ -caprolactone, yielding polymers with narrow polydispersities.<sup>71b</sup> The molecular weight of the produced polymers were low ( $< 15,000$  g/mol by GPC).

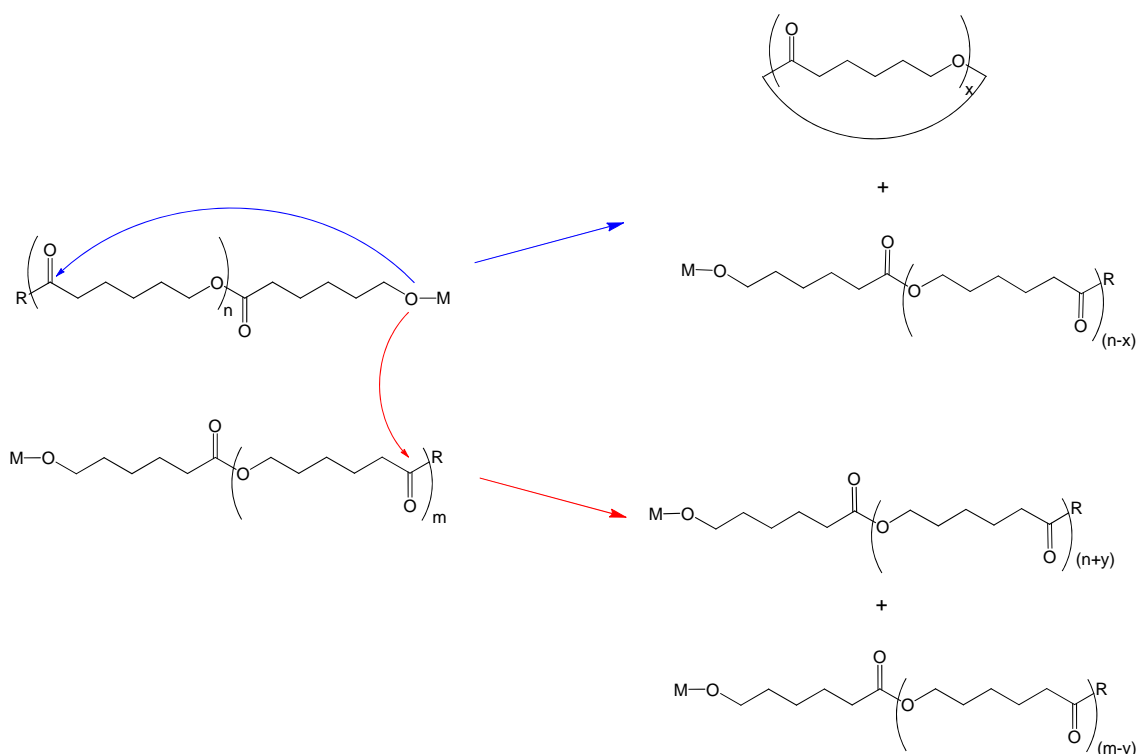
### 2.3.3 Coordination/insertion polymerisation

Coordination/insertion is the most common form of ring opening polymerisation. It is a pseudo-anionic ring opening polymerisation. The propagation step proceeds through the coordination of the monomer to the Lewis acidic catalyst metal centre *via* the exocyclic oxygen. Therefore, the carbonyl of the lactone is susceptible to nucleophilic attack by the alkoxide (Scheme 8). The growing polymer chain is attached to the metal centre *via* an alkoxide bond. At increased polymerisation times and temperatures, intermolecular and intramolecular back-biting can occur as side reactions. These can result in a broadening of the polydispersity and loss of control of the polymerisation (Scheme 9).<sup>66</sup>



**Scheme 8.** The coordination/insertion mechanism by a metal alkoxide species (M-OR).<sup>67</sup>

Complexes containing metals with empty *p*, *d* or *f* orbitals react as coordination catalysts, rather than anionic initiators. As mentioned in section 2.3.1, high molecular weight polymers can be produced *via* coordination/insertion polymerisation. This tends to occur as a living process, *i.e.* as a form of addition polymerisation where the ability of the growing chain to terminate has been removed. This enables greater control over the polymers molecular weight and narrow polydispersity indices.<sup>72</sup>



**Scheme 9.** Intermolecular (red) and intramolecular (blue) transesterification reactions in coordination/insertion polymerisation.<sup>80</sup>



Another benefit to this process is the ability to form stereoregular polymers, for instance polylactide or polymers of functionalised  $\epsilon$ -caprolactone. Coordination/insertion polymerisation limits the possibility of side reactions such as epimerisation, which occur regularly during the anionic polymerisation.<sup>86</sup>

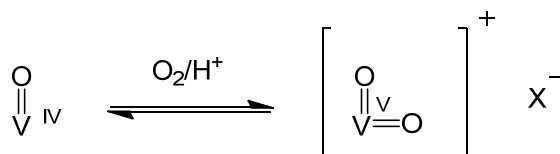
There are plenty of reports in the literature regarding the use of various metals for the ring opening polymerisation of cyclic esters *via* the coordination/insertion mechanism, the ones most commonly used for lactones are based on tin and aluminium.<sup>72a</sup> Typical metals used for the ring opening polymerisation of  $\epsilon$ -caprolactone include; magnesium,<sup>66, 67, 87</sup> calcium,<sup>66, 67, 87d, 88</sup> aluminium,<sup>66, 67, 72a, 89</sup> titanium,<sup>66, 67, 90</sup> iron,<sup>67, 91</sup> zinc,<sup>66, 67, 72a, 87c-d, 92</sup> tin,<sup>66, 67, 93</sup> lanthanides and rare earth metals.<sup>66, 67, 94</sup>

## 2.4 Vanadium complexes

As mentioned in sections 1.6 and 1.7, group V complexes have received substantial interest in their applicability for  $\alpha$ -olefin polymerisation, however this is not the case with regard to ring opening polymerisation of cyclic esters.

In 2005, Atlamsani and co-workers reported the use of vanadium complexes, *e.g.* vanadium/molybdenum heteropolyacids,  $\text{VOSO}_4$  and  $\text{VO}(\text{acac})_2$ , for the oligomerisation of  $\epsilon$ -caprolactone under an atmosphere of oxygen.<sup>95</sup> Under the same conditions, the vanadium heteropolyacid and  $\text{VOSO}_4$  displayed higher activities than their  $\text{VO}(\text{acac})_2$  counterpart, producing oligo( $\epsilon$ -caprolactone) with molecular weights of approximately 5,000 g/mol.

It was noted that when the polymerisation was conducted under an atmosphere of nitrogen, the Mo(VI)/V(V) heteropolyacid system saw a dramatic decrease in activity, the vanadium(IV) species,  $\text{VOSO}_4$  and  $\text{VO}(\text{acac})_2$ , showed no activity. Atlamsani *et al.* proposed that this is due to an intense green colour that was observed, when the heteropolyacids were used for the polymerisation under a dry nitrogen atmosphere. The intense green was associated with the conversion of the heteropolyacid to the reduced Mo(V)/V(IV) species. It is proposed that when the polymerisation was conducted under the dioxygen atmosphere, the dioxygen re-oxidised the inactive V(IV) species to an active dioxovanadium(V) cationic species (Scheme 10).



**Scheme 10.** Simplified redox activation mechanism of the vanadium complex postulated by Atlamsani *et al.* (Some ligands have been omitted for clarity).<sup>67</sup>

Efforts within our group have shown promise with the utilisation of chloride and alkoxide vanadium compounds for ring opening polymerisation of  $\epsilon$ -caprolactone. A family of organoimido vanadium(V) complexes were synthesised and screened for their ability to produce poly( $\epsilon$ -caprolactone).<sup>96</sup>

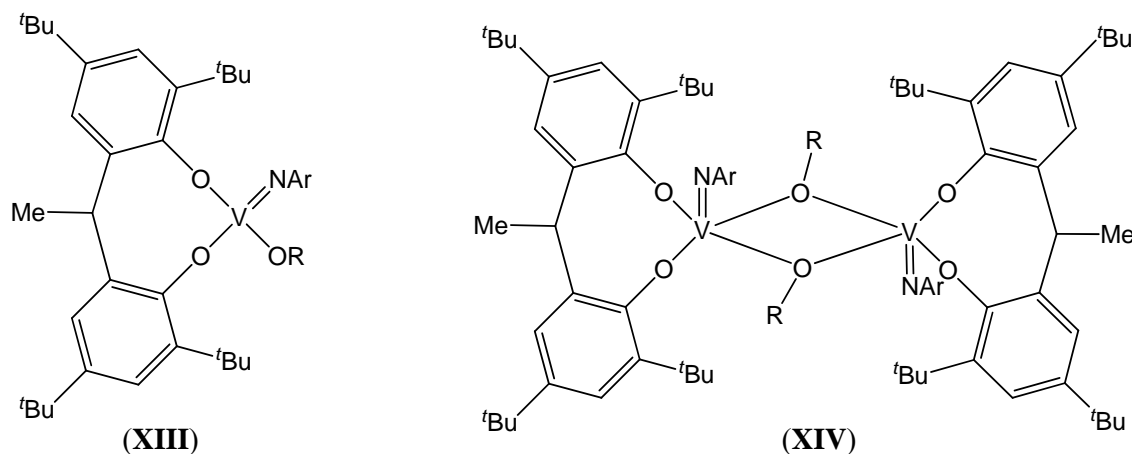


**Figure 8.** Organoimido vanadium(V) complexes. Typically R = Et, <sup>t</sup>Pr, <sup>n</sup>Pr, <sup>t</sup>Bu, Ar = 4-CH<sub>3</sub>C<sub>6</sub>H<sub>4</sub>, 4-ClC<sub>6</sub>H<sub>4</sub>, 4-CF<sub>3</sub>C<sub>6</sub>H<sub>4</sub>, C(CF<sub>3</sub>)<sub>2</sub>CH<sub>3</sub>, 4-MeOC<sub>6</sub>H<sub>4</sub>.

At 40 °C, monomer:metal ratio of 500:1, the dimeric species (**XIV**, Figure 8) were found to be more active than their mononuclear counterparts (**XIII**, Figure 8), ( $\geq 60\%$  and  $\leq 25\%$ , respectively). The highest conversions were produced by the dimeric pro-catalysts bearing propoxide bridges. Arbaoui *et al.* postulated that the propagating species was likely to be monomeric as a polymer chain is bulkier than a propoxide group. Therefore, the catalytic advantage must occur in the first stage of the polymerisation process, *i.e.* the coordination of the first molecule of  $\epsilon$ -caprolactone, and then its subsequent insertions into the V-OR bond.<sup>67</sup>

Arbaoui and co-workers also noted that the fluoride alkoxide group, OC(CH<sub>3</sub>)(CF<sub>3</sub>)<sub>2</sub>, led to an inactive pro-catalyst. It was assumed that the improvement in Lewis acidity of the metal centre was counterbalanced by the loss of nucleophilicity of the alkoxide group.<sup>67</sup>

Nomura and co-workers reported a similar system to Arbaoui's mononuclear pro-catalyst. They also observed poor activities; 57 % conversion after 48 hours and at 100 °C (monomer:metal ratio of 250:1).<sup>97</sup>

### **3. Aim of the study**

The aim of this study is to investigate a series of new complexes incorporating group V metals in combination with various chelating ligands (Figure 9), and to assess their ability as catalysts for the polymerisation of ethylene and ring opening polymerisation of  $\epsilon$ -caprolactone.

We have decided to focus our efforts on group V metals; vanadium species have proven their efficiency as catalysts for ethylene polymerisation.<sup>30, 31</sup> However, we believe there is room for improvement and by altering the polymerisation conditions and/or chelating ligands improvements upon literature results can be achieved. With regard to their ability as ring opening polymerisation for  $\epsilon$ -caprolactone, we wish to build upon this scarce literature field.

As mentioned in section 1.7, compared to vanadium little research has been done on its group V counterparts, niobium and tantalum. After successes with vanadium and those achieved recently with niobium by Marchetti *et al.*, we wish to investigate the potential for improving upon previously poor activities observed for both these metals, by altering polymerisation conditions and chelating ligands.

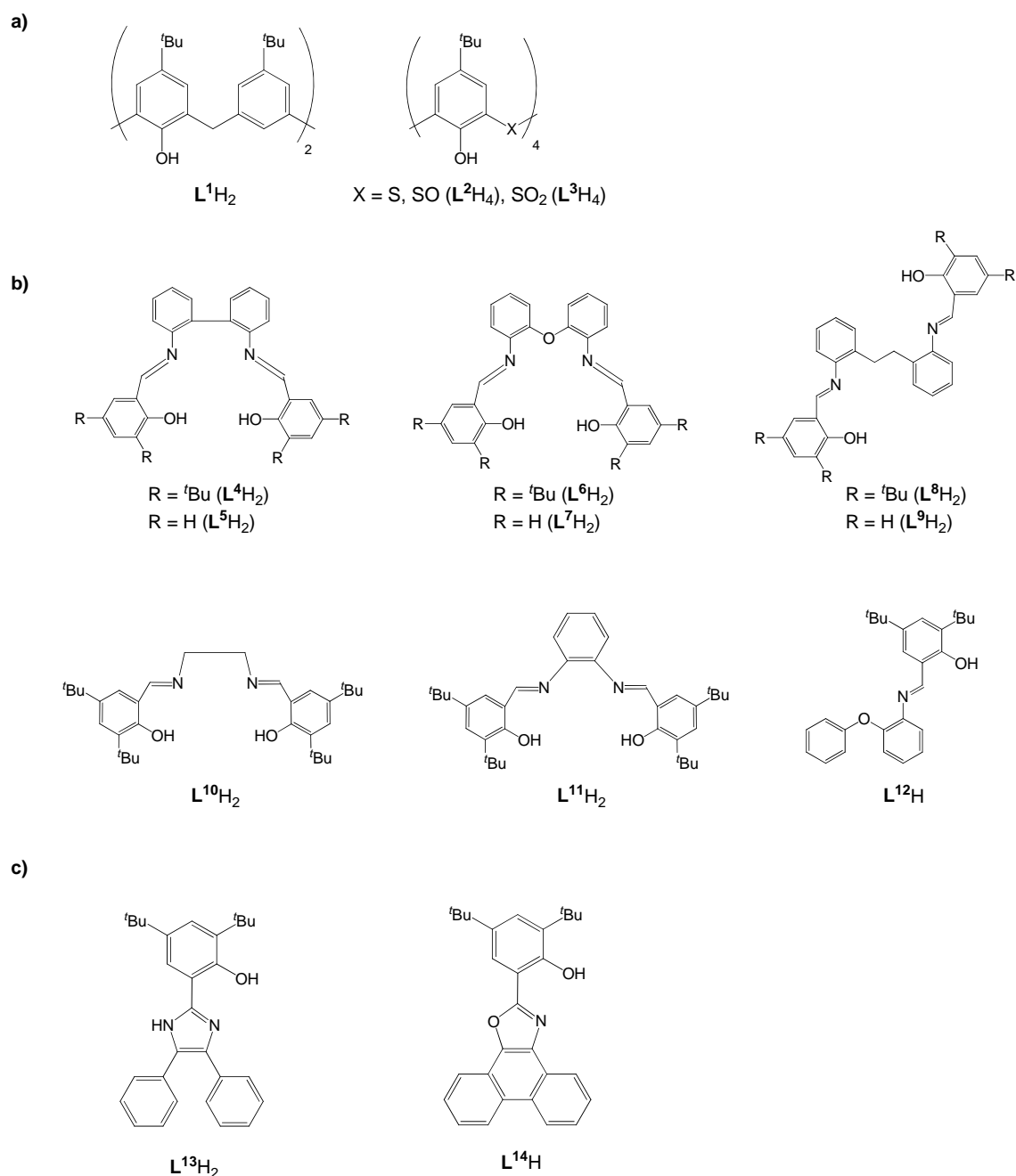


**Figure 9.** Chelating ligands used in this study **a)** calixarenes, **b)** phenoxy-imines, **c)** phenoxy-imine/imidazole and oxazole ligands.

All complexes have been fully characterised spectroscopically and wherever possible their molecular structure has been confirmed by single crystal X-ray diffraction studies. These complexes have all been screened for their ability to polymerise ethylene, and when appropriate for their ability for ring opening polymerisation of  $\epsilon$ -caprolactone. When deemed necessary, known complexes from the literature have also been synthesised to enable comparative studies under specific conditions to be achieved.

#### 4. Thesis overview

This study focuses on ethylene polymerisation and the ring opening polymerisation of  $\epsilon$ -caprolactone. Various mono- or multi-nuclear pro-catalyst systems have been synthesised and spectroscopically characterised, and then tested for their ability as polymerisation catalysts.

In the first results and discussion chapter, **Chapter 2**, the synthesis of multinuclear vanadium(V) alkoxide and imido/alkoxide complexes supported by 1,3-depleted calix[4]arene ligands have been screened for their ability to polymerise ethylene and for ring opening polymerisation of  $\epsilon$ -caprolactone.

In the second part of the study (**Chapter 3**), the focus is on oxovanadium(V) complexes supported by either thia, sulfinyl or sulfonyl calix[4]arene ligands. These systems will also be screened for their ability to produce polyethylene and poly( $\epsilon$ -caprolactone).

**Chapter 4** will shift the focus from vanadium(V) species to vanadium(III) pro-catalysts supported by various bridged phenoxy-imine systems. As in Chapters 2 and 3, complexes will also be screened for their efficiency as catalysts for polyethylene and poly( $\epsilon$ -caprolactone) production.

The fourth part of the study (**Chapter 5**) will involve the synthesis of a series of niobium(V) and tantalum(V) complexes, which are supported by phenoxy-imine/imidazole and oxazole ligands. All synthesised pro-catalysts will be assessed for polymerisation of ethylene.

All synthetic procedures, characterisation data and polymerisation methods are presented in the experimental section (**Chapter 6**).

- 1 J. A. Brydson, *Plastics Materials*, Butterworth-Heinemann, 7<sup>th</sup> Ed., 1999
- 2 Plastic Europe, *The compelling facts about plastics*, 2009
- 3 P. Bjacek, *Oil Gas*, 2008, **106**
- 4 British Plastics Federation, *Annual Review*, 2009
- 5 P.D. Gavens, M. Bottril, M. J.W. Kelland, J. McMeeking, *Comprehensive Organometallic Chemistry*, G. Wilkinson, F. G. A. Stone, E.W. Abel, Eds.: Pergamon Press: Oxford, 1982, **3**, 225
- 6 K. Ziegler, E. Hozkamp, H. Breil, H. Martin, *Angew. Chem.*, 1955, **67**, 541
- 7 G. Natta, P. Pino, G. Mazzanti, U. Giannini, *J. Am. Chem. Soc.*, 1957, **79**, 2975
- 8 K. Ziegler, Belgian Patent 533, 1954, **362**
- 9 W. Kaminsky, H. Sinn, *Adv. Organomet. Chem.*, 1980, **18**, 99
- 10 M. Brookhart, S. D Ittel, L. K. Johnson, *Chem. Rev.*, 2000, **100**, 1169
- 11 A. Clark, J. P. Hogan, R. L. Banks, W. C. Lanning, *Ind. Eng. Chem.*, 1956, **48**, 1152
- 12 E. Field, M. Feller, US 2,691,647, 1954
- 13 G. Natta, P. Pino, G. Mazzanti, U. Giannini, *J. Am. Chem. Soc.*, 1957, **79**, 2975
- 14 D. S. Breslow, N. R. Newburg, *J. Am. Chem. Soc.*, 1957, **79**, 5072
- 15 a) A. Andresen, H.G. Cordes, J. Herwig, W. Kaminsky, A. Merck, R. Mottweiler, J. Pein, H. Sinn, H. J. Vollmer, *Angew. Chem. Int. Ed. Engl.*, 1976, **15**, 630 b) H. Sinn, W. Kaminsky, H. J. Vollmer, R. Woldt, *Angew. Chem. Int. Ed. Engl.*, 1980, **19**, 390
- 16 A. L. McKnight, R. M. Waymouth, *Chem. Rev.*, 1998, **98**, 2587
- 17 M. Rowan, PhD Thesis, *University of East Anglia*, 2006
- 18 a) J. A. Ewen, *J. Am. Chem. Soc.*, 1984, **106**, 6355 b) J. A. Ewen, R. L. Jones, A. Razavi, J. D. Ferrara, *J. Am. Chem. Soc.*, 1988, **110**, 6255
- 19 a) K. H. Theopold, *Eur. J. Inorg. Chem.*, 1998, 15 b) U. Siemeling, *Chem. Rev.*, 2000, **100**, 1495 c) H. Butenschon, *Chem. Rev.*, 2000, **100**, 1527 d) J. Gromada, J. – F. Carpentier, A. Morteux, *Coord. Chem. Rev.*, 2004, **248**, 397
- 20 E. Kolodka, W. –J. Wang, S. Zhu, A. Hamielec, *Macromol. Rapid Commun.*, 2003, **24**, 311
- 21 a) J. E. Bercaw, Presented at 3<sup>rd</sup> Chemical Congress of North America, Toronto, Canada, June 1988 b) P. J. Shapiro, E. Bunel, W. P. Schaefer, J. E. Bercaw, *Organometallics*, 1990, **9**, 867

- 22 J. C. Stevens, *Surf. Sci. Catal.*, 1996, **101**, 11
- 23 W. Kaminsky, H. H. Brintzinger, F. R. W. P. Wild, *Angew. Chem. Int. Ed. Engl.*, 1985, **24**, 507
- 24 E. Y. X. Chen, T. J. Marks, *Chem. Rev.*, 2000, **100**, 1391
- 25 G. J. P. Britovsek, V. C. Gibson, D. F. Wass, *Angew. Chem. Int. Ed.*, 1999, **38**, 428
- 26 G. Natta, I. Pasquon, A. Zambelli, *J. Am. Chem. Soc.*, 1962, **84**, 1488
- 27 V. C. Gibson, S. K. Spitzmesser, *Chem. Rev.*, 2003, **103**, 283
- 28 a) D. Reardon, J. Guan, S. Gambarotta, G. P. A. Yap, *Organometallics*, 2002, **21**, 4390 b) Y. Ma, D. Reardon, S. Gambarotta, G. E. Yap, H. Zahalka, C. Lemay, *Organometallics*, 1999, **18**, 2773 c) K. Takaoki, T. Miyatake, *Macromol. Symp.*, 2000, **157**, 251 d) K. Nomura, A. Sagara, Y. Imanishi, *Macromolecules*, 2002, **35**, 1583
- 29 V. C. Gibson, A. K. Tomov, D. Zaher, M. R. J. Elsegood, S. H. Dale, *Chem. Commun.*, 2004, 1956
- 30 Y. Nakayama, H. Bando, Y. Sonobe, T. Fujita, *J. Mol. Catal. A*, 2004, **213**, 141
- 31 a) C. Redshaw, M. A. Rowan, D. M. Homden, S. H. Dale, M. R. J. Elsegood, S. Matsui, S. Matsuura, *Chem. Commun.*, 2006, 3329 b) C. Redshaw, M. A. Rowan, L. Warford, D. M. Homden, A. Arbaoui, M. R. J. Elsegood, S. H. Dale, T. Yamato, C. Pérez-Casas, S. Matsui, S. Matsuura, *Chem. Eur. J.*, 2007, **13**, 1090 c) C. Redshaw, L. Warford, S. H. Dale, M. R. J. Elsegood, *Chem. Commun.*, 2004, 1954
- 32 a) W. Wang, K. Nomura, *Macromolecules*, 2005, **38**, 5905 b) W. Wang, K. Nomura, *Adv. Synth. Catal.*, 2006, **348**, 743 c) W. Wang, J. Yamada, M. Fujiki, K. Nomura, *Catal. Commun.*, 2003, **4**, 159
- 33 T. Fujita, Y. Nakayama, H. Bando, Y. Sonobe, Y. Suzuki, *Chem. Lett.*, 2003, **32**, 766
- 34 H. Hagen, J. Boersma, G. van Koten, *Chem. Soc. Rev.*, 2002, **31**, 357
- 35 A. Gumboldt, J. Helberg, G. Schleitzer, *Makromol. Chem.*, 1967, **101**, 229
- 36 D. L. Christman, *J. Polymer Sci.: Part A-1*, 1972, **10**, 471
- 37 A. Jabri, I. Korobkov, S. Gambarotta, R. Duchateau, *Angew. Chem. Int. Ed.*, 2007, **46**, 6119
- 38 K. Czaja, M. Bialek, *Macromol. Rapid Commun.*, 1998, **19**, 163
- 39 A. Zambelli, G. Allegra, *Macromolecules*, 1980, **13**, 42
- 40 S. Gambarotta, *Coord. Chem. Rev.*, 2003, **237**, 229

- 41 a) R. Quijada, J. Dupont, D. Corrêa Silveira, M. L. Lacerda Miranda, R. B. Scipioni, *Macromol. Rapid Commun.*, 1995, **16** 357 b) J. Justino, A. Romão Dias, J. Ascenso, M. M. Marques, P. J. T. Tait, *Polym. Int.*, 1997, **44**, 407 c) J. H. Zimnoch dos Santos, A.E. Gerbase, K.C. Rodenbusch, G. Pozzebon Pires, M. Martinelli, K. Messias Bichinho, *J. Mol. Catal. A: Chem.*, 2002, **184**, 167
- 42 a) A. Nakamura, K. Mashima, *J. Organomet. Chem.*, 1995, **500**, 261 b) K. Mashima, S. Fujikawa, H. Urata, E. Tanaka, A. Nakamura, *J. Chem. Soc., Chem. Commun.*, 1994, 1623 c) K. Mashima, S. Fujikawa, Y. Tanaka, H. Urata, T. Oshiki, E. Tanaka, A. Nakamura, *Organometallics*, 1995, **14**, 2633 d) K. Mashima, S. Fujikawa, A. Nakamura, *J. Am. Chem. Soc.*, 1993, **115**, 10990 e) P. Jutzi, *Inorg. Chem.*, 1987, **6**, 123
- 43 C. –T. Chen, L. H. Doerrer, V. C. Williams, M. L. H. Green, *J. Chem. Soc., Dalton Trans.*, 2000, 967
- 44 a) L. H. Gade, *Chem. Commun.*, 2000, 173 b) D. Y. Dawson, J. Arnold, *Organometallics*, 1997, **16**, 1111
- 45 J. M. Decams, S. Daniele, L. G. Hubert-Pfalzgraf, J. Vaissermann, S. Lecocq, *Polyhedron*, 2001, **20**, 2405
- 46 J. Jaffart, C. Nayral, R. Choukroun, R. Mathieu, M. Etienne, *Eur. J. Inorg. Chem.*, 1998, 425
- 47 Y. Nakayama, N. Maeda, T. Shiono, *Stud. Surf. Sci. Catal.*, 2006, **161**, 165
- 48 C. Redshaw, D. M. Homden, M. A. Rowan, M. R. J. Elsegood, *Inorg. Chim. Acta.*, 2005, **358**, 4067
- 49 D. M. Homden, C. Redshaw, J. A. Wright, D. L. Hughes, M. R. J. Elsegood, *Inorg. Chem.*, 2008, **47**, 5799
- 50 C. Redshaw, M. A. Rowan, L. Warford, D. M. Homden, M. R. J. Elsegood, T. Yamato, C. Pérez-Casas, *Chem. Eur. J.*, 2007, **13**, 10129
- 51 a) F. Marchetti, G. Pampaloni, Y. Patil, A. M. R. Galletti, S. Zacchini, *J. Poly. Sci A.: Poly. Chem.*, 2011, **49**, 1664 b) F. Marchetti, G. Pampaloni, Y. Patil, A. M. R. Galletti, F. Renili, S. Zacchini, *Organometallics*, 2011, **30**, 1682
- 52 K. Michiue, T. Oshiki, K. Takai, M. Mitani, T. Fujita, *Organometallics*, 2009, **28**, 6450
- 53 a) K. Hakala, B. Löfgren, M. Polamo, M. Leskelä, *Macromol. Chem. Rapid Commun.*, 1997, **18**, 635 b) S. Feng, G. R. Roof, E. Y. –X. Chen, *Organometallics*,



- 2002, **21**, 832 c) J. M. Decker, S. J. Geib, T. Y. Meyer, *Organometallics*, 1999, **18**, 4417
- 54 A. Guttag, US patent 1994/2346929, 1994
- 55 C. Lefteri, *The Plastic Handbook*, Rotovision SA, 2008
- 56 B. Freedman and M. J. Diamond, US patent 1977/4017668, 1977
- 57 S. A. Braskem (for US only de-C.R.L.A. Morschbacker) WO patent 2009/070858 A1, 2009
- 58 a) C. X. F. Lan, S. H. Teoh, D. W. Hutmacher, *Polym. Int.*, 2007, **56**, 718 b) J. Peña, T. Corrales, I. Izquierdo-Barba, A. L. Doadrio, M. Vallet-Regi, *Polym. Degrad. Stab.*, 2006, **91**, 1424 c) M. J. Jenkins, K. L. Harrison, M. M. C. G. Silva, M. J. Whitaker, K. M. Shakesheff, S. M. Howdle, *Eur. Polym. J.*, 2006, **42**, 3145 d) D. W. Hutmacher, T. Schantz, I. Zein, K. W. Ng, S. Hin, T. Kim, C. Tan, J. *Biomed. Mater. Res.*, 2001, **55**, 203
- 59 a) V. R. Sunha, K. Bansal, R. Kaushik, R. Kumira, A. Trehan, *Int. J. Pharm.*, 2004, **278**, 1 b) R. Chandra, R. Rustgi, *Prog. Polym. Sci.*, 1998, **23**, 1273 c) D. R. Chen, J. Z. Bei, S. G. Wang, *Polym. Degrad. Stab.*, 2000, **67**, 455 d) E. Chiellini, R. Solaro, *Adv. Mater.*, 1996, **8**, 305 e) E. Mathiowitz, J. S. Jacob, Y. S. Jong, G. P. Carino, D. E. Chickering, P. Chaturvedi, C. A. Santos, K. Vijayaraghavan, S. Montgomery, M. Basset, C. Morrell, *Nature*, 1997, **386**, 410 f) S. Dumitriu, *Polymeric Biomaterials*, Marcel Dekker, New York, 2002
- 60 J. L. Hedrick, T. Magbitang, E. F. Connor, T. Glauser, W. Volksen, C. J. Hawker, V. Y. Lee, R. D. Miller, *Chem-Eur. J.*, 2002, **8**, 3308
- 61 P. Joshi, G. Madra, *Polym. Degrad. Stab.*, 2008, **93**, 1901
- 62 Y. Ikada, H. Tsuji, *Macromol. Rapid Commun.*, 2000, **21**, 117
- 63 O. Dechy-Cabaret, B. Martin-Vaca, D. Bourissou, *Chem. Rev.*, 2004, **104**, 6147
- 64 M. C. Rocca, G. Carr, A. B. Lambert, D. J. MacQuarrie, J. H. Clark, S. A. Solvay, US patent 2003/6531615 B2, 2003
- 65 M. Minami, S. Kozaki, US patent 2003/0023026 A1, 2003
- 66 M. Labet, W. Thielemans, *Chem. Soc. Rev.*, 2009, **38**, 3484
- 67 A. Arbaoui, C. Redshaw, *Polym. Chem.*, 2010, **1**, 801
- 68 W. H. Carothers, *Chem. Rev.*, 1931, **8**, 353
- 69 a) R. A. Gross, A. Kumar, B. Kalra, *Chem. Rev.*, 2001, **101**, 2097 b) R. T. MacDonald, S. K. Pulapura, Y. Y. Svirkin, R. A. Gross, D. L. Kaplan, J. Akkara,

- G. Swift, S. Wolk, *Macromolecules*, 1995, **28**, 6519 c) A. Córdova, T. Iversen, K. Hult, M. Martinelle, *Polymer*, 1998, **39**, 6519 d) S. Kobayashi, K. Takeya, S. Suda, H. Uyama, *Macromol. Chem. Phys.*, 1998, **199**, 1729
- 70 a) B. A. Rozenberg, *Pure Appl. Chem.*, 1981, **53**, 1715 b) K. Ito, Y. Hashizuka, Y. Yamashita, *Macromolecules*, 1977, **10**, 821 c) K. Ito, Y. Yamashita, *Macromolecules*, 1978, **11**, 68 d) M. Bero, G. Adamus, J. Kasperczyk, H. Janeczek, *Polym. Bull.*, 1993, **31**, 9
- 71 a) P. Kubisa, S. Penczek, *Prog. Polym. Sci.*, 1999, **24**, 1409 b) Y. Shibasaki, H. Sanada, M. Yokoi, F. Sanda, T. Endo, *Macromolecules*, 2000, **33**, 4316
- 72 a) W. Yao, Y. Mu, A. Gao, L. Ye, *Dalton Trans.*, 2008, 3199 b) A. –C. Albertsson, I. K. Varma, *Biomacromolecules*, 2003, **4**, 1466
- 73 a) B. Buchholz, DE patent 4005415, 1991 b) K. Enomoto, M. Ajioka, A. Yamaguchi, WO patent, 9312160, 1993 c) E. M. Filachione, C. H. Fisher, US patent 2396994, 1946 d) E. M. Filachione, C. H. Fisher, US patent, 2447693, 1948
- 74 C. Braud, R. Devarieux, A. Atlan, C. Ducos, V. Michel, *J. Chromatogr., B: Biomed. Sci. Appl.*, 1998, **706**, 73
- 75 a) C. K. Williams, *Chem. Soc. Rev.*, 2007, **36**, 1573 b) O. Coulembier, P. Degée, J. L. Hedrick, P. Dubois, *Prog. Polym. Sci.*, 2006, **31**, 723
- 76 A. Mahapatro, A. Kumar, R. A. Gross, *Biomacromolecules*, 2004, **5**, 62
- 77 H. Dong, H. –D. Wang, S. –G. Cao, J. –C. Shen, *Biotechnol. Lett.*, 1998, **20**, 905
- 78 F. J. Van Natta, J. W. Hill, W. H. Carother, *J. Am. Chem. Soc.*, 1934, **56**, 455
- 79 A. Duda, T. Biela, J. Libiszowski, P. Dubois, D. Mecerreyes, R. Jérôme, *Polymer Degrad. Stabil.*, 1998, **59**, 215
- 80 A. Arbaoui, PhD Thesis, *University of East Anglia*, 2009
- 81 G. L. Brode, J. V. Koleske, *J. Macromol. Sci. Chem.*, 1972, **A6**, 1109
- 82 A. Deffieux, S. Boileau, *Macromolecules*, 1976, **9**, 369
- 83 M. Basko, P. Kubisa, *J. Polm. Sci. Polym. Chem.*, 2006, **44**, 7071
- 84 T. Endo, Y. Shibasaki, F. Sanda, *J. Polym. Sci. Polym. Chem.*, 2002, **40**, 2190
- 85 a) H. Seikigushi, C. Clarisse, *Makromol. Chem.*, 1976, **177**, 591 b) G. Jiang, G. S. Walker, I. A. Jones, C. D. Rudd, *J. Appl. Polymer Sci.*, 2006, **102**, 3900
- 86 S. Penczek, M. Cypryk, A. Duda, P. Kubisa, S. Slomkowski, *Prog. Polym. Sci.*, 2007, **32**, 247

- 
- 87 a) M. -L. Shueh, Y. -S. Wang, B. -H. Huang, C. -Y. Kuo, C. -C. Lin, *Macromolecules*, 2004, **37**, 5155 b) T. -L. Yu, C. -C. Wu, C. -C. Chen, B. -H. Huang, J. Wu, C. -C. Lin, *Polymer*, 2005, **46**, 5909 c) L. F. Sánchez-Barba, D. L. Hughes, S. Humphrey, M. Bochmann, *Organometallics*, 2006, **25**, 1012 d) L. E. Breyfogle, C. K. Williams, V. G. Young, M. A. Hillmyer, W. B. Tolman, *Dalton Trans.*, 2006, 928 e) Y. Sarazin, R. H. Howard, D. L. Hughes, S. M. Humphrey, M. Bochmann, *Dalton Trans.*, 2006, 340 f) W. -Y. Lee, H. -H. Hsieh, C. -C. Hsieh, H. M. Lee, G. -H. Lee, J. -H. Huang, T. -C. Wu, S. H. Chuang, *J. Organomet. Chem.*, 2007, **692**, 1131
- 88 a) Z. Zhong, P. J. Dijkstra, C. Birg, M. Westerhausen, J. Feijen, *Macromolecules*, 2001, **34**, 3863 b) Z. Zhong, S. Schneiderbauer, P. J. Dijkstra, M. Westerhausen, J. Feijen, *Polym. Bull.*, 2003, **51**, 175
- 89 a) C. H. Huang, F. C. Wang, B. -T. Ko, T. -L. Yu, C. -C. Lin, *Macromolecules*, 2001, **34**, 356 b) R. -C. Yu, C. -H. Hung, J. -H. Hung, H. -Y. Lee, J. -T. Chen, *Inorg. Chem.*, 2002, **41**, 6450 c) D. Chakraborty, E. Y. -X. Chen, *Organometallics*, 2002, **21**, 1438 d) L. M. Alcazar-Roman, B. J. O'Keefe, M. A. Hillmyer, W. B. Tolman, *Dalton Trans.*, 2003, 3082 e) J. Lewiński, P. Horeglad, M. Dranka, I. Justyniak, *Inorg. Chem.*, 2004, **43**, 5789 f) N. Nomura, T. Aoyama, R. Ishii, T. Kondo, *Macromolecules*, 2005, **38**, 5363 g) J. Lewiński, P. Horeglad, K. Wójcik, I. Justyniak, *Organometallics*, 2005, **24**, 4588 h) S. Millione, F. Grisi, R. Centore, A. Tuzi, *Organometallics*, 2006, **25**, 266 i) S. Dagorne, F. Le Bideau, R. Welter, S. Bellemin-Lapponnaz, A. Maise-Francois, *Chem. Eur. J.*, 2007, **13**, 3202 j) M. Bouyahyi, E. Grunova, N. Marquet, E. Kirillov, C. M. Thomas, T. Roisnel, J. -F. Carpentier, *Organometallics*, 2008, **27**, 5815 k) A. Arbaoui, C. Redshaw, D. L. Hughes, *Chem. Comm.*, 2008, 4717
- 90 a) D. Takeuchi, T. Nakamura, T. Aida, *Macromolecules*, 2000, **33**, 725 b) A. J. Chmura, M. G. Davidson, M. D. Jones, M. D. Lunn, M. F. Mahon, *Dalton Trans.*, 2006, 887 c) Y. Takashima, Y. Nakayama, T. Hiro, H. Yasuda, A. Harada, *J. Organomet. Chem.*, 2004, **689**, 612 d) A. J. Chmura, M. G. Davidson, M. D. Jones, M. D. Lunn, M. F. Mahon, A. F. Johnson, P. Khunkamchoo, S. L. Roberts, S. S. F. Wong, *Macromolecules*, 2006, **39**, 7250
- 91 a) B. J. O'Keefe, S. M. Monnier, M. A. Hillmyer, W. B. Tolman, *J. Am. Chem. Soc.*, 2001, **123**, 339 b) B. J. O'Keefe, L. E. Breyfogle, M. A. Hillmyer, W. B.

- Tolman, *J. Am. Chem. Soc.*, 2002, **124**, 4384 c) M. –Z. Chen, H. –M. Sun, W. –F. Li, Z. –G. Wang, Q. Shen, Y. Zhang, *J. Organomet. Chem.*, 2006, **691**, 2489 d) D. S. McGuinness, E. L. Marshall, V. C. Gibson, J. W. Steed, *J. Polym. Sci. Polym. Chem.*, 2003, **41**, 3798 e) V. C. Gibson, E. L. Marshall, D. Navarro-Llobet, A. J. P. White, D. J. Williams, *J. Chem. Soc., Dalton Trans.*, 2002, 4321
- 92 a) M. D. Hannant, M. Schormann, M. Bochmann, *Dalton Trans.*, 2002, 4071 b) C. M. Silvernail, L. J. Yao, L. M. R. Hill, M. A. Hillmyer, W. B. Tolman, *Inorg. Chem.*, 2007, **46**, 6565 c) Y. D. M. Champouret, W. J. Nodes, J. A. Scrimshire, K. Singh, G. A. Solan, I. Young, *Dalton Trans.*, 2007, 4565
- 93 a) H. R. Kricheldorf, M. V. Sumbél, I. Kreiser-Saunderses, *Macromolecules*, 1991, **24**, 1944 b) H. R. Kricheldorf, S. –R. Lee, *Macromolecules*, 1996, **29**, 8669 c) H. R. Kricheldorf, S. Eggerstedt, *Macromol. Chem. Phys.*, 1998, **199**, 283 d) S. Penczek, A. Duda, A. Kowalski, J. Libiszowski, K. Majerska, T. Biela, *Macromol. Symp.*, 2000, 157, 61 e) A. Kowalski, J. Libiszowski, A. Duda, S. Penczek, *Macromolecules*, 2000, **33**, 1964
- 94 a) F. M. Kerton, A. C. Whitwood, C. E. Williams, *Dalton Trans.*, 2004, 2237 b) M. Yamashita, Y. Takemoto, E. Ihara, H. Yasuda, *Macromolecules*, 1996, **29**, 1798 c) Y. Shen, Z. Shen, Y. Zhang, K. Yao, *Macromolecules*, 1996, **29**, 8289
- 95 Y. Mahha, A. Atlamsani, J. –C. Blais, M. Tessier, J. –M. Brégeault, L. Salles, *J. Mol. Catal. A: Chem.*, 2005, **234**, 63
- 96 A. Arbaoui, C. Redshaw, D. M. Homden, J. A. Wright, M. R. J. Elsegood, *Dalton Trans.*, 2009, 8911
- 97 J. Yamada, K. Nomura, *Organometallics*, 2005, **24**, 3621

## **Chapter 2**

### **Vanadium(V) pro-catalysts supported by 1,3-depleted calix[4]arenes**

## 1. Introduction

As mentioned in Chapter 1, throughout the last decade the search for new ligand sets capable of forming efficient catalytic systems for either  $\alpha$ -olefin polymerisation or the ring opening of lactones has met with considerable success.<sup>1</sup> One recent example of highly efficient systems for the polymerisation of ethylene was published by Redshaw *et al.*, in which vanadyl pro-catalysts supported by a oxacalix[3]arene ligand, displayed activities over 90,000 g/mmol.h.bar.<sup>2</sup> Activities within the same range (75,200 g/mmol.h.bar) were also produced by utilising vanadium-based imido-alkoxide pro-catalysts bearing bisphenolate ligands.<sup>3</sup> However, these two findings are surpassed by results produced when investigating the use of vanadyl di- and tri-aryloxide  $-(CH_2)$ -bridged systems, which achieved extremely high activities (166,000 g/mmol.h.bar).<sup>4</sup>

Calixarenes can be viewed as cyclic analogues of such bi-phenols. The cyclic structures are produced by the condensation reaction between *para*-substituted phenols with formaldehyde. By varying the reaction temperature or equivalent of base, the size of the produced calixarene can be manipulated. The most commonly reported metallocalixarene systems tend to be complexes utilising the calix[4, 6 or 8]arenes.<sup>5</sup> The standard formula for *p-tert*-butylcalix[*n*]arene, where *n* is the number of phenolic units within the macrocycle, and X is the linking group between the phenolic units (this will be discussed further in Chapter 3). A typical calixarene compound (Figure 10) is shown in the ‘cone’ conformation, other conformations do arise, however the cone conformation is the only one described herein.

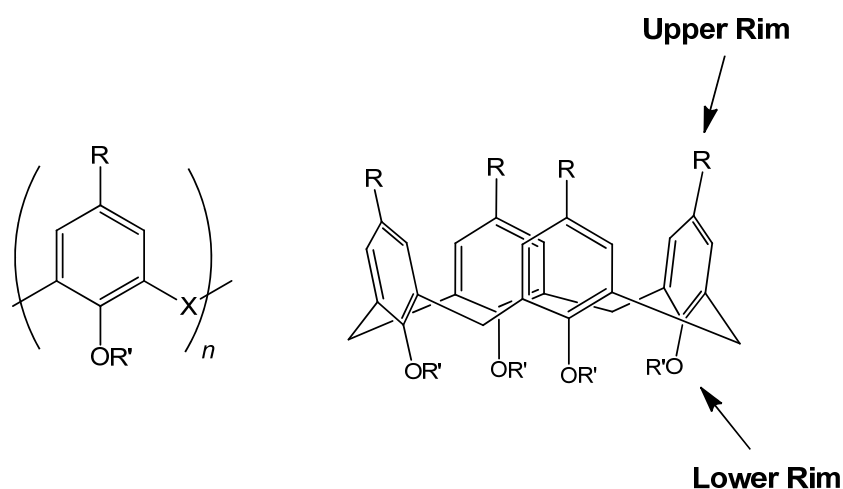


**Figure 10.** Calixarene phenolic sub-unit. *p-tert*-butylcalix[4]arene in the cone conformation, indicating the lower and upper rims of the calixarene molecule. (Typically, R = H, alkyl, aryl, NH<sub>2</sub>, CO<sub>2</sub>H; R' = H, alkyl).

Calixarenes form highly organised multimetallic architectures for various applications such as; catalysis,<sup>5</sup> magnetism,<sup>6</sup> medicine,<sup>7</sup> sensors,<sup>8</sup> metal organic frameworks<sup>9</sup> and other nano-technologies.<sup>6, 10</sup>

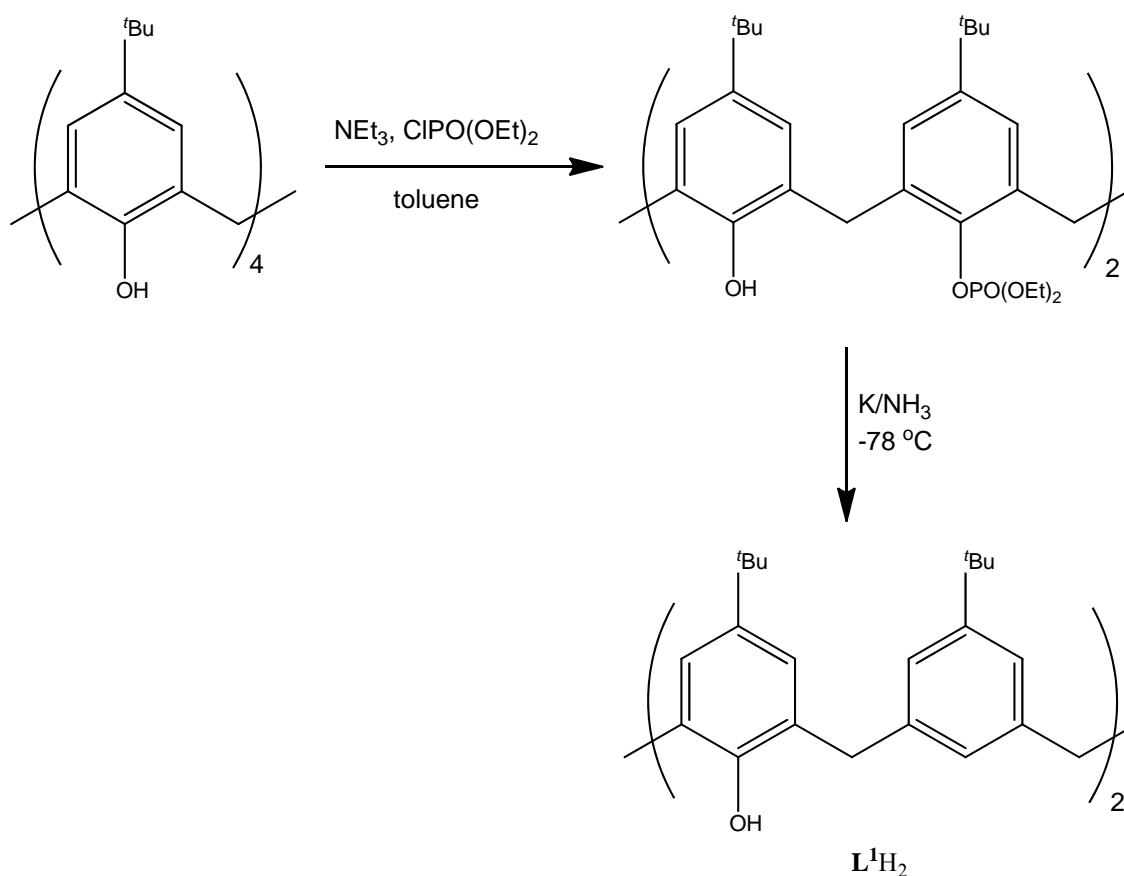
Calixarene analogues can be synthesised with ease, on large scales and at cheap cost. The functionalities on either the lower or upper rim of the calixarenes can also be easily altered, enabling numerous different functionalities to be added to the calixarene backbone. Transition metal calix[4]arenes have been used in a range of polymerisations from ring opening metathesis to polyethylene with varying degrees of success.<sup>11</sup> The main focus of this chapter will be altering the functionality on the lower rim of the calixarene, to investigate any potential benefit on the efficiency of the pro-catalysts for the polymerisation of ethylene and  $\epsilon$ -caprolactone.

### 1.1 Depleted calix[4]arenes

Although there has been extensive research into calixarenes as ancillary ligands, the related depleted calixarenes have not undergone such scrutiny, partly due to their recent discovery.

In the early 1990s, synthetic routes to 1,2- and 1,3-depleted calix[4]arenes were first reported by Biali and co-workers.<sup>12</sup> These involve the parent calix[4]arene molecule undergoing a Birch reduction to produce the final product, *i.e.* depleted calixarene (Scheme 11).

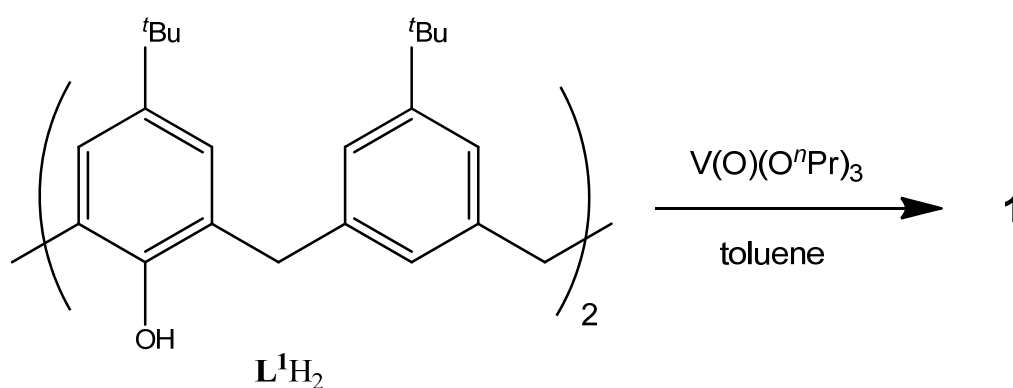
The coordination chemistry of such depleted calixarenes is only just emerging,<sup>13</sup> and their use in olefin polymerisation catalysis is restricted to a patent on group IV systems,<sup>14</sup> and more recently a number of titanacalix[4]arenes.<sup>15</sup> Espinas *et al.* reported the synthesis of a family of titanium complexes, supported by a variety of calix[4]arene moieties, activities for the polymerisation of ethylene, upon activation with MAO, were in the range of 14-770 g/mmol.h.<sup>15</sup> To date, there are no reports of vanadium depleted systems and their activity towards ethylene or ring opening polymerisations.



**Scheme 11.** The synthetic route for producing 1,3-depleted calix[4]arene,  $L^1H_2$ .

## 2. Results and Discussion

### 2.1 Vanadium(V) alkoxide 1,3-depleted calix[4]arenes



**Scheme 12.** Synthesis of vanadium(V) 1,3-depleted calix[4]arene complex **1**

The dinuclear vanadium 1,3-depleted calix[4]arene was produced *via* the reaction of the 1,3-depleted calix[4]arene ligand,  $L^1H_2$ , with vanadium oxytriisopropoxide,  $[V(O)(O^iPr)_3]$  (Scheme 12). The dark red solution was heated at reflux overnight and then cooled, the



volatile components were removed under *vacuo*. The residue was extracted into ‘hot’ acetonitrile, after prolonged standing at ambient temperature red plates of **1** formed. These were suitable for X-ray diffraction studies; a molecular structure of **1** is shown in Figure 11.

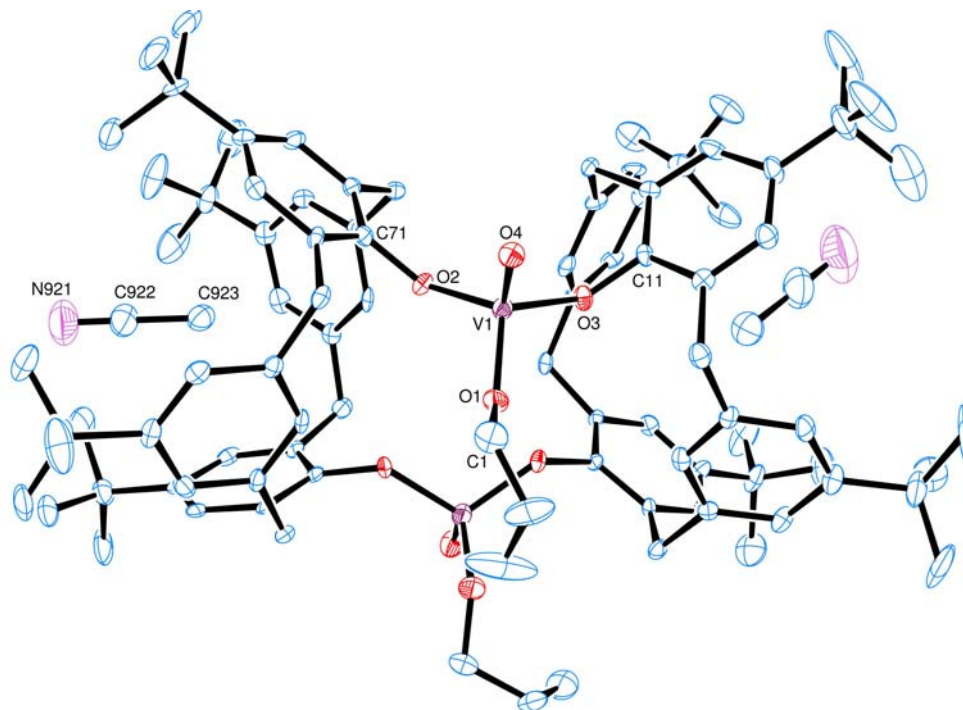


**Figure 11.** View of a molecule of  $[\text{VO}(\text{O}^i\text{Pr})\text{L}^1]_2(2\text{MeCN})$  (**1**(2MeCN)) indicating the atom numbering scheme. Hydrogen atoms have been omitted for clarity. Thermal ellipsoids are drawn at the 30 % probability level. Selected bond lengths (Å) and angles (°): V(1)-O(3) 1.780(2), V(1)-O(2) 1.778(2), V(1)-O(1) 1.743(2), V(1)-O(4) 1.581(2), O(3)-V(1)-O(2) 111.93(10), O(3)-V(1)-O(1) 109.67(12), O(3)-V(1)-O(4) 106.97(12), O(1)-V(1)-O(2) 110.37(11), O(4)-V(1)-O(2) 110.17(12), O(4)-V(1)-O(1) 107.58(12).

In the dimeric structure of **1**, one phenolic O atom from each calixarene ligand is linked through a VO(O<sup>*i*</sup>Pr) bridge; the second O atom from each calixarene ligand is bridged through a second VO(O<sup>*i*</sup>Pr) group. The two calixarene ligands (and the two bridging groups) are related by a *pseudo*-twofold symmetry axis. Both vanadium centres are four-coordinate, with approximately tetrahedral geometries. There is an acetonitrile molecule in the cavities of both calixarene ligands.

In addition to **1**, deep-red plates of the hydrolysis product (**2**) were also isolated. The formation of **2** could be accounted for by two equivalents of water getting into the reaction solution.

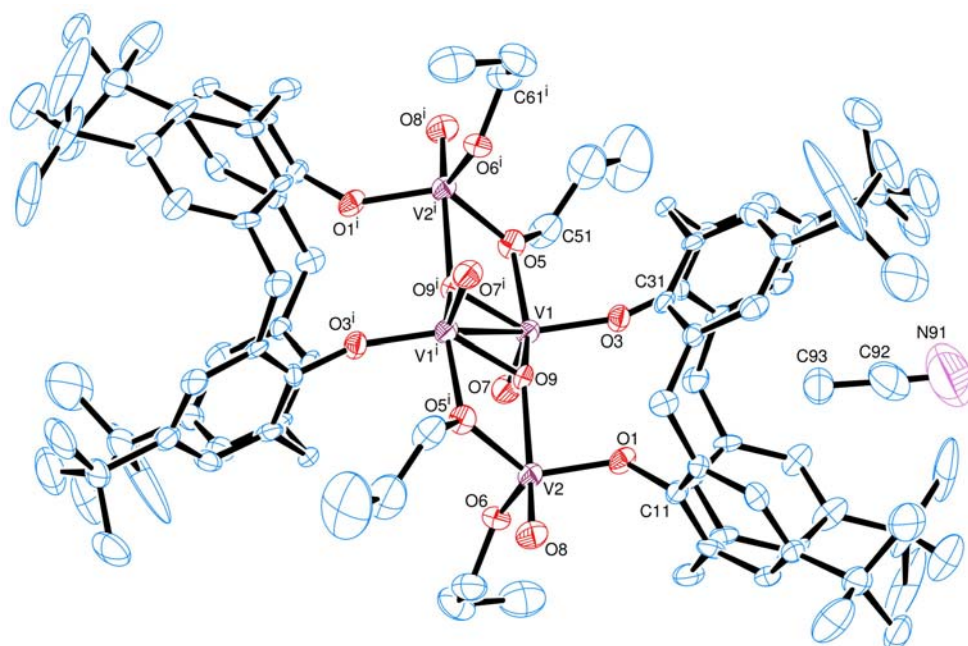


**Figure 12.** View of a molecule of  $\{[\text{VO}(\text{O}^i\text{Pr})]_2(\mu\text{-O})\text{L}^1\}_2(\text{MeCN})$  (**2**(MeCN)) indicating the atom numbering scheme. Hydrogen atoms have been omitted for clarity. Thermal ellipsoids are drawn at the 30 % probability level.

The complex dimeric molecule **2** lies about a centre of symmetry. The two calixarene ligands are linked through a  $\text{V}_4\text{O}_4$  network. The metal centre in complex **2** can be described as an inorganic core, consisting of four vanadium metal centres (Figure 13). There is a molecule of solvent, acetonitrile, in the cone cavity of each calixarene ligand.

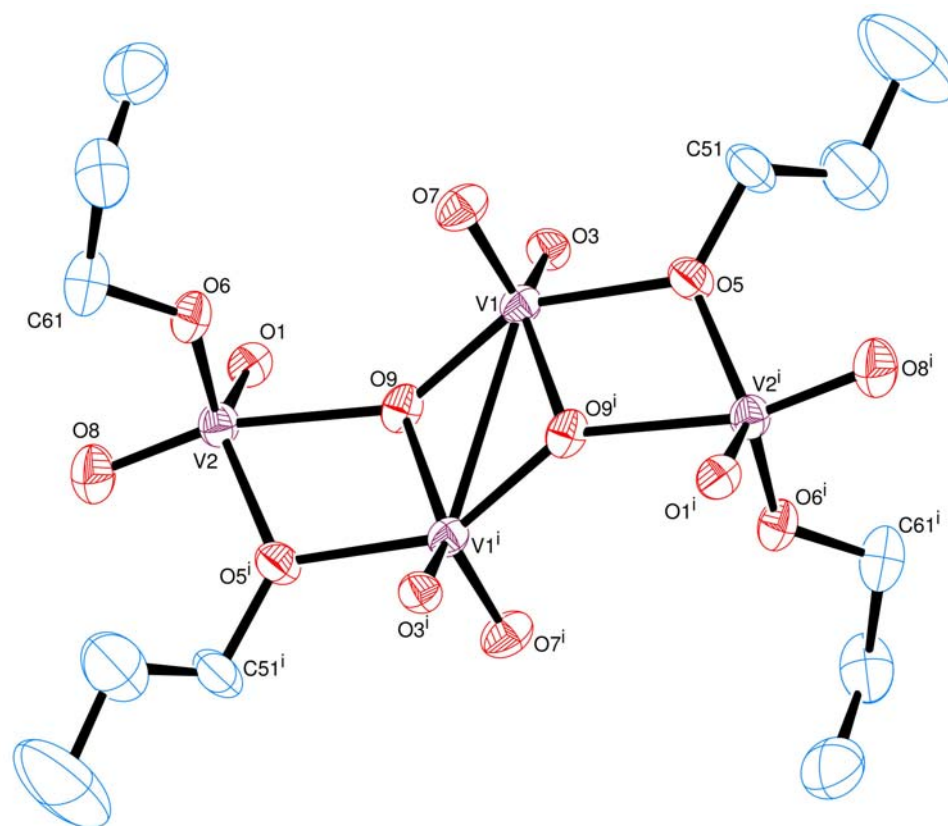
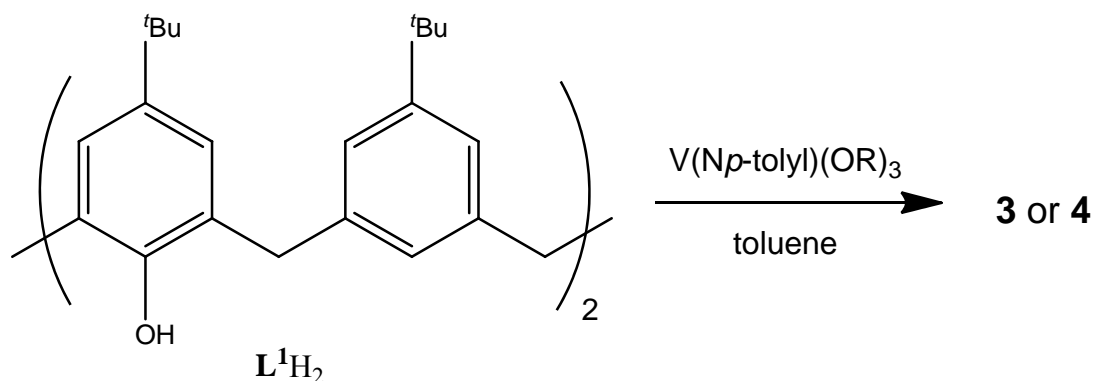


**Figure 13.** View of the inorganic core of **2** showing the atom numbering scheme and revealing the geometry around the vanadium centre. Thermal ellipsoids are represented at the 30 % probability level. Selected bond lengths (Å) and angles (°): V(1)-O(3) 1.766(4), V(1)-O(5) 2.042(4), V(1)-O(7) 1.573(4), V(1)-O(9) 1.857(4), V(1)-O(9<sup>1</sup>) 1.877(4), O(3)-V(1)-O(5) 89.79(18), O(3)-V(1)-O(7) 109.0(2), O(3)-V(1)-O(9) 99.55(19), O(3)-V(1)-O(9<sup>1</sup>) 137.16(17), V(1)-O(9)-V(2) 144.1(2), V(1)-O(9)-V(1<sup>1</sup>) 100.4(2), O(8)-V(2)-O(9) 163.5(2).

Each vanadium atom is 5-coordinate: V(1) has a square pyramidal pattern with the vanadyl oxygen, O(7), in the apical site, whereas the pattern of V(2) is closer to trigonal bipyramidal with the vanadyl O(8) and a  $\mu^3$ -O atom, O(9), in the axial positions. Both metals are bonded to a vanadyl O, a phenolic O and a bridging O<sup>n</sup>Pr ligand; the shell of V(1) is completed by two  $\mu^3$ -O ligands, whereas V(2) has one  $\mu^3$ -O and a terminal O<sup>n</sup>Pr ligand.

## 2.2 Vanadium(V) imido-alkoxide 1,3-depleted calix[4]arenes



**Scheme 13.** Synthesis of vanadium(V) imido-alkoxide 1,3-depleted calix[4]arene complexes,  $[V(Np\text{-tolyl})(OR)L^1]_2$  R =  $n$ Pr **3**, R =  $t$ Bu **4**.

The vanadium(V) imido-alkoxide 1,3-depleted calix[4]arene, **3**, was prepared in the same manner as complex **1** (Scheme 13) using  $[V(Np\text{-tolyl})(O^nPr)_3]$  as the vanadium source. After extraction into hot acetonitrile, and following prolonged standing at room temperature, yellow block crystals of **3** were formed, which were characterised by X-ray diffraction (Figure 14).

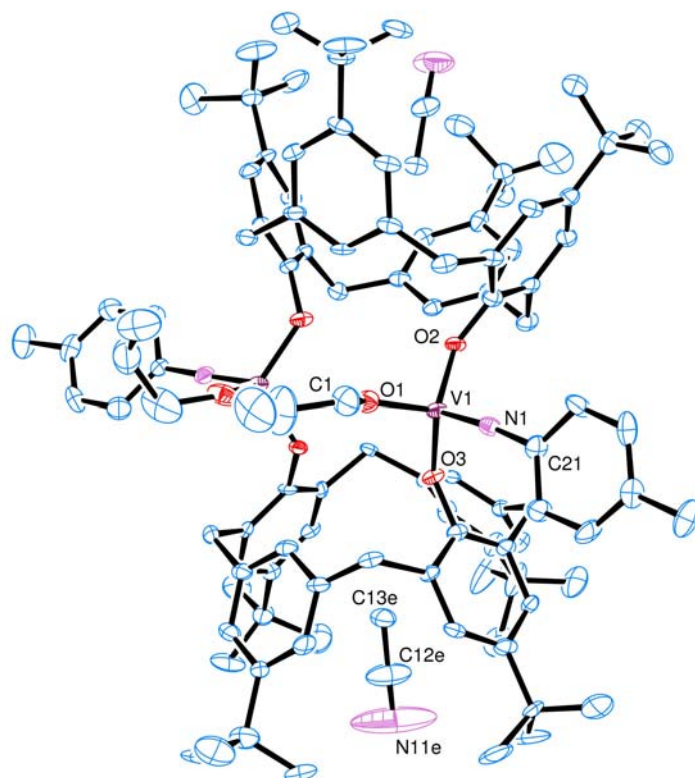


**Figure 14.** View of a molecule of  $[V(Np\text{-tolyl})(O^iPr)L^1]_2(2MeCN)$ , (**3**(2MeCN)), indicating the atom numbering scheme. Hydrogen atoms have been omitted for clarity. Thermal ellipsoids are drawn at the 30 % probability level. Selected bond lengths (Å) and angles (°): V(1)-O(2) 1.820(5), V(1)-O(3) 1.792(6), V(1)-N(1) 1.641(8), V(1)-O(1) 1.790(6), N(1)-V(1)-O(2) 107.7(3), O(1)-V(1)-O(2) 111.8(3), O(3)-V(1)-O(2) 112.5(2), N(1)-V(1)-O(1) 103.6(3), N(1)-V(1)-O(3) 108.0(3), O(3)-V(1)-O(1) 112.7(3).

Complex **4** was prepared in the same manner as complex **1** from a solution of  $L^1H_2$  and  $[V(Np\text{-tolyl})(O^iBu)_3]$ . The solution was cooled and volatile components removed under vacuum. The orange/brown residue was extracted into hot acetonitrile and left to stand at room temperature. Yellow lath crystals were formed which were characterised by X-ray diffraction (Figure 15).

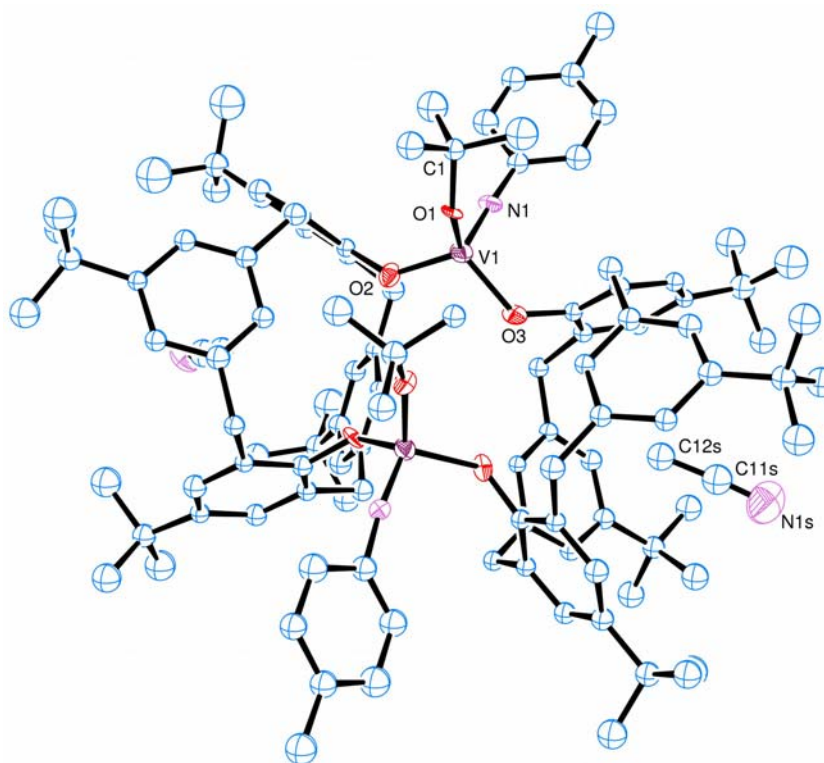


**Figure 15.** View of one of the three independent (but very similar) molecules of  $[V(Np\text{-tolyl})(O^t\text{Bu})L^1]_2(2\text{MeCN})$  (**4**(2MeCN)), indicating the atom numbering scheme. Hydrogen atoms have been omitted for clarity. Thermal ellipsoids are drawn at the 30 % probability level. Selected bond lengths (Å) and angles ( $^\circ$ ): V(1)-O(2) 1.829(12), V(1)-O(3) 1.799(12), V(1)-N(1) 1.649(14), V(1)-O(1) 1.753(12), O(3)-V(1)-O(2) 112.7(4), N(1)-V(1)-O(2) 106.3(6), O(1)-V(1)-O(2) 114.0(5), N(1)-V(1)-O(3) 109.3(5), O(1)-V(1)-O(3) 109.2(4), N(1)-V(1)-O(1) 104.9(6).

The calixarene complex molecule of **3** and the three independent calixarene molecules in **4** are also dimeric molecules, and resemble **1** in many respects. Each comprises two vanadium atoms (four-coordinate, with tetrahedral coordination pattern) linked through the phenolate O atoms of the two calixarene ions. There are also  $O^i\text{Pr}$  (or  $O^t\text{Bu}$ ) and  $Np\text{-tolyl}$  ligands on each vanadium atom, and an acetonitrile molecule lies in the cone of each calixarene unit. The whole molecule is arranged with approximately  $2mm$  symmetry. The *pseudo*-twofold axis passes through the midpoint of the V...V vector and relates the pairs of  $O^i\text{Pr}$  (or  $O^t\text{Bu}$ ),  $Np\text{-tolyl}$  and calixarene ligands.

The imido-alkoxide complexes **3** and **4**, can be compared to some imido-alkoxide vanadium(V) complexes bearing bisphenolate ligands that have been previously synthesised in the group (Complex **XIV** Chapter 1, section 2.4, crystal structure shown in Figure 16).<sup>3</sup> As mentioned previously, calix[4]arene and its 1,3-depleted counterpart

can be viewed as cyclic analogues of biphenol ligands. As this is the case, comparisons can be made between the 1,3-depleted vanadium(V) imido-alkoxide complexes, **3** and **4**, and the bisphenol vanadium(V) imido-alkoxide complexes synthesised by Arbaoui *et al.*<sup>3</sup>

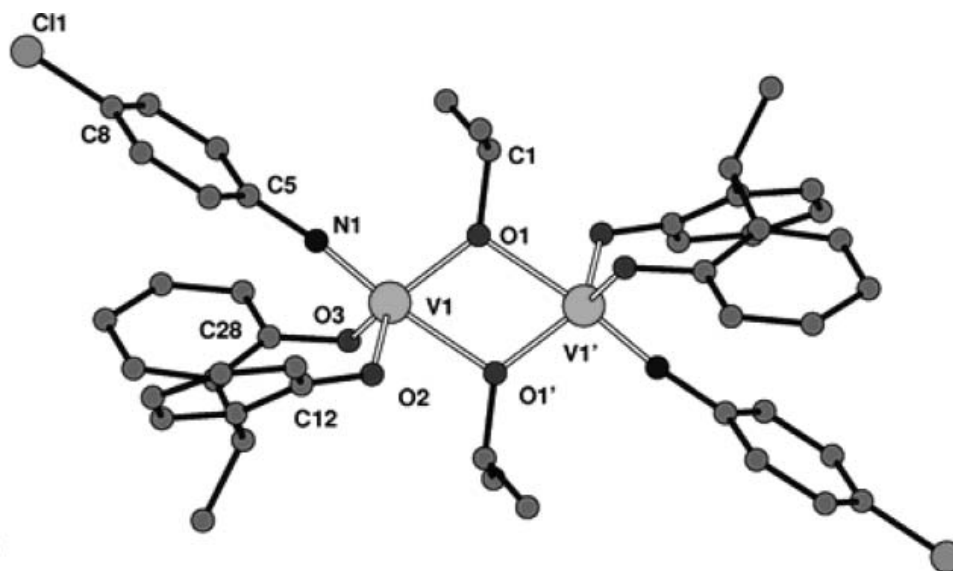


**Figure 16.** Dimeric aryylimido-alkoxide vanadium(V) complex **XIV** as described by Arbaoui *et al.*<sup>3, 16</sup>

Complexes **1–4** contain vanadium/oxygen cage networks sandwiched between two ligand units, which are similar to those observed in **XIV**. Crystallographic data comparing complexes **1–4** and **XIV**, are collated in Table 3.

**Table 3.** Selected bond lengths (Å) and angles (°) for **1–4**, compared to complex **XIV**.

	<b>XIV</b>	<b>1</b>	<b>2</b>	<b>3</b>	<b>4</b>
V(1)-N(1)	1.661(3)	-	-	1.641(8)	1.649(14)
V(1)-O(1)	1.885(3)	1.743(2)	-	1.790(6)	1.753(12)
V(1)-O(3)	1.836(2)	1.780(2)	1.766(4)	1.792(6)	1.799(12)
V(1)-O(1')	2.172(2)	-	1.857(4)	-	-
N(1)-V(1)-O(1)	99.34(13)	-	-	103.6(3)	104.9(6)
N(1)-V(1)-O(2)	99.11(13)	-	-	107.7(3)	109.3(5)
O(1) or O(5)-V(1)- O(3)	117.55(11)	109.67(12)	89.79(18)	112.7(3)	109.2(4)
V(1)-O(1) or O(9)- V(1')	107.73(11)	-	100.4(2)	-	-

By comparing the bond angles and lengths, it is apparent that there is little difference between the bond lengths in complex **XIV** and complexes **1-4**. When comparing the bond angles around the vanadium metals centres, it is noted, that the angles formed between the phenolic oxygen, metal centre and alkoxide oxygen (O(1)-V(1)-O(2)), are all similar to complex **XIV**. However, the other bonds angles are larger for the metallocalixarene complexes in comparison to the bisphenolate ligand system. This is most likely due to the rigid metallocalixarene backbone, whereas the phenol rings in the bisphenolate complex have more flexibility. For instance, the chelating rings in **XIV** adopt a flattened chair conformation, with O(2)-V(1)-O(3) angles in the range of 109.68(7) to 112.19(6)<sup>o</sup>.<sup>16</sup> These are similar to related oxo vanadium(V) bisphenolate compounds that stated angles of approximately 106<sup>o</sup>.<sup>17</sup> The two phenolic oxygens in the depleted calix[4]arene systems are on opposing rings, in the 1,3 position. Due to steric constrictions, they are unable to bind to the same metal centre as observed in **XIV**.

### 2.3 Ethylene polymerisation

Complexes **1-4** were screened for their ability to polymerise ethylene in the presence of either dimethylaluminium chloride (DMAC) or methylaluminium chloride (MADC) with the re-activating substance ethyl trichloroacetate (ETA). Temperature and number of equivalents of co-catalyst were also investigated over 15 minute periods to study the effects upon the vanadium(V) complexes.

#### 2.3.1 Temperature screening

Complexes **1-4** were screened over a range of temperatures (20-80 °C, Table 4) in the presence of either DMAC or MADC with the re-activator ETA. All parameters, such as time, were kept the same for each run allowing for comparisons between pro-catalyst activities.



**Table 4.** Polyethylene screening results for pro-catalysts **1-4**.<sup>a</sup>

Run	Pro-catalyst ( $\mu\text{mol}$ )	Co-catalyst	Temp ( $^{\circ}\text{C}$ )	Yield PE(g) <sup>b</sup>	Activity <sup>c</sup> ( $\times 10^3$ )
1	<b>1</b> (0.25)	DMAC	20	1.34	10.8
2	<b>1</b> (0.25)	DMAC	40	2.07	16.5
3	<b>1</b> (0.25)	DMAC	80	3.95	31.6
4	<b>1</b> (0.25)	MADC	20	1.96	15.7
5	<b>1</b> (0.25)	MADC	40	2.78	22.2
6	<b>1</b> (0.25)	MADC	60	2.18	17.4
7	<b>1</b> (0.25)	MADC	80	2.63	21.0
8	<b>2</b> (0.25)	DMAC	20	2.47	4.9
9	<b>2</b> (0.25)	DMAC	40	2.49	10.0
10	<b>2</b> (0.25)	DMAC	60	3.27	13.1
11	<b>2</b> (0.25)	DMAC	80	4.10	16.4
12	<b>2</b> (0.25)	MADC	20	1.26	5.0
13	<b>2</b> (0.25)	MADC	40	1.99	8.0
14	<b>2</b> (0.25)	MADC	80	2.99	12.0
15	<b>3</b> (0.25)	DMAC	20	1.08	8.6
16	<b>3</b> (0.25)	DMAC	40	1.56	12.5
17	<b>3</b> (0.25)	DMAC	60	1.86	14.9
18	<b>3</b> (0.25)	DMAC	80	2.65	21.2
19	<b>3</b> (0.25)	MADC	20	1.12	9.0
20	<b>3</b> (0.25)	MADC	40	1.59	12.7
21	<b>3</b> (0.25)	MADC	60	1.60	12.8
22	<b>3</b> (0.25)	MADC	80	2.51	20.1
23	<b>4</b> (0.25)	DMAC	20	1.65	13.2
24	<b>4</b> (0.25)	DMAC	40	2.55	20.4
25	<b>4</b> (0.25)	DMAC	60	1.33	10.6
26	<b>4</b> (0.25)	DMAC	80	1.11	8.9
27	<b>4</b> (0.25)	MADC	20	1.44	11.5
28	<b>4</b> (0.25)	MADC	40	1.48	11.8
29	<b>4</b> (0.25)	MADC	60	2.08	16.6
30	<b>4</b> (0.25)	MADC	80	0.95	7.6

<sup>a</sup>1 bar ethylene Schlenk tests carried out in toluene (200 mL) in the presence of ETA (0.05 mL) over 15 min; reaction was quenched with dilute HCl, washed with methanol (50 mL) and dried for 12 h. at 80  $^{\circ}\text{C}$ ,

<sup>b</sup> g per pro-catalyst, <sup>c</sup>g/mmol.h.bar per V centre.

Pro-catalysts **1** and **3** behaved in a similar manner when using either DMAC or MADC as co-catalyst over a range of temperatures (20-80 °C) (Figure 17). In particular, both exhibited enhanced catalytic activity (runs 1-3 and 15-20 - DMAC; runs 4-7 and 19-22 - MADC) at elevated temperatures (80 °C). Pro-catalyst **2**, enhanced thermal stability was observed at 80 °C in the presence of both DMAC (run 11) and MADC (run 14). For the *tert*-butoxide system, **4**, the thermal stability is reduced, the highest activities were observed at 40 °C (run 24) when using DMAC, and 60 °C (run 29) when using MADC. At 80 °C, in the presence of 2000 equivalents of co-catalyst, the activity orders  $1 > 3 > 2 > 4$  for DMAC and  $1 \approx 3 > 2 > 4$  for MADC were observed. In general, there was a change in the polymer morphology (from a thick jelly-like solid to a fine white powder) at higher temperatures, which started at 60 °C.

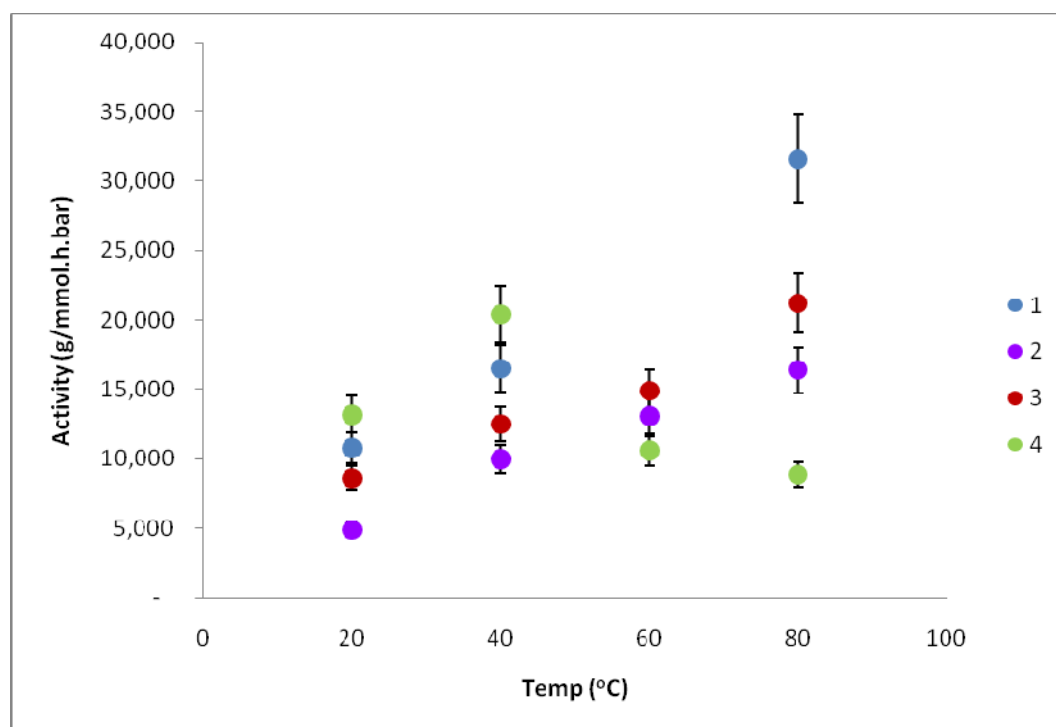


**Figure 17.** Polyethylene screening results varying temperature for pro-catalysts **1–4** (utilising DMAC).

### 2.3.2 Equivalent of co-catalyst

The effect of varying the concentration of co-catalyst was also investigated to note if there would be an overall impact on observed catalytic activity. It was also observed as to what extent the different co-catalysts and varying concentrations would have on pro-catalysts **1**, **3** and **4**. Temperature, time and pro-catalyst concentration were all kept constant to enable comparisons between the performances of the three pro-catalysts.

**Table 5.** Varying co-catalyst and concentration, using pro-catalysts **1**, **3** and **4**.<sup>a</sup>

Run	Pro-catalyst ( $\mu\text{mol}$ )	Co-catalyst	[Al]/[V]	Time (min)	Temp ( $^{\circ}\text{C}$ )	Yield PE(g) <sup>c</sup>	Activity <sup>d</sup> ( $\times 10^3$ )
1	<b>1</b> (0.25)	DMAC	2000	15	20	1.52	12.2
2	<b>1</b> (0.25)	DMAC	4000	15	20	2.04	16.3
3 <sup>b</sup>	<b>1</b> (0.15)	DMAC	6000	10	20	1.55	31.0
4 <sup>b</sup>	<b>1</b> (0.15)	DMAC	8000	10	20	2.19	42.4
5	<b>1</b> (0.25)	MADC	1000	15	20	1.48	11.8
6	<b>1</b> (0.25)	MADC	2000	15	20	1.49	11.9
7	<b>1</b> (0.25)	MADC	4000	15	20	1.90	15.2
8 <sup>b</sup>	<b>1</b> (0.15)	MADC	6000	10	20	1.79	35.8
9 <sup>b</sup>	<b>1</b> (0.15)	MADC	8000	10	20	1.95	39.0
10	<b>3</b> (0.25)	DMAC	1000	15	20	1.25	10.0
11	<b>3</b> (0.25)	DMAC	3000	15	20	1.37	11.0
12 <sup>b</sup>	<b>3</b> (0.15)	DMAC	6000	10	20	1.41	28.1
13 <sup>b</sup>	<b>3</b> (0.15)	DMAC	8000	10	20	1.99	39.9
14	<b>3</b> (0.25)	MADC	1000	15	20	0.60	4.8
15	<b>3</b> (0.25)	MADC	2000	15	20	1.38	11.1
16	<b>3</b> (0.25)	MADC	3000	15	20	1.99	15.9
17	<b>3</b> (0.25)	MADC	4000	15	20	2.51	20.1
18 <sup>b</sup>	<b>3</b> (0.15)	MADC	6000	10	20	2.07	41.3
19 <sup>b</sup>	<b>3</b> (0.15)	MADC	8000	10	20	1.85	36.9
20	<b>4</b> (0.25)	DMAC	1000	15	20	1.95	15.6
21	<b>4</b> (0.25)	DMAC	3000	15	20	2.06	16.5
22 <sup>b</sup>	<b>4</b> (0.15)	DMAC	6000	10	20	1.03	20.5
23 <sup>b</sup>	<b>4</b> (0.15)	DMAC	8000	10	20	1.42	28.5
24	<b>4</b> (0.25)	MADC	1000	15	20	1.23	9.8
25	<b>4</b> (0.25)	MADC	2000	15	20	1.40	11.1
26	<b>4</b> (0.25)	MADC	3000	15	20	1.76	14.1
27	<b>4</b> (0.25)	MADC	4000	15	20	2.72	21.8
28 <sup>b</sup>	<b>4</b> (0.15)	MADC	6000	10	20	1.16	23.3
29 <sup>b</sup>	<b>4</b> (0.15)	MADC	8000	10	20	2.00	40.1

<sup>a</sup>1 bar ethylene Schlenk tests carried out in toluene (200 mL) in the presence of ETA (0.05 mL) over 15 min; reaction was quenched with dilute HCl, washed with methanol (50 mL) and dried for 12 h. at 80  $^{\circ}\text{C}$ ,

<sup>b</sup> 0.025 mL ETA, <sup>c</sup> g per pro-catalyst, <sup>d</sup> g/mmol.h.bar per V centre.

There is a general increase in observed activity on increasing the co-catalyst concentration, though in the case of **3**, the activity peaks at 6000 equivalents for MADC (run 18) (Figure 18). Overall, there appears to be little benefit in using MADC over DMAC. For pro-catalyst **1**, the activities for increasing concentration of either DMAC or MADC follow the same trend, with the highest activities  $\sim 40,000$  g/mmol.h.bar being observed with 8000 equivalent of co-catalyst (runs 4 and 9).

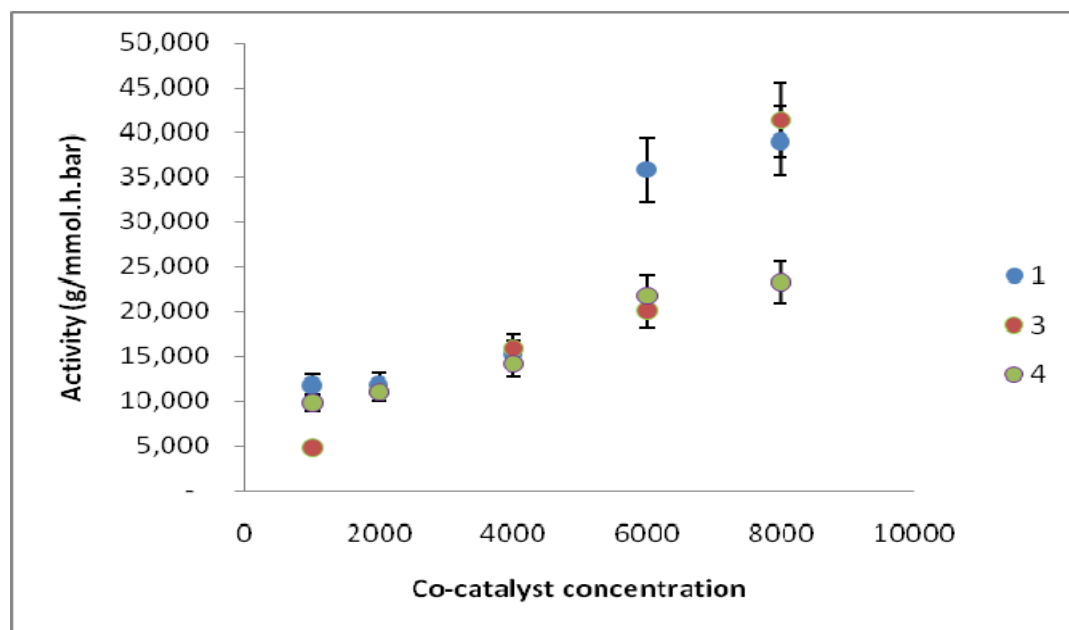


**Figure 18.** Polyethylene screening results varying co-catalyst concentration for pro-catalysts **1**, **3** and **4** (utilising MADC).

Activities in approximately the same range were noted for **3**, however these were achieved at 8000 equivalents of DMAC (run 13) and with 6000 equivalents of MADC (run 18). Whereas for **1** and **3**, there was little difference in the range of activities when comparing co-catalysts DMAC and MADC, with pro-catalyst **4**, there is a notable difference when comparing results achieved with 8000 equivalents of co-catalyst (runs 23 and 29). This is most likely due to sterics around the metal centre; complex **4** has the bulkier *tert*-butoxide group attached to the vanadium.

### 2.3.3 Industrial ethylene screening

Pro-catalysts **1** and **3** were also submitted for industrial screening to observe whether either pro-catalyst showed any degree of activity for ethylene polymerisation under more robust, heterogenous industrial conditions.

Firstly the pro-catalysts were screened using either triethylaluminum (TEA) or diethylaluminum chloride (DEAC) as co-catalyst. The polymerisation conditions were at 220 °C, 29 bar ethylene fed in on demand, and in the presence of hydrogen and a 10 minute polymerisation time. However under these conditions, no polymer was formed.<sup>18</sup> Pro-catalysts **1** and **3** were also screened under silica-supported slurry conditions. During this process, the pro-catalysts were screened using a technique referred to as ‘pore-filling’ or ‘incipient wetness’. This requires the pro-catalyst to be supported on silica to produce a free flowing powder. This method was conducted under less harsh polymerisation conditions than the previous technique (15.2 bar, 70 °C). MAO and DEAC were used as co-catalysts.

**Table 6.** Results for ethylene polymerisation runs (supported silica-catalyst) using pro-catalysts **1** and **3**.<sup>a</sup>

Run	Pro-catalyst (μmol)	Co-catalyst	[Al]/[V]	Time (min)	Temp (°C)	Yield PE(g)	Activity <sup>b</sup>
1	<b>1</b> (5.0)	MAO	1700	60	70	4.02	30
2	<b>3</b> (5.1)	MAO	1650	60	70	1.80	10
3	<b>3</b> (3.0)	DEAC	1600	60	70	0.60	10

<sup>a</sup>15.2 bar ethylene partial pressure slurry polymerization tests carried out in isobutane in the presence of TiBAL as scavenger, <sup>b</sup>g/mmol.h.bar per V centre.

For the silica-supported systems screened for ethylene activity under slurry conditions, polymers were formed, however activities were rather disappointing at  $\leq 30$  g/mmol.h.bar. It needs to be taken into account that such industrial conditions tend to utilise low equivalents of co-catalyst and high temperatures. The above screening results (shown in Table 4-6) show that pro-catalysts **1-4** show the highest activities at approximately 8000 equivalents of co-catalyst. It is also worth noting that at 60 °C the morphology of the produced polymer changed, indicating potential degradation of the pro-catalyst.

#### 2.4 ε-Caprolactone polymerisation

Complexes **1**, **3** and **4** were also screened for their ability to polymerise ε-caprolactone. Pro-catalyst **4** was subjected to temperature, time, monomer and co-initiator studies. No

polymer was observed at 20-40 °C. The polymerisation results for these studies are shown in Table 7.

**Table 7.**  $\epsilon$ -Caprolactone polymerisation data for complex **4**.<sup>a</sup>

Run	Monomer / metal	Equiv. BnOH	Time (h)	Temp (°C)	Conversion <sup>b</sup>	$M_n$ calculated <sup>c</sup> (g/mol)	$M_n$ measured <sup>d</sup> (g/mmol)	PDI <sup>e</sup>
1	400	5	72	60	8	3.7	0.5	2.1
2	400	5	72	80	21	9.6	2.6	1.2
3	600	5	72	80	12	5.5	2.9	1.2
4	800	5	72	80	-	-	-	-
5	400	0	72	80	-	-	-	-
6	400	1	72	80	18	8.2	3.5	1.4
7	400	10	72	80	12	5.5	0.8	2.0
8	400	5	12	80	-	-	-	-
9	400	5	24	80	15	6.8	2.1	1.1
10	400	5	48	80	20	9.1	5.3	1.2

<sup>a</sup> Conditions: 20 mL of toluene; 2 mL of  $\epsilon$ -caprolactone; benzyl alcohol taken from a 0.97 M solution in toluene; <sup>b</sup> calculated by <sup>1</sup>H NMR; <sup>c</sup>  $\times 10^3$  <sup>d</sup>  $M_n$  measured =  $0.58 \times M_n$  (GPC  $\times 10^3$ ).<sup>19</sup> <sup>e</sup> Polydispersity index.

Complex **4** was active for the ring opening polymerisation of  $\epsilon$ -caprolactone. However, it was inactive at room temperature and 40 °C. From Table 7, it is evident that as the temperature was increased, the conversion from monomer to polymer also increased (Table 7, runs 1-2). The polydispersity index decreased as the temperature increased, indicating that increasing the temperature also prevents side reactions from occurring. The percentage conversion appeared to reach optimum conversion at around 48 hours, as both 48 hours and 72 hours observed approximately the same rate of conversion. The conditions that produced the most polymer were noted to be at 72 h, with 5 equivalents of co-initiator (run 2).

The conditions which produced the most poly( $\epsilon$ -caprolactone) were then used to screen complexes **1** and **3** (Table 8).

**Table 8.**  $\epsilon$ -Caprolactone polymerisation data for complex **1**, **3** and **4**.<sup>a</sup>

Run	Pro-catalyst	Conversion <sup>b</sup> (%)	$M_n$ calculated <sup>c</sup> (g/mol)	$M_n$ measured <sup>d</sup> (g/mol)	PDI <sup>e</sup>
1	<b>1</b>	94	42.9	6.6	1.5
2	<b>3</b>	46	21.0	6.1	1.2
3	<b>4</b>	21	9.6	2.6	1.2

<sup>a</sup> Conditions: monomer/metal = 400; 72 h; 80 °C; 20 mL of toluene; 2 mL of  $\epsilon$ -caprolactone; 5 equivalent of benzyl alcohol (from a 0.97 M solution in toluene); <sup>b</sup> calculated by <sup>1</sup>H NMR; <sup>c</sup>  $\times 10^3$  <sup>d</sup>  $M_n$  measured =  $0.58 \times M_n$  (GPC  $\times 10^3$ ).<sup>19</sup> <sup>e</sup> Polydispersity index.

The results showed that the less sterically hindered complex **1** had the highest rates of conversion (> 90 %, run 1) in comparison to its imido-alkoxide counterparts, complexes **3** and **4** ( $\leq 46$  %, runs 2 and 3, respectively). Due to complexes **3** and **4** essentially being isostructural, we can infer that the presence of the bulkier alkoxide in **4** (<sup>t</sup>Bu) is the reason for the poorer conversion compared with **3** (<sup>n</sup>Pr). Also given the propagating polymeric chain is bulkier than a *tert*-butyl group, the smaller the groups around the metal centre, the more beneficial the effect regarding the initiation step of the polymerisation.

As mentioned in the introductory chapter, there are limited reports in the literature for the use of vanadium in the ring opening polymerisation of  $\epsilon$ -caprolactone.<sup>3,20</sup> Arbaoui *et al.* observed conversions of  $\sim 60$  % at 40 °C after 24 h, with molecular weights of *ca.* 11,000 and a polydispersity index of 1.1 when using complex **XIV**. The polydispersity index values for polymers produced from complexes **1**, **3** and **4** are similar to those observed with complex **XIV** (PDI  $\sim 1.1$ ). This is indicative with the polymerisation occurring without side reactions. The molecular weights for the less sterically hindered complexes (**1** and **3**) were similar to those produced for complex **XIV** ( $M_w$ 's between 12,000–13,000). However, the molecular weights of the polymers produced by **4** ( $M_w \leq 5000$ ) are analogues with Atlamsani and co-workers reports on heteropolyacids based on vanadium and molybdenum,  $\text{VO}(\text{SO}_4)$  and  $\text{VO}(\text{acac})_2$ . The heteropolyacid complexes and  $\text{VO}(\text{SO}_4)$  oligo( $\epsilon$ -caprolactone) with molecular weights of 4,900 g/mol with polydispersity index of approximately 1.7.

### 3. Conclusion

A new family of 1,3-depleted calix[4]arene complexes incorporating either an alkoxide or imido-alkoxide vanadium(V) centres have been synthesised and structurally analysed. All complexes were investigated for their effectiveness as ethylene polymerisation catalysts. The choice of co-catalyst, either DMAC or MADC, has little or no overall effect on the activity of the pro-catalyst. The concentration of the chosen co-catalyst has a dramatic result on polymerisation activity, with a general observed trend of increasing co-catalyst correlating with increasing pro-catalyst activity. All pro-catalysts were shown to be highly active for the polymerisation of ethylene under the utilised conditions.<sup>21</sup> Unfortunately, such activities were not matched under more robust industrial conditions ( $\leq 30$  g/mmol.h.bar).

The imido-alkoxide vanadium(V) complexes and dinuclear alkoxide complexes were also screened for their ability for  $\epsilon$ -caprolactone polymerisation. The conversion value was dictated by the steric hinderance on the vanadium(V) metal centre. The highest conversion ( $> 90$  %) observed for the alkoxide ligand with *n*-propoxide, and the lowest conversion ( $\sim 20$  %) for the imido-alkoxide ligand with *tert*-butoxide. The less sterically hindered *n*-propoxide complexes were able to produce polymers with higher molecular weights, in comparison to the more sterically *t*-butoxide complex. All pro-catalysts produced low molecular weight polymers with low polydispersity values comparable to literature reports.<sup>3, 20</sup> However, the overall conversion rates can be viewed as low when compared to literature reviews.<sup>1c</sup>



- 
- 1 a) V. Busico, *Dalton Trans.*, 2009, 8794 b) D. Takeuchi, *Dalton Trans.*, 2010, 311  
c) A. Arbaoui, C. Redshaw, *Polym. Chem.* 2010, **1**, 801
  - 2 C. Redshaw, M. Rowan, D. M. Homden, M. R. J. Elsegood, T. Yamato, C. Perez-Casas, *Chem. Eur. J.*, 2007, **13**, 10129
  - 3 A. Arbaoui, C. Redshaw, D. M. Homden, J. A. Wright, M. R. J. Elsegood, *Dalton Trans.*, 2009, 8911
  - 4 a) C. Redshaw, L. Warford, S. H. Dale, M. R. J. Elsegood, *Chem. Commun.*, 2004, 1954 b) C. Redshaw, *Dalton Trans.*, 2010, **39**, 5595
  - 5 D. M. Homden, C. Redshaw, *Chem. Rev.*, 2008, **108**, 5086
  - 6 a) S. Kennedy, G. Karotsis, C. M. Beavers, S. J. Teat, E. K. Brechin, S. J. Dalgarno, *Angew. Chem. Int. Ed.*, 2010, **49**, 4205 b) A. Wei, S. L. Tripp, J. Liu, T. Kasama, R. E. Dunin-Borkowski, *Supramolecular Chem.*, 2009, **21**, 189
  - 7 a) K. Langa, J. Mosinger, D. M. Wagnerová, *Coord. Chem. Rev.*, 2004, **248**, 321 b) T. -L. Kao, C. -C. Wang, Y. -T. Pan, Y. -J. Shiao, J. -Y. Yen, C. -M. Shu, G. -H. Lee, S. -M. Peng, W. -S. Chung, *J. Org. Chem.*, 2005, **70**, 2912 c) V. Lamare, J. F. Dozol, S. Fuangswasdi, F. Arnaud-Neu, P. Thuéry, M. Nierlich, Z. Asfari, J. Vicens, *J. Chem. Soc., Perkin Trans.*, 1999, **2**, 271
  - 8 a) I. -T. Ho, J. -H. Chu, W. -S. Chung, *Eur. J. Org. Chem.*, 2011, 1472 b) C. Han, H. Li, *Anal. Bioanal. Chem.*, 2010, **397**, 1437 c) I. Leray, B. Valeur, *Eur. J. Inorg. Chem.*, 2009, 3525
  - 9 a) Y. -J. Liu, J. -S. Huang, S. S. -Y. Chui, C. -H. Li, J. -L. Zuo, N. Y. Zhu, C. -M. Che, *Inorg. Chem.*, 2008, **47**, 11514 b) C. -Q. Liu, J. B. Lambert, L. Fu, *J. Am. Chem. Soc.*, 2003, **125**, 6452
  - 10 Y. -S. Zheng, A. Ji, X. -J. Chen, J. -L. Zhou, *Chem. Commun.*, 2007, 3398
  - 11 a) Y-S. Zheng, L-Q. Ying, Z-Q. Shen, *Polymer*, 2000, **41**, 1641 b) J. Ling, Z. Shen, W. Zhu, *J. Polym. Sci. A*, 2003, **41**, 1390 c) Y. Chen, Y. Zhang, Z. Shen, R. Kou, L. Chen, *Eur. Polym. J.*, 2001, **37**, 1181 d) O. V. Ozerov, N. P. Rath, F. T. Ladipo, *J. Organomet. Chem.*, 1999, **586**, 223 e) C. Capacchione, P. Neri, A. Proto, *Inorg. Chem. Comm.*, 2003, **6**, 339 f) C. Huang, J. Ahn, S. Kwon, J. Kim, J. Lee, Y. Han, H. Kim, *Applied Cat A*, 2003, **258**, 173 g) L. Giannini, A. Caselli, E. Solari, C. Floriani, A. C.-Villa, C. Rizzoli, *Chem. Bio.*, Oxford University Press, Oxford, 1999 h) L. Giannini, A. Caselli, E. Solari, C. Floriani, A. C-Villa, C. Rizzoli, N. Re, A. Sgamellotti, *J. Am. Chem. Soc.*, 1997, **119**, 9198 i) R. A. Kemp, D. S. Brown,

- M. Lattman, J. Li, *J. Mol. Catal. A.*, 1999, **149**, 125 j) C. Limberg, *Inorg. Chem. Eur. J.*, 2007, **21**, 3303 k) M. Frediani, D. Semeril, M. Dominique, F. Rizzolo, A. M. Papini, P. Frediani, L. Rosi, *Int. J. Polym. Sci.*, 2010, **2010**, 1 l) C. Redshaw, D. M. Homden, D. L. Hughes, J. A. Wright, M. R. J. Elsegood, *Dalton Trans.*, 2009, **7**, 1231
- 12 F. Grynszpan, Z. Goren, S. E. Biali, *J. Org. Chem.*, 1991, **56**, 532
- 13 E. Tzadka, I. Goldberg, A. Vigalok, *Chem. Commun.* 2009, 2041
- 14 United States Patent, Nagy S., Patent No. US 6,984,599 B2, Jan 10, 2006
- 15 J. Espinas, U. Darbost, J. Pelletier, E. Jeanneau, C. Duchamp, F. Bayard, O. Boyron, J. Thivolle-Cazart, J.-M. Basset, M. Taoufik, I. Bonnamour, *Eur. J. Inorg. Chem.*, 2010, **9**, 1349
- 16 A. Arbaoui, PhD Thesis, *University of East Anglia*, 2009
- 17 P. J. Toscano, E. J. Schermerhorn, C. Dettelbacher, D. Macherone, J. Zubieta, *J. Chem. Soc., Chem. Commun.*, 1991, 933
- 18 S. Nagy (Lyondell Chemical Company), Personal Communication
- 19 A. Kowalski, A. Duda, S. Penczek, *Macromolecules*, 1998, **31**, 2114
- 20 Y. Mahha, A. Atlamsani, J.-C. Blais, M. Tessier, J.-M. Bregeault, L. Salles, *J. Mol. Catal. A: Chem.*, 2005, **234**, 63
- 21 V. C. Gibson, G. J. P. Britovsek, D. F. Wass, *Angew. Chem. Int. Ed.*, 1999, **38**, 428

## **Chapter 3**

### **Oxovanadium(V) complexes bearing sulfur-bridged calix[4]arenes**

## 1. Introduction

As mentioned previously (Chapter 2, section 1), calixarenes are emerging as a versatile class of ligands.<sup>1</sup> This is mainly due to their flexibility and ease with which the ligand backbone can be altered. Varying the functionality on the lower rim of calix[4]arene in the ‘cone’ confirmation was described in Chapter 2. The possibility of altering the linking groups between the phenol rings has been proven to be beneficial when compared against unmodified calix[4]arene systems (Figure 19). For example, the Redshaw group have experienced great success in the past by altering the methylene linkers to form oxacalixarenes (complex **III**, Chapter 1).<sup>2</sup> These systems showed dramatic improvements as vanadium-based ethylene polymerisation catalysts. In this chapter, the main focus will be on thia, sulfinyl or sulfonyl calix[4]arene ligands (X = S, SO or SO<sub>2</sub>, respectively).

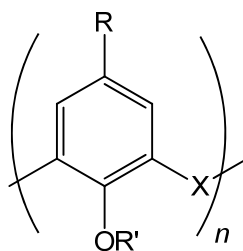


**Figure 19.** Calix[*n*]arene (Typically, R = H, alkyl, aryl, NH<sub>2</sub>, CO<sub>2</sub>H; R' = H, alkyl; X = CH<sub>2</sub>, CH<sub>2</sub>OCH<sub>2</sub>, S, NR).

In recent years, a number of reviews have been published regarding the chemistry of thiacalixarenes, varying from their synthesis to their application.<sup>3</sup> Sano *et al.* first reported a multi-step synthesis to produce thiacalixarenes.<sup>4</sup> In the same year, Miyano and co-workers reported a simpler one-step method for producing thiacalix[4]arene in higher yields by reacting calix[4]arene with sulfur.<sup>5</sup> From this, the sulfur-oxidised relatives of *p-tert*-butyl-sulfinylcalix[4]arene and *p-tert*-butyl-sulfonylcalix[4]arene may be prepared.<sup>6</sup> Like the oxacalixarenes, thiacalixarenes show distinctly different behaviour from their methylene-linked calixarene relatives. This is due to the linking sulfur moieties having different electronic and structural characteristics compared to the methylene bridges. Therefore, it is assumed that thiacalixarenes would infer new properties in metal-based systems compared to the more conventional calixarene class as host molecules.<sup>3e</sup>

As discussed in Chapter 2, section 1, calixarenes can have various functionalities attached to the lower and upper rim of the calixarene, this is also true for thiacalixarenes. However in this section only *p*-*tert*-butylthiacalix[4]arene will be discussed.

Like their calixarene counterparts, thiacalixarenes also possess great flexibility within the calixarene framework, this enables various conformations to be formed. Thiacalix[4]arene forms the same conformations as calix[4]arene. Figure 20 shows four possible conformations for the calix[4]arene moiety.

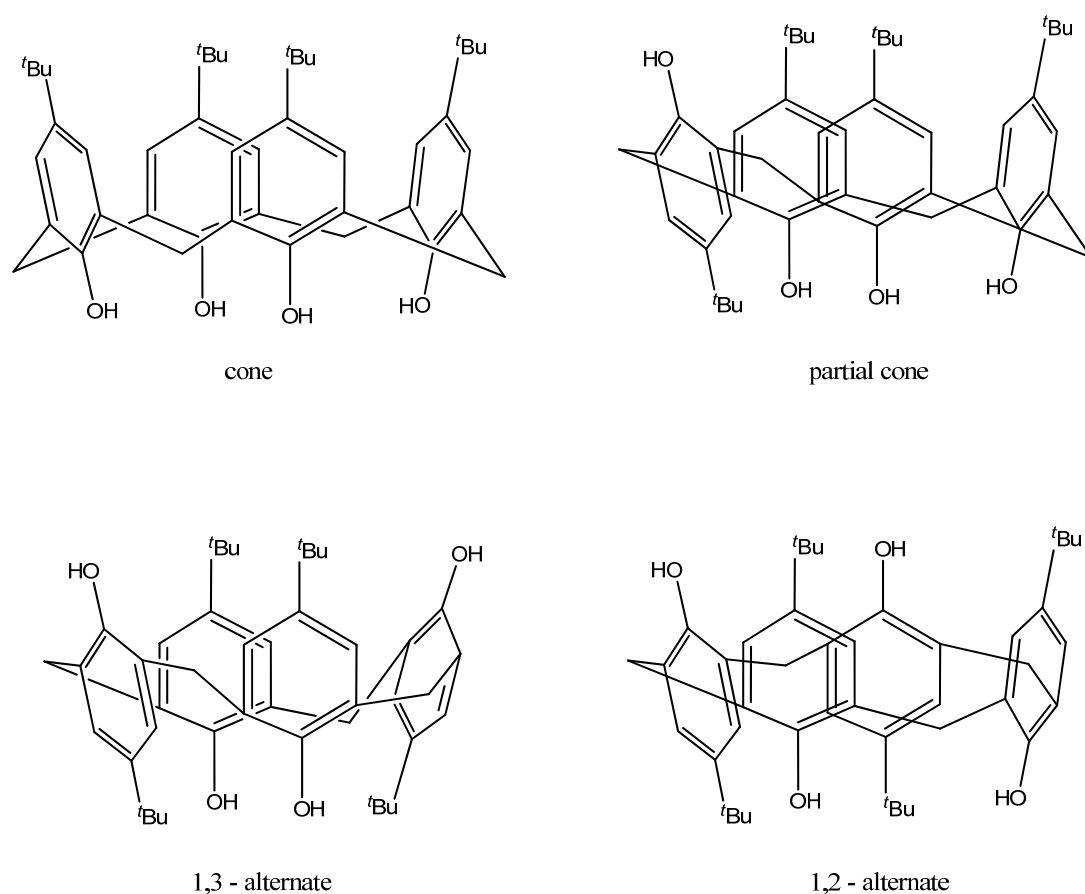


**Figure 20.** Four conformations of calix[4]arene.

In the majority of cases the methylene-bridged calix[4]arene behaves as a tetradentate ligand, bonding to a metal ion through the phenolic oxygen atoms.<sup>7</sup> However for thiacalixarenes, the C-S bonds are longer than the bridging methylene linkers in calix[4]arene, and the additional donating sulfur atoms in the linkers, means there is potential for four chelating sites within the lower cavity of the thiacalix[4]arene ring (Figure 21).<sup>3e</sup>

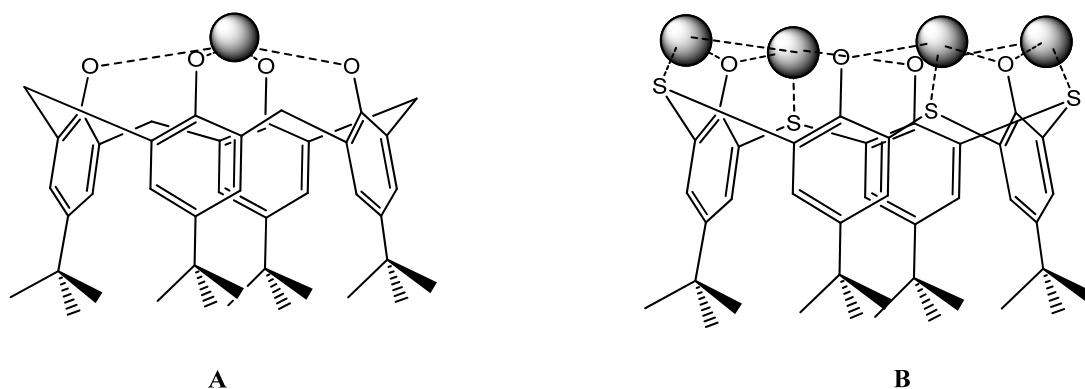


**Figure 21.** A) Mono-nuclear tetra-anionic calix[4]arene system. B) Tetra-nuclear tetra-anionic thiacalix[4]arene complex.

Thiacalixarenes have been utilised for various applications; modified thiacalixarenes have been used for environmental applications such as removing small chlorinated organic molecules from water.<sup>8</sup> Miyano and co-workers noted that the thiacalixarene moieties showed superior selectivity in comparison to the corresponding methylene-bridged analogues used within the study. Thiacalixarenes have shown high affinity for complexing metals; because of this they have been used for the separation and removal of heavy-metal ions ( $\text{Co}^{2+}$ ,  $\text{Ni}^{2+}$ ,  $\text{Cu}^{2+}$ ,  $\text{Zn}^{2+}$ ) in water and as pre-column chelating reagents for HPLC. Interestingly, they do not retain the alkaline-earth-metal ions  $\text{Mg}^{2+}$  and  $\text{Ca}^{2+}$ .<sup>9</sup> Kaiwara and co-workers investigated the use of thia and sulfonylcalixarenes for the removal and separation of metal ions, such as copper and lanthanides.<sup>10</sup> Due to the ease at which thiacalixarene metal complexes can be synthesised, potassium salts have been produced which show the capacity to absorb several guest molecules, such as methanol.<sup>11</sup> Lanthanide complexes were capable of energy-transfer luminescence, which can be applied to dye lasers and luminescent probes because of their long lifetimes and narrow emission bands.<sup>12</sup> A dinuclear titanium complex of the -S- bridged ligand set has been employed as a Lewis acid catalyst in the Mukaiyama-aldol reaction of aryl aldehydes with silyl enol ethers,<sup>13</sup> and as a catalyst in the cyclotrimerization of alkynes.<sup>14</sup> Regarding polymerisation catalysis, there is only one publication which studies di-nuclear titanium *p*-*tert*-butylthiacalixarenes. The synthesised pro-catalysts showed poor activity ( $\leq 25$  g/mmol.h.bar) in the presence of methylaluminoxane (MAO) over a temperature range of 0-50 °C; however the produced polymer had broad molecular weight distributions (PDI 2.6-41.3).<sup>15</sup>

### 1.1 Vanadium thiacalixarenes

To date, there are no reports of vanadium complexes with either the thia, sulfinyl or sulfonylcalix[4]arene ligand being used for either ethylene or  $\epsilon$ -caprolactone polymerisation. However, research has been conducted on various vanadyl complexes utilising sulfur bridged phenolate ligands for the polymerisation of ethylene.<sup>16, 17</sup> In 2000 Miyatake reported the use of vanadium and titanium catalysts, bearing thio- and sulfonyl-bridged bisphenolates, for the synthesis of ultra-high-molecular-weight poly( $\alpha$ -olefin)s.<sup>16</sup> However the titanium complexes displayed greater activities than the vanadium species for the polymerisation of ethylene ( $\leq 3,090$  g/mmol.h.). When comparing activities between the titanium complexes bearing the sulfonyl linker and thia linker, the sulfonyl group appeared to have a detrimental effect on the activity of the catalyst, when in the presence of various co-catalysts (*e.g.* MAO).

Homden and co-workers observed high activities for complex **XV** ( $\leq 33,040$  g/mmol.h.bar) when in the presence of DMAC and the re-activator ETA (Figure 22).<sup>17</sup> When screened under the same conditions, pro-catalysts **XV** and **XVII** produced approximately the same levels of activity ( $\sim 20,000$  g/mmol.h.bar), showing no obvious beneficial effect by having the donating oxygen being present in the bridge. The highest activities were observed when employing 20000 equivalents of DMAC at 60 °C. These activities were surpassed when the pro-catalyst contained both a chelating ligand and a vanadyl group. It was noted that there was a significant drop in activities when the polymerisations were carried out in the presence of either MAO or TMA.

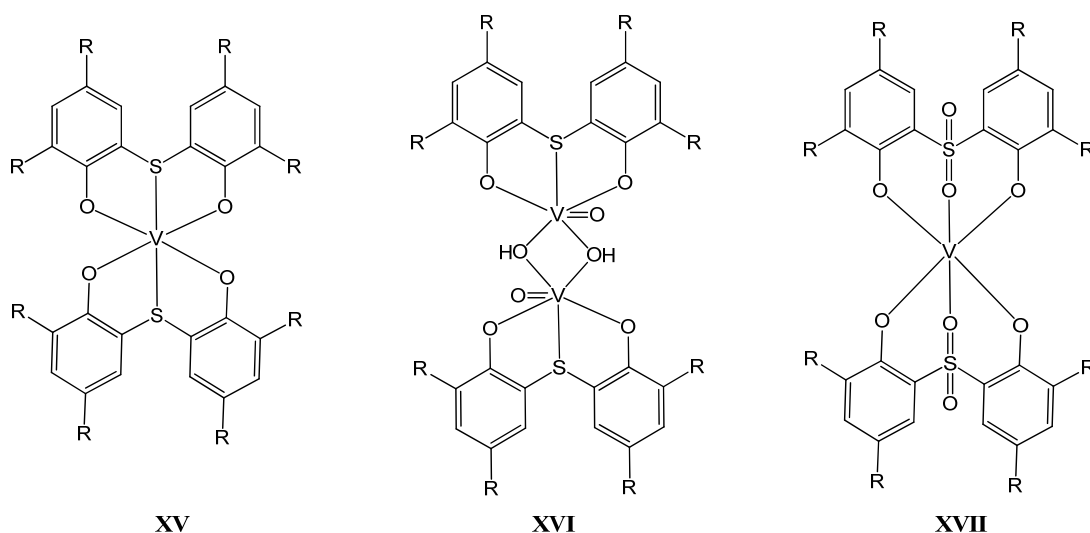


**Figure 22.** Vanadium(IV and V) complexes bearing sulfur-bridged phenolate ligands.

Limberg *et al.* have investigated the use of oxovanadium calixarene complexes, including thiacalixarenes, for the oxidative dehydrogenation (ODH) of light alkanes and methanol.<sup>1c, 18</sup> One of the complexes involved in their study was a mono-nuclear vanadium thiacalix[4]arene complex **XVIII** (Figure 23).

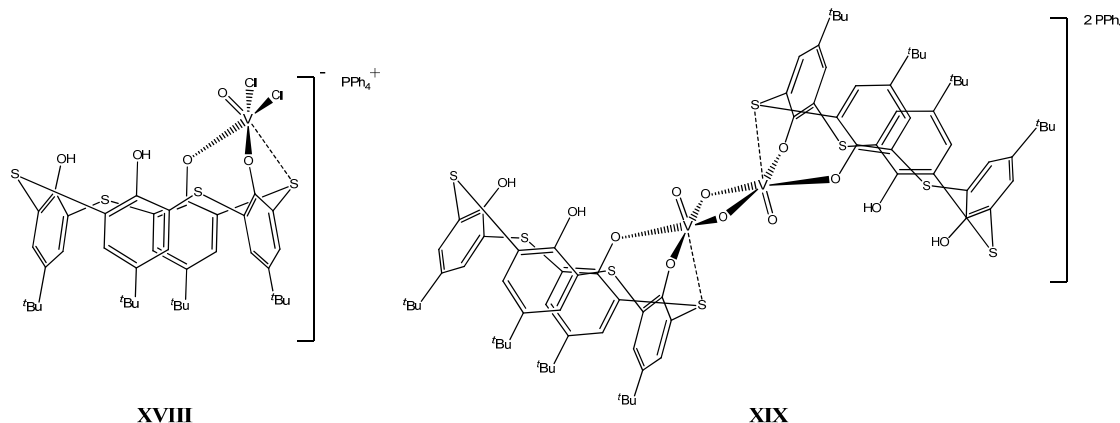


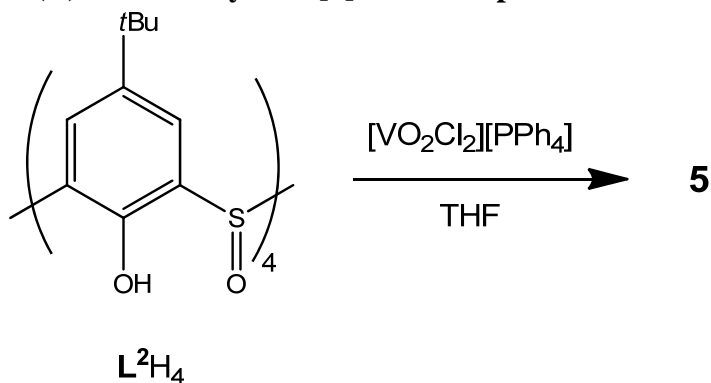
**Figure 23.** Oxovanadium(V) tetrathiacalix[4]arene complexes, **XVIII** and **XIX**.

Limberg and co-workers observed that complex **XIX** showed higher activities than **XVIII**, however both catalysts showed improved activities in comparison to oxovanadium(V) complexes containing ‘classical’ calixarene ligands.

Building on Limberg’s synthetic methodology, vanadium complexes supported by sulfonyl and sulfinylcalix[4]arene frameworks were prepared herein. These structures, as well as the “Limberg” complex **XVIII**, were screened for their efficiency as ethylene and  $\epsilon$ -caprolactone polymerisation catalysts. It was hoped that like the oxacalix[3]arene systems, improved activities would be observed.

## 2. Results and Discussion

### 2.1 Oxovanadium(V) tetrasulfinylcalix[4]arene complex



**Scheme 14.** Synthesis of oxovanadium(V) tetrasulfinylcalix[4]arene (**5**).



The mono-nuclear complex, **5**, was synthesised following the same method as described by Limberg *et al.* to produce complex **XVIII**.<sup>18</sup> One equivalent of  $[\text{VO}_2\text{Cl}_2][\text{PPh}_4]$  and the *p-tert*-butylsulfinylcalix[4]arene ligand,  $\text{L}^2\text{H}_4$ , were reacted in tetrahydrofuran at room temperature (Scheme 14). Volatile components were removed under vacuum and the dark blue precipitate was extracted into dichloromethane. The solution was layered with hexane and after prolonged standing grey/blue plates were formed. The crystals were suitable for X-ray diffraction studies (Figure 24).

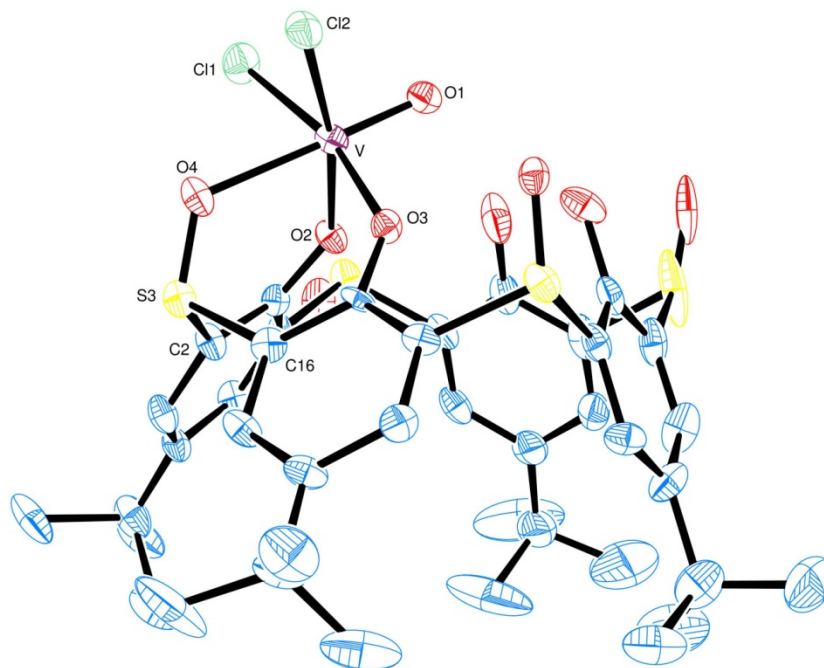
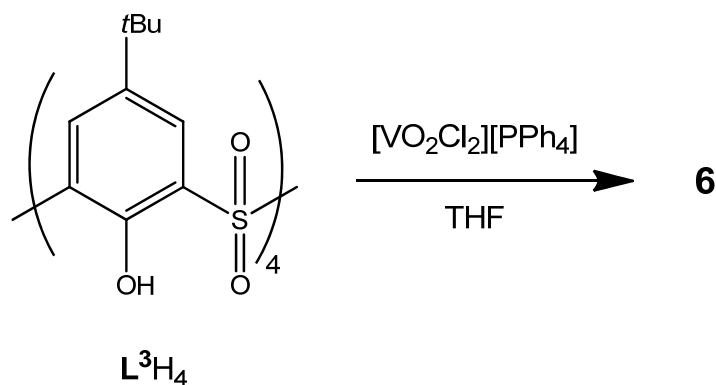


**Figure 24.** The anion  $[\text{VOCl}_2(\text{L}^2\text{H}_2)]^-$  (**5**), indicating the atom numbering scheme. Thermal ellipsoids are drawn at the 30 % probability level. Selected bond lengths (Å) and angles ( $^\circ$ ): V(1)-O(1) 1.933(4), V(1)-O(2) 1.919(4), V(1)-O(9) 1.575(4), V(1)-O(5) 2.192(4), V(1)-Cl(1) 2.293(2), V(1)-Cl(2) 2.2860(18), O(1)-V(1)-O(9) 95.47(18), O(1)-V(1)-Cl(1) 87.45(13), O(1)-V(1)-O(5) 84.85(15), Cl(1)-V(1)-Cl(2) 92.56(7).

The vanadium centre adopts a distorted octahedral geometry with the oxygen of one of the sulfinyl bridges incorporated in the coordination sphere. This oxygen [O(5)] is *trans* to the oxo group [O(9)] and the bond to vanadium is somewhat elongated [V(1)-O(5) 2.192(4) Å] compared with the other V-O bonds (Figure 24), but is similar to other reported V-O(S) bonds.<sup>19</sup> The calixarene ligand retains the cone conformation, and the vanadium centre sits 1.24 Å above the O(1), O(2), O(5) plane. Oxygen atoms O(6), O(7), and O(8) all exhibit conformational disorder with the O atoms predominantly in the ‘out’ position. The minor component lies ‘up’, as does O(5) which does not exhibit

disorder. The structure contains two dichloromethane molecules of crystallisation; one is well defined within the calixarene cone, the other, substantially disordered, lies exo to the cone. The two phenol groups make intramolecular H-bonds.

## 2.2 Oxovanadium(V) tetrasulfonylcalix[4]arene complex



**Scheme 15.** Synthesis of oxovanadium(V) tetrasulfonylcalix[4]arene, **6**.

Oxovanadium(V) tetrasulfonylcalix[4]arene, **6**, was synthesised following an adapted version of Limberg's method used for complex **5** (Scheme 15). *p*-*tert*-Butylsulfonylcalix[4]arene,  $\mathbf{L}^3\mathbf{H}_4$ , and one equivalent of  $[\text{VO}_2\text{Cl}_2][\text{PPh}_4]$  were stirred in tetrahydrofuran. After 48 hours, the volatile components were removed under *vacuo* and the purple/blue residue was extracted into dichloromethane, which was layered with hexane. After prolonged standing at ambient temperature, purple prisms were formed which were suitable for X-ray diffraction (Figure 25).

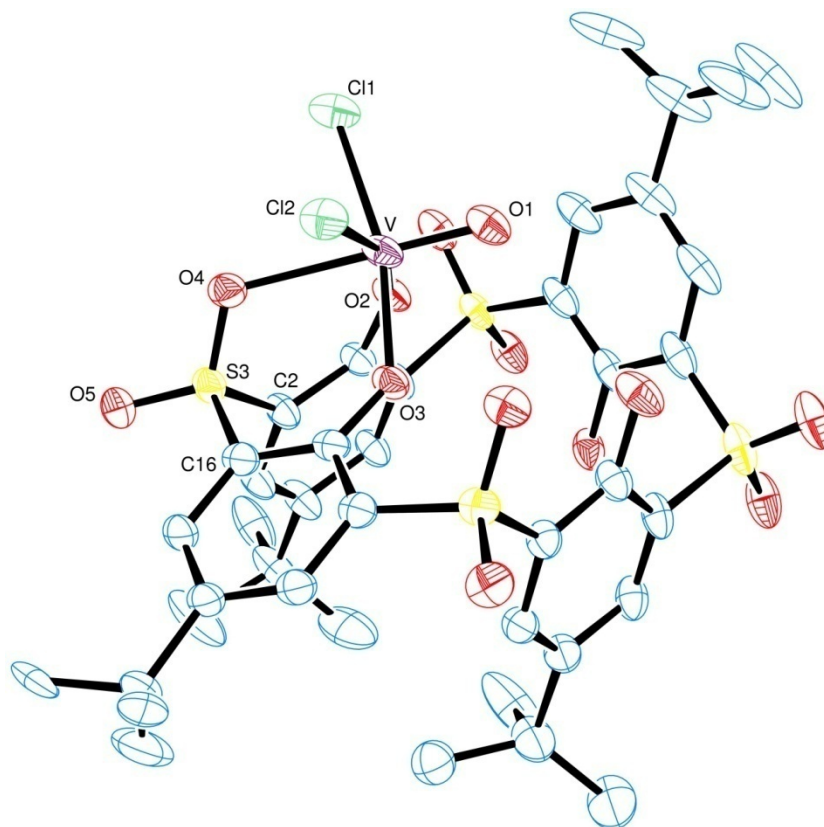


**Figure 25.** View of the anion  $[\text{VOCl}_2(\text{L}^3\text{H}_2)]^-$  (**6**), indicating the atom numbering scheme. Minor disorder components have been omitted for clarity. Thermal ellipsoids are drawn at the 30 % probability level. Selected bond lengths (Å) and angles (°): V(1)-O(1) 1.895(3), V(1)-O(2) 1.937(3), V(1)-O(5) 2.357(3), V(1)-O(9) 1.577(3), V(1)-Cl(1) 2.2771(14), V(1)-Cl(2) 2.2904(12); O(1)-V(1)-O(2) 86.62(12), O(5)-V(1)-O(9) 177.53(13).

In **6**, the coordination of the  $\text{V}=\text{OCl}_2$  unit to the calixarene is very similar to that adopted in **5**. However, the calixarene in **6** adopts an ‘up-up-up-down’ conformation rather than the cone observed in **5**. As in **5** there are two intramolecular H-bonds, but in this case the calixarene conformation facilitates an additional centrosymmetric pair of intermolecular H-bonds between phenol group O(4)-H(4) and one oxygen of an  $\text{SO}_2$  group on a neighbouring molecule (Figure. 26).

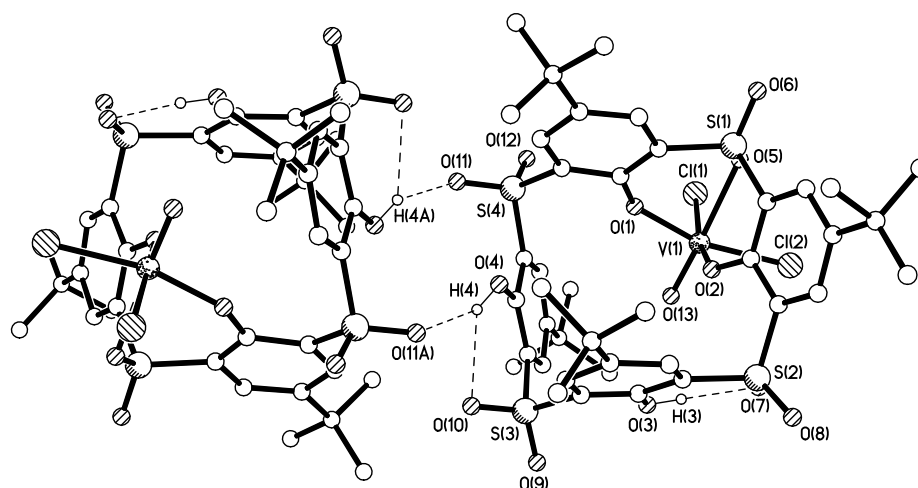


**Figure 26.** View of **6** showing intra- and inter-molecular H-bonding. O(3)–H(3)···O(7), H(3)···O(7) = 1.89Å; O(4)–H(4)···O(10), H(4)···O(10) = 2.24Å; and O(4)–H(4)···O(11A), H(4)···O(11A) = 2.30Å, symmetry operator A =  $-x+2, -y, -z$ .

As in **5**, Limberg's complex **XVIII** (Figure 23, molecular structure Figure 27) contains a calixarene ligand in the cone conformation, and the vanadium metal centre is positioned above the calixarene. However, the vanadium is shifted out of the plane defined by O2, O3, C11 and C12 in the direction of the terminal O1. The observed bond length between the vanadium and terminal oxygen atom, (V–O1 0.3539(9) Å) in **XVIII** is typical for oxo ligands in oxovanadium(V) calixarene complexes.<sup>2, 20</sup> The vanadium is also coordinated to one of the thioethers (S3) with a bond length of 2.7553(16) Å, this is shorter than the van der Waals radii of vanadium and sulfur, indicating a coordinative interaction.<sup>18</sup> It is longer than vanadium-thioether bonds in similar compounds produced by Mattes *et al.* however, Limberg states that this could be due to the *trans* influence from the terminal oxygen (O1).<sup>18</sup> As with complexes **5** and **6**, the vanadium atom in **XVIII** is coordinated within a distorted octahedral environment.

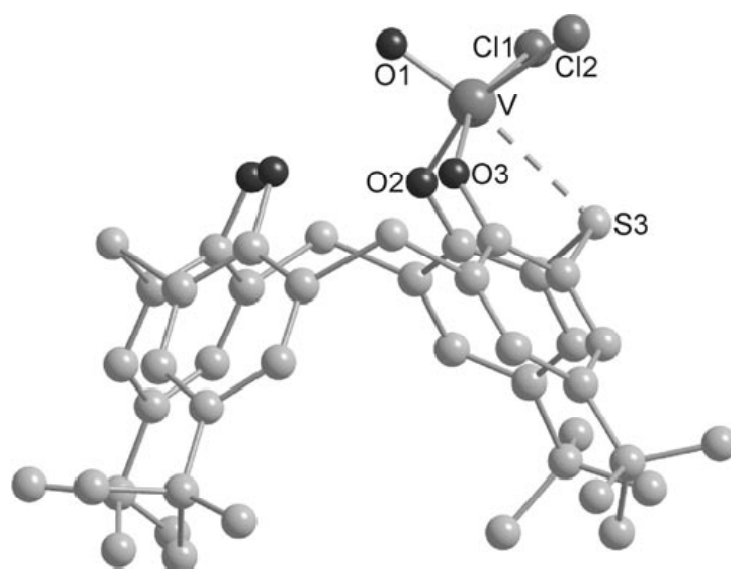


**Figure 27.** View of the anion  $[\text{VOCl}_2(p\text{-tert-butylcalix}[4,\text{S}]\text{areneH}_2)]^-$  (**XVIII**), indicating the atom numbering scheme.

Considering the previously discussed similarities between the three structures, it is worth comparing the structures to observe whether the differing bridges have any effect on the vanadium centres environment. In Table 9, bond lengths and angles between the three compounds are compared.

**Table 9.** Selected bond lengths (Å) and angles (°) for **5** and **6** compared to complex **XVIII**.

	<b>XVIII</b>	<b>5</b>	<b>6</b>
V-O1	1.592(4)	1.575(4)	1.577(3)
V-O2	1.904(4)	1.933(4)	1.895(3)
V-O3	1.877(5)	1.919(4)	1.937(3)
V-O4	-	2.192(4)	2.357(3)
V-Cl1	2.305(2)	2.293(2)	2.2771(14)
V-Cl2	2.308(2)	2.2860(18)	2.2904(12)
V-S3	2.7553(16)	-	-
O1-V-O2	97.18(18)	95.36(17)	-
O1-V-O3	98.81(18)	95.73(73)	86.62(12)
O1-V-Cl1	101.28(15)	97.09(15)	-
O1-V-Cl2	102.06(15)	96.88(14)	-
O1-V-S3	172.50(15)	-	-
O1-V-O4	-	178.98(19)	177.53(13)

The vanadium centre in **5** and **6** is in a similar environment to that observed in complex **XVIII**. The bond lengths and angles in the three structures are analogous to those of **XVIII**, with O4 in **5** and **6** adopting the same position as S3 in **XVIII**, with similar bond lengths and angles.

Due to these structural similarities, Limberg's complex **XVIII** was synthesised, to enable comparison studies between the three complexes for their ability to polymerise ethylene and  $\epsilon$ -caprolactone.

### 2.3 Ethylene polymerisation

Complexes **XVIII**, **5** and **6** were screened for their ability to polymerise ethylene in the presence of either dimethylaluminium chloride (DMAC) or methylaluminium dichloride (MADC) with the re-activating substance ethyl trichloroacetate (ETA). Temperature and equivalent of co-catalyst were also investigated over a 15 minute period to study the effects upon the oxovanadium(V) complexes.

#### 2.3.1 Temperature screening

Complexes **XVIII**, **5** and **6** were screened over a range of temperatures (20-80 °C, Table 10). Complex **XVIII** was screened in the presence of DMAC and MADC with the re-activator ETA. Pro-catalysts **5** and **6** were screened in the presence of MADC with the re-activator ETA. All parameters, such as time, were kept the same for each run allowing for comparisons between pro-catalyst activities. The known highly active pro-catalyst [V(O)*p-tert*-butylhexahomotrioxacalix[3]arene] **III**, was used as a comparison (benchmark).<sup>2</sup> **III** has shown high activities (92,500 g/mmol.h.bar, Chapter 1, section 1.6) surpassing those produced by methylene-bridged calixarenes under the same conditions (1,400 g/mmol.h.bar).

**Table 10.** Results for ethylene polymerisation runs using pro-catalysts **XVIII**, **5** and **6**.<sup>a</sup>

Run	Pro-catalyst ( $\mu\text{mol}$ )	Co-catalyst	Temp ( $^{\circ}\text{C}$ )	Yield PE(g)	Activity <sup>b</sup> ( $\times 10^3$ )
1	<b>XVIII</b>	DMAC	20	0.75	12.0
2	<b>XVIII</b>	DMAC	40	0.80	12.8
3	<b>XVIII</b>	DMAC	60	0.86	13.8
4	<b>XVIII</b>	DMAC	80	0.74	11.8
5	<b>XVIII</b>	MADC	20	1.05	16.8
6	<b>XVIII</b>	MADC	40	1.33	21.3
7	<b>XVIII</b>	MADC	60	1.63	26.1
8	<b>XVIII</b>	MADC	80	1.20	19.2
9	<b>5</b>	MADC	20	1.72	27.5
10	<b>5</b>	MADC	40	1.27	20.3
11	<b>5</b>	MADC	60	2.22	35.4
12	<b>5</b>	MADC	80	2.32	37.4
13	<b>6</b>	MADC	20	1.61	25.7
14	<b>6</b>	MADC	40	2.00	31.9
15	<b>6</b>	MADC	60	2.77	44.4
16	<b>6</b>	MADC	80	2.33	37.4

<sup>a</sup>0.25  $\mu\text{mol}$  pro-catalyst, 6000 [Al]:[V], 1 bar ethylene Schlenk tests carried out in toluene (200 mL) in the presence of ETA (0.05 mL) over 15 min, reaction was quenched with dilute HCl, washed with methanol (50 mL) and dried for 12 h. at 80  $^{\circ}\text{C}$ . <sup>b</sup>g/mmol.h.bar.

Due to the moderate activities observed with **XVIII** when using DMAC as co-catalyst ( $\leq 11800$  g/mmol.h.bar, runs 1-4), it was decided to screen **5** and **6** only with MADC/ETA. All pro-catalysts showed very high activities in the presence of MADC (26,100-44,400 g/mmol.h.bar, runs 7, 12 and 15).<sup>21</sup> **5**/MADC exhibited activities comparable with those of **XVIII**/MADC, with enhanced thermal stability (run 12). Due to **XVIII** and **6** observing optimised temperatures at 60  $^{\circ}\text{C}$ , a run was conducted at 60  $^{\circ}\text{C}$  using the known pro-catalyst [V(O)*p-tert*-butylhexahomotrioxacalix[3]arene] **III**,<sub>2</sub> as a benchmark for activity. All four pro-catalysts were screened under the same conditions, 6000 equivalents MADC, 15 minutes, to compare the effect the calixarene linker has on the activity of the oxovanadium(V) pro-catalyst (Figure 28).

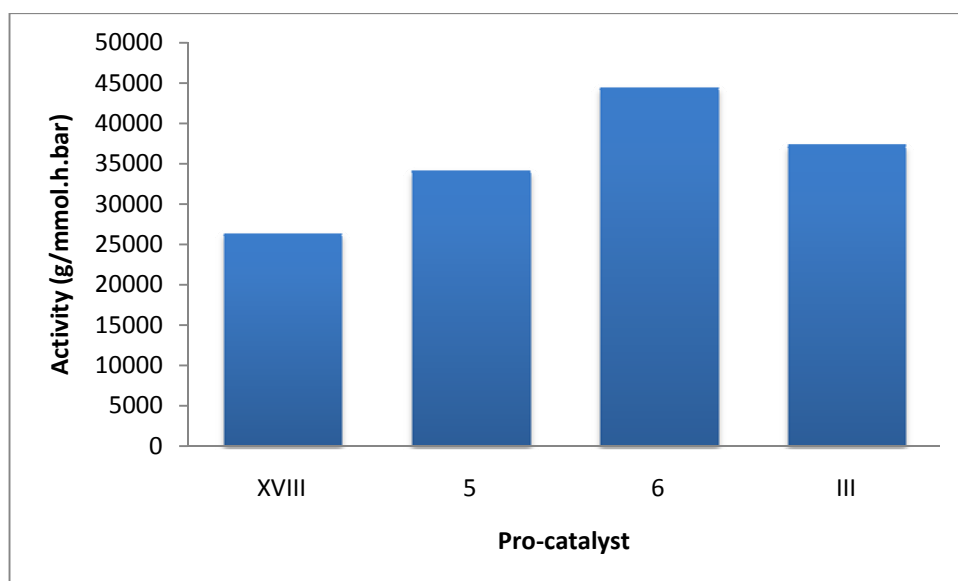


**Figure 28.** The activities of the four pro-catalysts, screened under the same polymerisation conditions. (Conditions; 0.25  $\mu\text{mol}$  pro-catalyst, 6000 [MADC]:[V], 1 bar ethylene Schlenk tests carried out in toluene (200 mL) in the presence of ETA (0.05 mL), at 60  $^{\circ}\text{C}$ , over 15 min).

The comparative screening study of pro-catalysts **XVIII**, **5**, **6** and **III** under the same conditions (60  $^{\circ}\text{C}$  and 6000 equivalents of MADC, Figure 28) led to the observed activity order **6**>**III**>**5**>**XVIII**. The sulfonyl-bridged ligand set, **6**, promoted the highest observed activities. It is thought that this sulfonyl ligand set is able to stabilise the active species through O  $\rightarrow$  V interactions. Such stabilisation is also possible in the systems using **2** and **4**, but not in that employing pro-catalyst **1**.

Selected polymer data from temperature runs in Table 10 are shown in Table 11. All pro-catalysts afforded high molecular weight, linear polyethylene; typical melting points by DSC were in the range of 138-140  $^{\circ}\text{C}$  for runs from Figure 28. From Table 11, it is evident that there is a direct correlation between temperature and the produced polymers molecular weight; at higher temperatures the molecular weight decreases. The highest molecular weights (1,140,000 and 994,000, for runs 9 and 14, respectively) being associated with 40  $^{\circ}\text{C}$ . The range of PDIs measured was in the range 2.7-6.5, the lowest being observed at higher temperatures (80  $^{\circ}\text{C}$ ).



**Table 11.** Selected results for ethylene polymerisation runs using pro-catalysts **XVIII**, **5** and **6**.<sup>a</sup>

Run	Pro-catalyst	Co-catalyst	Temp (°C)	$M_w^b$	$M_n^c$	PDI <sup>d</sup>
6	<b>XVIII</b>	MADC	60	4.01	1.03	3.9
9	<b>5</b>	MADC	40	11.4	17.3	6.5
14	<b>6</b>	MADC	40	9.94	2.31	4.3
16	<b>6</b>	MADC	80	1.30	0.49	2.7

<sup>a</sup>1 bar ethylene Schlenk tests carried out in toluene (200 mL) in the presence of ETA (0.05 mL) over 15 min, reaction was quenched with dilute HCl, washed with methanol (50 mL) and dried for 12 h. at 80 °C.

<sup>b</sup> Weight average molecular weight ( $\times 10^5$ ). <sup>c</sup> Number average molecular weight ( $\times 10^5$ ). <sup>d</sup> Polydispersity index.

### 2.3.2 Equivalent of co-catalyst

The effect of varying the type of co-catalyst and concentration of co-catalyst was investigated to note if there would be an overall impact on the activity of the pro-catalysts. Temperature, time and pro-catalyst concentration were all kept constant to enable comparisons between the performances of the three pro-catalysts made.

**Table 12.** Results for ethylene polymerisation runs using pro-catalysts **XVIII**, **5** and **6**.<sup>a</sup>

Run	Pro-catalyst	Co-catalyst	[Al]:[V]	Yield PE(g)	Activity <sup>c</sup> ( $\times 10^3$ )
1 <sup>b</sup>	<b>XVIII</b>	DMAC	2000	0.39	3.1
2 <sup>b</sup>	<b>XVIII</b>	DMAC	4000	0.96	7.7
3 <sup>b</sup>	<b>XVIII</b>	DMAC	6000	2.00	16.0
4 <sup>b</sup>	<b>XVIII</b>	DMAC	8000	1.84	14.7
5	<b>XVIII</b>	MADC	2000	0.07	1.1
6	<b>XVIII</b>	MADC	4000	0.53	8.5
7	<b>XVIII</b>	MADC	6000	1.2	19.2
8	<b>XVIII</b>	MADC	8000	1.09	17.4
9	<b>5</b>	DMAC	6000	0.01	0.2
10	<b>5</b>	DMAC	8000	0.06	1.0
11	<b>5</b>	MADC	4000	0.12	1.8
12	<b>5</b>	MADC	8000	1.58	25.3
13	<b>6</b>	DMAC	2000	0.40	6.4
14	<b>6</b>	DMAC	4000	1.27	20.3
15	<b>6</b>	DMAC	6000	1.26	20.1
16	<b>6</b>	DMAC	8000	1.57	25.1
17	<b>6</b>	MADC	2000	0.03	0.4
18	<b>6</b>	MADC	4000	1.31	20.2
19	<b>6</b>	MADC	6000	1.74	27.9
20	<b>6</b>	MADC	8000	1.61	25.7

<sup>a</sup>1 bar ethylene Schlenk tests carried out at room temperature, in toluene (200 mL) in the presence of ETA (0.05 mL) over 15 min, reaction was quenched with dilute HCl, washed with methanol (50 mL) and dried for 12 h. at 80 °C. <sup>b</sup> in toluene (150 mL) in the presence of ETA (0.1 mL). <sup>c</sup>g/mmol.h.bar.

In the case of pro-catalyst **XVIII** /DMAC, varying the [Al]:[V] ratio at 20 °C led to an increase from about 3,000 g/mmol.h.bar (run 1) at 2000:1 to 16,000 g/mmol.h.bar (run 3) at 6000:1. Further increases in the [Al]:[V] ratio were detrimental to the observed activity. In the case of MADC, similar trends were observed, with somewhat higher optimised observed activities (runs 7 and 8). In the case of pro-catalyst **5**, activities using DMAC were unimpressive (< 1,000 g/mmol.h.bar), and so this system was not studied further. By contrast, **5**/MADC exhibited activities comparable with those of

**XVIII**/MADC. Pro-catalyst **6**/DMAC exhibited impressive activities which improved on increasing the [Al]:[V] ratio (runs 13 – 16). In the case of pro-catalyst **6**/MADC, the activities peaked at a [Al]:[V] ratio of 6000:1 (run 19); use of  $\leq 2000$  equivalents of MADC led to a dramatic reduction in the observed activity (run 17).

As mentioned in Chapter 2, calixarenes can be viewed as cyclic analogues of phenolates. Homden and co-workers observed that there was no beneficial effect when comparing the thia (**XV**) and sulfonyl (**XVII**) phenolate complexes (20,500 vs. 21,600 g/mmol.h.bar, respectively, chapter 3, section 1.1).<sup>16</sup> Whereas the above results have shown that when utilising the calixarene moieties, the presence of donating oxygens in the calixarene linkers increase the pro-catalysts observed activities.

Complexes **XVIII**, **5** and **6** were also screened for their ability to polymerise  $\epsilon$ -caprolactone under various conditions, such as altering temperature (20–80 °C), time (12–72 hours) and varying the equivalent of benzyl alcohol (0 to 5 eq.). However, these systems, under the conditions employed (monomer:metal (400:1); 25–80 °C; 20 mL toluene) were inactive.

Ring opening polymerisation by the coordination/insertion method (Chapter 1, section 2.3.3) occurs *via* the  $\epsilon$ -caprolactone monomer undergoing nucleophilic attack from the metal alkoxide species. However, the oxovanadium(V) systems discussed (**XVIII**, **5** and **6**) do not possess an alkoxide species. To try and overcome this, a co-initiator (*e.g.* benzyl alcohol) was added to the polymerisation solutions. The lack of polymer suggests that due to the anionic nature of the oxovanadium complexes, the alcohol is unable to produce the active alkoxide species through nucleophilic attack of the vanadium metal centre, which in turn prevents the initiation step of the polymerisation from occurring.

### 3. Conclusion

Following on from the work of Limberg on a oxovanadium thiacalix[4]arene complex, two new vanadyl complexes have been synthesised utilising sulfinyl and sulfonyl calix[4]arenes, producing a family of sulfur-bridged oxovanadium complexes. All complexes have been synthesised and fully characterised. They have then been investigated for their effectiveness as polymerisation catalysts for ethylene. The type of co-catalyst, molar equivalents of co-catalyst and temperature for polymerisation screening were investigated. MADC was proven to give the highest activities for all

three pro-catalysts. Elevated temperatures (60 °C) gave the highest activities and the lowest PDI values for the produced polymers. However, high temperatures also proved detrimental to polymer molecular weight, with the highest molecular weights being observed at 40 °C. The sulfonyl system gave the highest activities in comparison to the thia- and sulfinyl- calix[4]arene systems. This is thought to be due to the beneficial effect of the donating oxygen atoms present on the linkers between the phenolic units of the calixarene, stabilising the vanadium centre through O → V interactions. Under the conditions used, the sulfonyl pro-catalyst out-performed the [V(O)*p*-*tert*-butylhexahomotrioxacalix[3]arene] (**III**), 44,400 vs. 37,300 g/mmol.h.bar, respectively. Unfortunately, under the conditions screened all three systems showed to be inactive for  $\epsilon$ -caprolactone polymerisation.

- 1 a) C. Redshaw, *Coord. Chem. Rev.*, 2003, **244**, 45 b) D. M. Homden, C. Redshaw, *Chem. Rev.*, 2008, **108**, 5086 c) C. Limberg, *Eur. J. Inorg. Chem.*, 2007, 3303
- 2 C. Redshaw, M. A. Rowan, L. Warford, D. M. Homden, A. Arbaoui, M. R. J. Elsegood, S. H. Dale, T. Yamato, C. P. Casas, S. Matsui, *Chem. Eur. J.*, 2007, **13**, 1090
- 3 a) S. Cherenok, V. Kalchenko, *Top. Heterocyc. Chem.*, 2009, **20**, 229 b) H. Tsue, K. Ishibashi, R. Tamura, *Top. Heterocyc. Chem.*, 2008, **17**, 73 c) T. Kajiwara, N. Iki, M. Yamashita, *Coord. Chem. Rev.*, 2007, **251**, 1734 d) W. -S. Zhang, Y. An, R. Liu, B. Gong, L. He, *Mini-Rev. Org. Chem.*, 2007, **4**, 143 e) N. Morohashi, F. Narumi, N. Iki, T. Hattori, S. Miyano, *Chem. Rev.*, 2006, **106**, 5291 f) P. Lhotak, *Eur. J. Org. Chem.*, 2004, **8**, 1675 g) D. C. Gutsche, *Calixarenes*, 2001, 1
- 4 T. Sone, Y. Ohba, K. Moriya, H. Kumada, K. Ita, *Tetrahedron*, 1997, **53**, 10689
- 5 H. Kumagai, M. Hasegawa, S. Miyanari, Y. Sugawa, Y. Sato, T. Hori, S. Ueda, H. Kamiyama, S. Miyano, *Tetrahedron Lett.*, 1997, **38**, 3971
- 6 N. Morohashi, N. Iki, A. Sugawara, S. Miyano, *Tetrahedron*, 2001, **57**, 5557
- 7 a) B. Castellano, E. Solari, C. Floriani, R. Scopeliti, N. Re, *Inorg. Chem.*, 1999, 3406 b) M. Chisholm, K. Folting, W. E. Streib, D. -D. Wu, *Inorg. Chem.*, 1999, **38**, 5219 c) P. D. Beer, G. D. Brindley, O. D. Fox, A. Grieve, M. I. Ogden, F. Szemes, M. G. B. Drew, *J. Chem. Soc., Dalton Trans.*, 2002, 3101 d) U. Radius, J. Attner, *Inorg. Chem.*, 2004, **43**, 8587
- 8 N. Iki, T. Fujimoto, T. Shindo, K. Koyama, S. Miyano, *Chem. Lett.*, 1999, 777
- 9 a) H. Matsumiya, T. Ishida, N. Iki, S. Miyano, *Anal. Chim. Acta.*, 2003, **478**, 163 b) H. Matsumiya, H. Masai, Y. Terazono, N. Iki, S. Miyano, *Bull. Chem. Soc. Jpn.*, 2003, **76**, 133 c) H. Matsumiya, N. Iki, S. Miyano, M. Hiraide, *Anal. Bioanal. Chem.*, 2004, **379**, 867 d) H. Matsumiya, M. Hirade, *Bull. Chem. Soc. Jpn.*, 2005, **78**, 1939
- 10 a) T. Kajiwara, N. Kon, S. Yokozawa, T. Ito, N. Iki, S. Miyano, *J. Am. Chem. Soc.*, 2002, **124**, 11274 b) T. Kajiwara, H. Wu, T. Ito, N. Iki, S. Miyano, *Angew. Chem. Int. Ed.*, 2004, **43**, 1832
- 11 a) K. Endo, Y. Kondo, Y. Aoyama, F. Hamada, *Tetrahedron Lett.*, 2003, **44**, 1355 b) Y. Kondo, K. Endo, F. Hamada, *Chem. Commun.*, 2005, 711

- 12 a) N. Iki, T. Horiuchi, H. Oka, K. Koyama, N. Morohashi, C. Kabuto, S. Miyano, *J. Chem. Soc., Perkin Trans.*, 2001, **2**, 2219 b) T. Horiuchi, N. Iki, H. Oka, S. Miyano, *Bull. Chem. Soc. Jpn.*, 2002, **75**, 2615
- 13 N. Morohashi, T. Hattori, K. Yokomakura, C. Kabuto, S. Miyano, *Tetrahedron Lett.*, 2002, **43**, 7769
- 14 N. Morohashi, K. Yokomakura, T. Hattori, S. Miyano, *Tetrahedron Lett.*, 2006, **47**, 1157
- 15 A. Proto, F. Giugliano, C. Capacchione, *Eur. Polym. J.*, 2009, **45**, 2138
- 16 a) K. Takaoki, T. Miyatake, *Macromol. Symp.*, 2000, **157**, 251 b) M. Fujita, Y. Seki, T. Miyatake, *J. Polym. Sci.: Part A: Polym. Chem.*, 2004, **42**, 1107
- 17 D. M. Homden, C. Redshaw, L. Warford, D. L. Hughes, J. A. Wright, S. H. Dale, M. R. J. Elsegood, *Dalton Trans.*, 2009, 8900
- 18 E. Hoppe, C. Limberg, *Chem. Eur. J.*, 2007, **13**, 7006
- 19 a) R. Mulhaupt, F. G. Sernetz, S. Fokken, J. Okuda, *Macromolecules*, 1997, **30**, 1562 b) C. J. Schaverien, A. Vanderlinden, N. Meijboom, C. Ganter, A. G. Orpen, *J. Am. Chem. Soc.*, 1995, **117**, 3008 c) P. Sobota, Z. Janas, L. B. Jerzykiewicz, K. Przybylak, K. Szczegot, *Eur. J. Inorg. Chem.*, 2004, 1639 d) K. Takaoki, T. Miyatake, *Macromol. Symp.*, 2000, **157**, 251 e) Y. Takashima, Y. Nakayama, T. Hirao, H. Yasuda, A. Harada, *J. Organomet. Chem.*, 2004, **689**, 612 f) Z. Janas, D. Wisniewska, L. B. Jerzykiewicz, P. Sobota, K. Drabent, K. Szczegot, *Dalton Trans.*, 2007, 2065 g) Z. Janas, D. Godbole, T. Nerkowski, K. Szczegot, *Dalton Trans.*, 2009, 8846 h) B. Lian, H. Ma, T.P. Spaniol, J. Okuda, *Dalton Trans.*, 2009, 9033
- 20 a) E. Hoppe, C. Limberg, B. Ziemer, C. Mügge, *J. Mol. Catal. A.*, 2006, **251**, 34 b) E. Hoppe, C. Limberg, B. Ziemer, *Inorg. Chem.*, 2006, **45**, 8308 c) B. Castellano, E. Solari, C. Floriani, R. Scopelliti, N. Re., *Inorg. Chem.*, 1999, **38**, 3406 d) V. C. Gibson, C. Redshaw, M. R. J. Elsegood, *J. Chem. Soc. Dalton Trans.*, 2001, 767
- 21 V. C. Gibson, G. J. P. Britovsek, D. F. Wass, *Angew. Chem. Int. Ed.*, 1999, **38**, 428

## **Chapter 4**

### **Vanadium(III) pro-catalysts bearing phenoxy-imine ligands**

## 1. Introduction

As well as oxacalix[3]arenes proving themselves as beneficial chelating ligands for vanadium-based ethylene polymerisation catalysis, phenoxy-imine based systems have also shown very high activities (Chapter 1, section 1.6).<sup>1</sup> Fujita and co-workers have proven that the ancillary phenoxy-imine (FI) ligand can produce highly active systems for various early transition metals and when exposed to different  $\alpha$ -olefins, which is discussed in numerous reviews.<sup>2</sup>

Initial results showed group IV transition metal complexes bearing phenoxy-imine ligands displayed very high activities in the presence of MAO (550,000 g/mmol.h.bar), for ethylene polymerisation at room temperature and atmospheric ethylene pressure.<sup>3</sup> The FI zirconium(IV) complexes (Figure 29) exhibited activities 20 times greater than previously observed when employing the metallocene catalytic system,  $\text{Cp}_2\text{ZrCl}_2/\text{MAO}$ , under similar conditions.

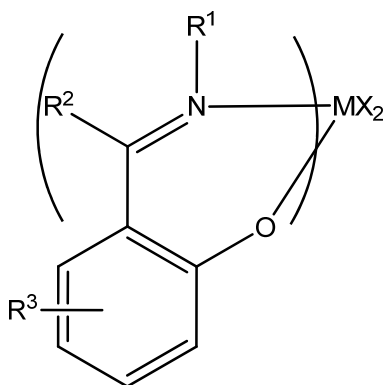


**Figure 29.** Generic formula for phenoxy-imine (FI) complexes. Typically  $M = \text{Zr}, \text{Ti}, \text{Hf}, \text{V}$ ;  $R^1, R^2$  and  $R^3 = \text{H}, \text{alkyl}, \text{aryl}$ ;  $X = \text{Cl}$ .

These results have since been extended by Fujita and other groups, such as Coates *et al.*, by altering substituents on the ligand framework,<sup>2, 4</sup> supporting on  $\text{MgCl}_2$ <sup>1a, 2, 4b, 5</sup> and utilising various other transition metals, such as titanium,<sup>1a-b, 2, 4b, 6</sup> hafnium,<sup>2a,c-d, 4a, 7</sup> nickel<sup>8</sup> and vanadium.<sup>1, 2a,d, 9</sup>

Other  $\alpha$ -olefins have been investigated to see if early phenoxy-imine successes could be repeated beyond ethylene polymerisation, *e.g.* propylene<sup>4b, 6d, 7b, 10</sup> and co-polymerising other  $\alpha$ -olefins with ethylene.<sup>4a,c, 6e, 11</sup> The produced polypropylene had ultra-high molecular weight, with low polydispersities. It was also observed that the regio- and



stereo-chemistry of the polymer could be controlled by the substituents on the pro-catalyst.<sup>7b</sup>

### 1.1 Bridged phenoxy-imine ligands

Due to the successes of the salicylaldiminato systems when utilised for olefin polymerisation catalysis, numerous groups have now built upon Fujita's original work by producing bridged phenoxy-imine systems for numerous applications, including the possibility of observing useful cooperative effects.

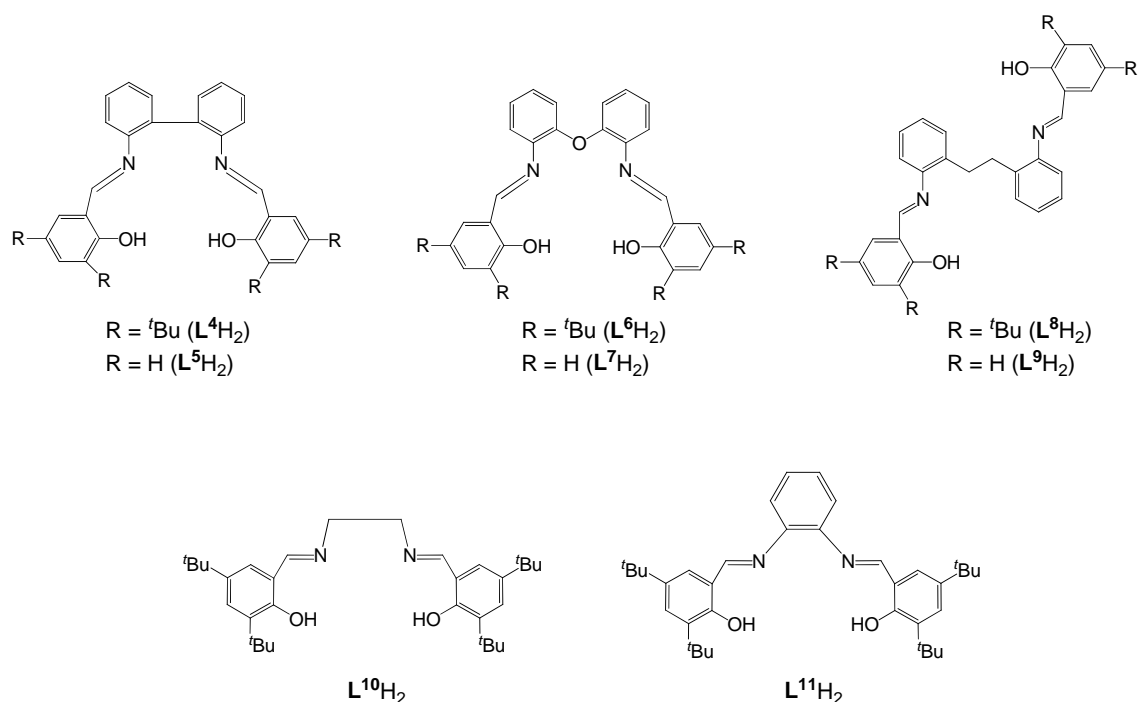


**Figure 30.** Bridged phenoxy-imine ligands used within this study.

The ligands **L<sup>4</sup>H<sub>2</sub>** and **L<sup>5</sup>H<sub>2</sub>** (Figure 30) have been previously utilised for their therapeutic applications treating disorders such as Parkinson's and Alzheimer's disease.<sup>12</sup> However, Gibson *et al.* has utilised these ligands as well as the Schiff base systems **L<sup>8</sup>H<sub>2</sub>-L<sup>10</sup>H<sub>2</sub>**, for the ring opening polymerisation of lactide by complexation with aluminium to prepare numerous initiators.<sup>13</sup> Gibson and co-workers also utilised **L<sup>8</sup>H<sub>2</sub>** and **L<sup>9</sup>H<sub>2</sub>** in studies preparing group IV catalysts for the polymerisation of ethylene. The titanium complexes exhibited higher activities, upon activation with MAO, than their zirconium counterparts. However, overall the activities can be classified as high (2,600 g/mmol.h.bar).<sup>14</sup> The oxygen-bridged chelating ligands, **L<sup>6</sup>H<sub>2</sub>** and **L<sup>7</sup>H<sub>2</sub>**, have also been scrutinised for their potential as Schiff base catalytic systems,

when complexed with group IV metals, for the polymerisation of  $\alpha$ -olefins.<sup>15</sup> Oleinik *et al.* noted that even at elevated temperatures ( $\leq 70$  °C) the dititanium(IV) pro-catalysts were capable of producing ultra-high molecular weight polyethylene.

Recently, Bialek *et al.* reported various transition metal complexes of tetradentate and bidentate Schiff bases, based on the salicylaldehyde versions of  $\mathbf{L}^{10}\text{H}_2$  and  $\mathbf{L}^{11}\text{H}_2$  (complexes **XX** and **XXI**, section 2.3, Figure 34), for the polymerisation of ethylene.<sup>16</sup> They noted that irrespective of the co-catalysts used, the vanadium and zirconium pro-catalysts produced linear high molecular weight polyethylene. The support and immobilisation of 1,2-cyclohexylenebis(5-chlorosalicylideneiminato)vanadium(IV) pro-catalyst on magnesium increased activities for ethylene homopolymerisation and its co-polymerisation with 1-octene.<sup>17</sup>

Redshaw and co-workers have also reported the use of bridged phenoxy-imine systems for the polymerisation ethylene.<sup>18</sup> Vanadium(V) pro-catalysts bearing a C-capped tris(phenolate) ligand with an imine pendant arm were highly active (2,450-6,800 g/mmol.h.bar), in the presence of DMAC and ETA, for the polymerisation of ethylene. These activities are analogues with those produced by various vanadium sulfur bridge phenoxy-imine complexes for the homopolymerisation of ethylene (1,050-11,130 g/mmol.h.bar) and co-polymerisation of ethylene/1-hexene.<sup>19</sup> A general feature of this chemistry is the adoption of mononuclear pro-catalysts. However, in a number of other polymerisation systems, beneficial cooperative effects are witnessed, leading to either improved catalytic performance or differing polymer properties.<sup>20</sup>

The bridged phenoxy-imine ligand systems mentioned above ( $\mathbf{L}^1\text{H}^2\text{-L}^{11}\text{H}_2$ ) were prepared and then complexed with vanadium to produce various vanadium(III) pro-catalysts. All complexes were screened for their ability to polymerise ethylene and  $\epsilon$ -caprolactone, to observe if the differing linkers or multinuclear *vs.* mononuclear systems would have an impact on either the pro-catalysts activity or the morphology of the produced polymers.

## 2. Results and Discussion

### 2.1 Ligand synthesis

The phenoxy-imine ligands,  $\mathbf{L}^1\text{H}_2\text{-L}^{11}\text{H}_2$  (Figure 30), were prepared in good yields by reacting either 3,5-di-*tert*-butyl-hydroxybenzaldehyde or salicylaldehyde with the corresponding amine following the literature procedure.<sup>14</sup> It proved possible to obtain

X-ray quality crystals of the ligand  $L^8H_2$ , by crystallisation from chloroform/methanol. The molecular structure is shown in Figure 31, with selected bond lengths and angles given in the caption.

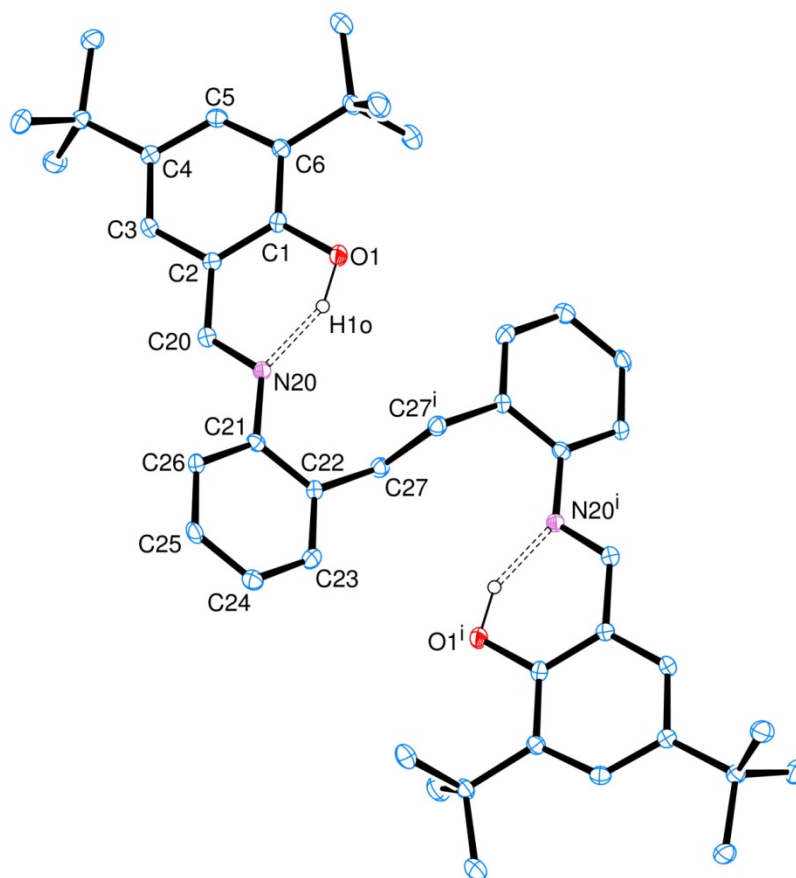
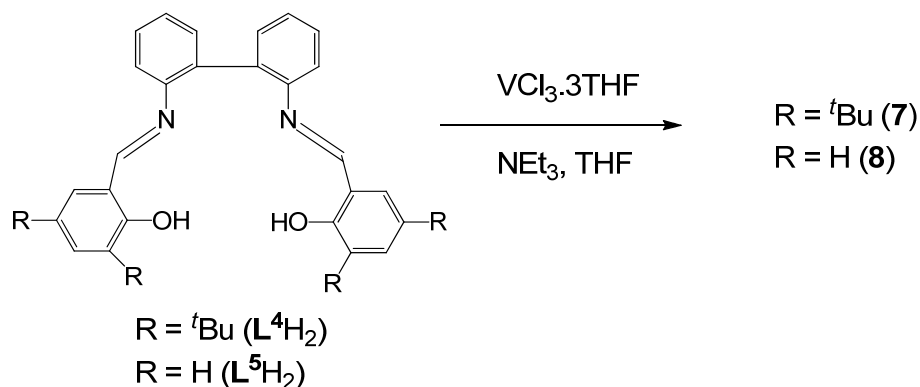


**Figure 31.** View of molecule  $L^8H_2$  indicating the atom numbering scheme. Thermal ellipsoids are drawn at the 50 % probability level. Selected bond lengths (Å) and angles ( $^\circ$ ): O(1)-C(1) 1.357(2), O(1)-H(10) 1.00(3), C(1)-C(2) 1.412(3), N(20)-C(21) 1.423(2), C(1)-O(1)-H(10) 105.8(16), O(1)-C(1)-C(6) 119.80(18), C(6)-C(1)-C(2) 119.41(17), N(20)-C(20)-C(2) 12.17(19).

The molecule lies about a centre of symmetry at the mid-point of the C(27)-C(27') bond, and thus has an 'S-shape' rather than curved in a 'C-shape' as it would when enfolding a metal centre. The phenolic hydrogen atom (in each half of the molecule) was refined freely and is directed towards the imino nitrogen with which it forms a hydrogen bond, O(1)-H(10) $\cdots$ N(20) 1.63 Å.

## 2.2 Vanadium(III) phenoxy-imine complexes



**Scheme 16.** Synthesis of vanadium(III) phenoxy-imine pro-catalysts **7** and **8**.

The mononuclear complexes **7** and **8** were synthesised following the Wu *et al.* literature method used to produce phenoxy-imine vanadium(III) systems **XXII** and **XXIII** (Figure 42).<sup>9c</sup> One equivalent of  $[\text{VCl}_3 \cdot 3\text{THF}]$ , slight excess of the base triethylamine and the corresponding ligand,  $\text{L}^4\text{H}_2$  or  $\text{L}^5\text{H}_2$ , were reacted in tetrahydrofuran at room temperature (Scheme 16). Volatile components were concentrated under vacuum, and the reaction solution filtered. The solution was layered with hexane and after prolonged standing the vanadium(III) complexes, **7** and **8** were formed. Dark red/black crystals of **8** were suitable for X-ray diffraction studies (Figure 32).

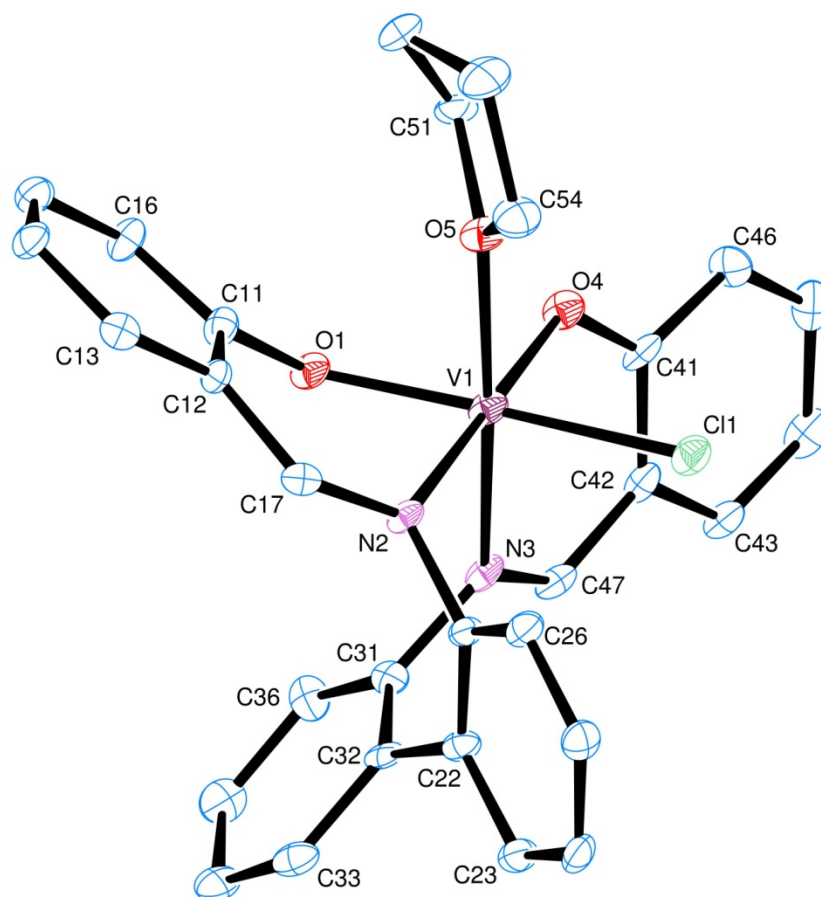
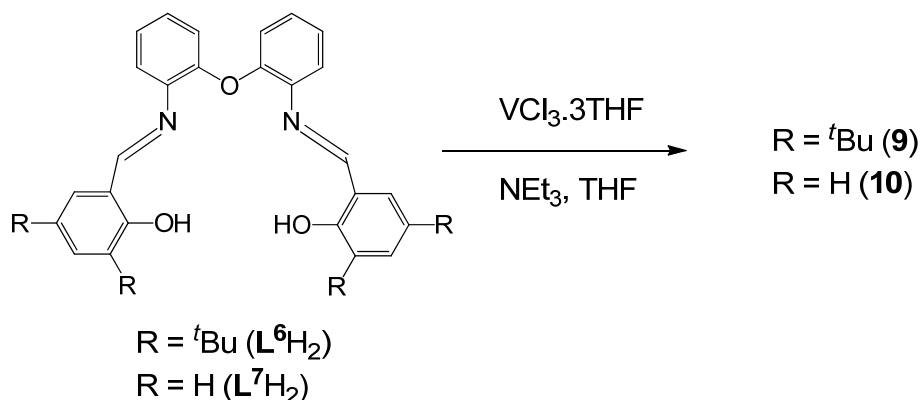


**Figure 32.** View of molecule of  $[\text{VCl}(\text{THF})\text{L}^5]$  (**8**) indicating the atom numbering scheme. Hydrogen atoms and the minor disorder component have been omitted for clarity. Thermal ellipsoids are drawn at the 50 % probability level. Selected bond lengths (Å) and angles ( $^\circ$ ): V(1)-O(1) 1.926(4), V(1)-N(2) 2.107(5), V(1)-N(3) 2.092(5), V(1)-O(4) 1.917(5), V(1)-O(5) 2.127(4), V(1)-Cl(1) 2.353(2); O(1)-V(1)-N(2) 83.8(2), O(1)-V(1)-O(4) 96.41(19), O(1)-V(1)-Cl(1) 169.19(15), N(2)-V(1)-N(3) 89.7(2), O(5)-V(1)-Cl(1) 88.77(13).

Compound **2** crystallises with two independent V-complex molecules in the cell. These are very similar in conformation, each with a six-coordinate vanadium atom with an octahedral coordination pattern. Three of the  $\text{N}_2\text{O}_2$  donor atoms of each  $\text{L}^{2-}$  ligand are arranged in a meridional mode with the remaining O atom bonding normal to the meridional plane. The two remaining sites are filled by a chloride ion (*trans* to the fourth donor atom) and a THF ligand (*trans* to an imido N atom). In the folding of the  $\text{L}^{2-}$  ligand around the metal centre, there is twisting of  $71.7^\circ$  about the N(2)-C(21) bond (and equivalent N(7)-C(71) bond in the second molecule) and  $54.5^\circ$  about the

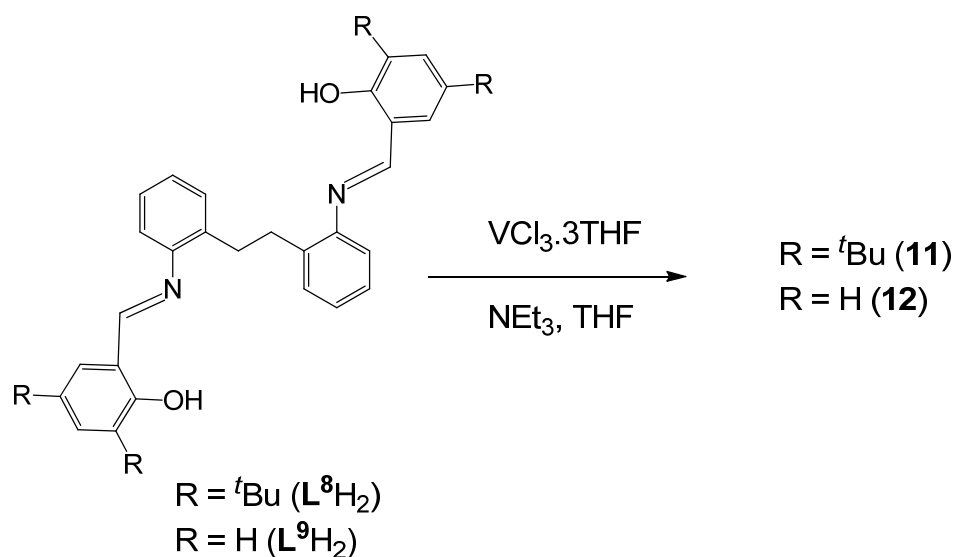
N(3)-C(31) and its equivalent bond; the rotation between the two phenyl groups, as about C(22)-C(32), is 55°.

There is also slight disorder in one of the THF ligands. Both THF ligands have a 'twisted' conformation, with C(51,52) and C(102,103) out of the planes of the other atoms in each ring. There are also one and a half solvent (THF) molecules in the asymmetric unit; the half-molecule is disordered about a centre of symmetry. In the molecule of O(11), C(111) is the out-of-plane atom in an envelope conformation of this ring. The disordered molecule of O(12) has a 'twisted' shape, with O(12) and C(124) on either side of the plane through C(121,122,123). Intermolecular contacts are at normal van der Waals' distances.



**Scheme 17.** Synthesis of vanadium(III) phenoxy-imine pro-catalysts **9** and **10**.

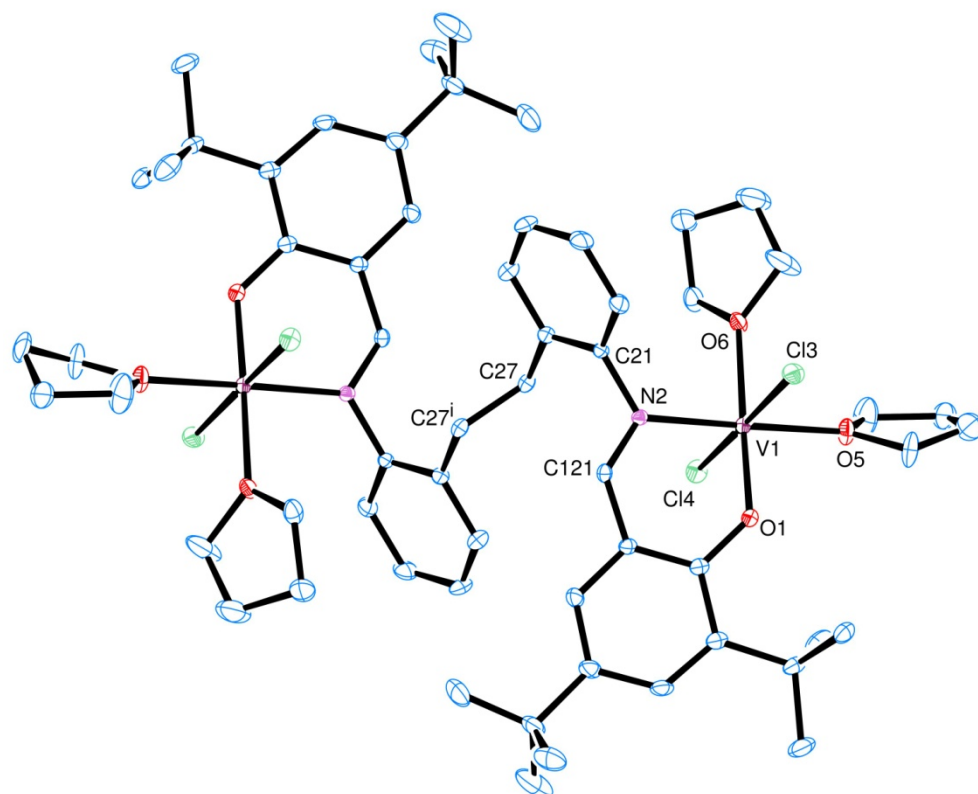
Complexes **9** and **10** were synthesised following the same procedure used to synthesise pro-catalysts **7** and **8**. [ $\text{VCl}_3 \cdot 3\text{THF}$ ], triethylamine and ligands  $\mathbf{L}^6\text{H}_2$  or  $\mathbf{L}^7\text{H}_2$ , were reacted in tetrahydrofuran at room temperature (Scheme 17). Volatile components were concentrated under vacuum, and the reaction solution filtered. The solution was layered with hexane to form **9** and **10**, respectively. Dark red precipitates were formed for **9** and **10**, which were characterised by various techniques, including; elemental analysis, mass spectrometry and Evans' magnetic moment.<sup>21</sup>



**Scheme 18.** Synthesis of vanadium(III) phenoxy-imine pro-catalysts **11** and **12**.

Treatment of either  $\text{L}^8\text{H}_2$  or  $\text{L}^9\text{H}_2$  with excess of  $[\text{VCl}_3 \cdot 3\text{THF}]$  in tetrahydrofuran afforded, following work-up, dark red complexes **11** and **12** (Scheme 18). Crystals of **11** suitable for X-ray crystallography were grown by slow diffusion of hexane into a THF solution of **11** at ambient temperature. The molecular structure is depicted in Figure 33, with selected bond lengths and angles given in the caption.

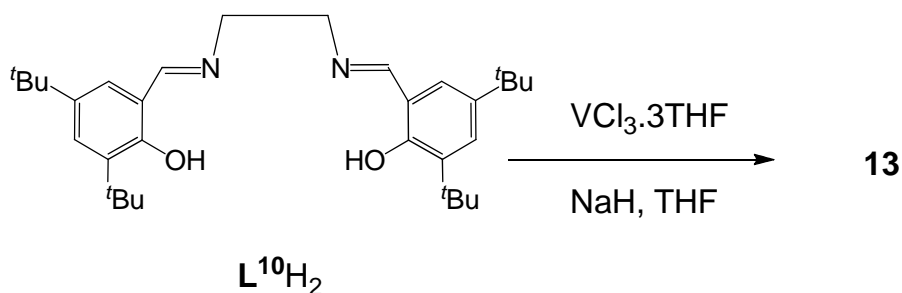
Regardless of whether the ligands  $\text{L}^8\text{H}_2$  or  $\text{L}^9\text{H}_2$  were treated with one or two equivalents of  $[\text{VCl}_3 \cdot 3\text{THF}]$ , the di-nuclear species was always obtained. The use of two equivalents of vanadium, rather than one, increased the obtained yields of the respective compounds.



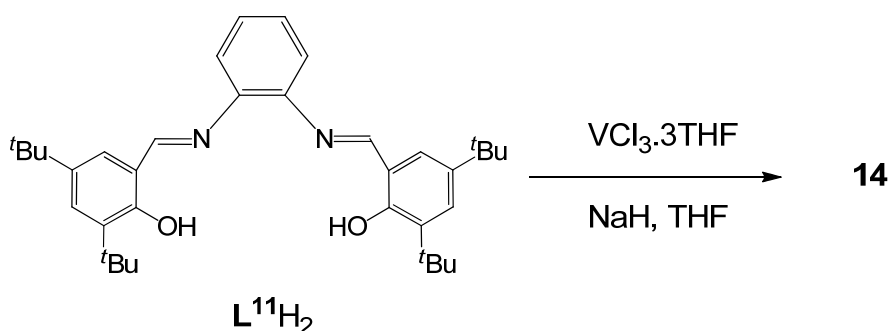
**Figure 33.** View of molecule  $[\{VCl_2(THF)_2\}_2L^8]$  (**11**) indicating the atom numbering scheme. Hydrogen atoms and the minor disorder component have been omitted for clarity. Thermal ellipsoids are drawn at the 50 % probability level. Selected bond lengths (Å) and angles ( $^\circ$ ): V-O(1) 1.870(2), V-N(2) 2.087(2), V-Cl(3) 2.3546(9), V-O(5) 2.107, V-O(6) 2.117(2), V-Cl(4) 2.358(9), O(1)-V-N(2) 89.56(9), O(1)-V-O(5) 92.12(9), O(1)-V-O(6) 177.31(9), N(2)-V-O(5) 177.87(9), N(2)-V-O(6) 92.60(9).

Interestingly here, the ligand rather than acting in tetra-dentate fashion as observed previously,<sup>14</sup> prefers to act as a bis-bi-dentate ligand, binding to a vanadium centre at either end of the ligand. The *centro*-symmetry is retained about the C(27)-C(27') bond midpoint and there is rotation about the C(21)-N(2) bond to allow the coordination of the V centres. Six-fold coordination, in an octahedral pattern, is achieved by the ligation of two chloride ligands (mutually *trans*, Cl(3)-V-Cl(4) 176.20(4) $^\circ$  and two *cis*-THF molecules (opposite the iminophenolate N and O atoms, O(5)-V-O(6) 85.68(9) $^\circ$  at each V centre.



**Scheme 19.** Synthesis of vanadium(III) phenoxy-imine pro-catalyst **13**

The *tert*-butylated vanadium(III) species **13** (Scheme 19) was prepared following literature methods used to synthesise the known salicylaldehyde vanadium(III) counterpart (**XX**, Figure 34).<sup>22</sup> Recently **XX** was used in studies by Bialek and co-workers to investigate its efficiency towards ethylene polymerisation and copolymerisation (Chapter 4, section 1.1).<sup>16, 17</sup> Complex **13** was formed in good yields (64 %) as a dark red/orange powder.

**Scheme 20.** Synthesis of vanadium(III) phenoxy-imine pro-catalyst **14**

Pro-catalyst **14** was prepared following the same procedure for **13**. Like **13**, the salicylaldehyde counterpart of **14** (**XXI**, Figure 34) has been used previously for polymerisation of ethylene.<sup>16, 17</sup> Unfortunately single crystals of **14** suitable for X-ray diffraction were not obtainable, however **14** was isolated as a dark red/orange precipitate solid characterised by various techniques, *viz* mass spectrometry, IR and Evans' magnetic moment.<sup>21</sup>

### 2.3 Known vanadium(III) phenoxy-imine complexes

As mentioned above, the salicylaldehyde counterparts of **13** and **14**, **XX** and **XXI**, are known in the literature, and have been employed as catalysts for the polymerisation of ethylene. Both of these complexes were prepared and used within the study to enable

comparisons to be made between the *tert*-butyl species **13** and **14**, to observe if steric issues regarding the large *tert*-butyl groups could affect the activity of the pro-catalysts. Vanadium(III) complexes bearing a phenoxy-imine ligand (**XXII** and **XXIII**, Figure 34), previously prepared and screened for their ability to polymerise ethylene by Wu *et al.*,<sup>9c</sup> were also prepared to enable comparisons between bridged phenoxy-imine systems and phenoxy-imine complexes without a bridge.

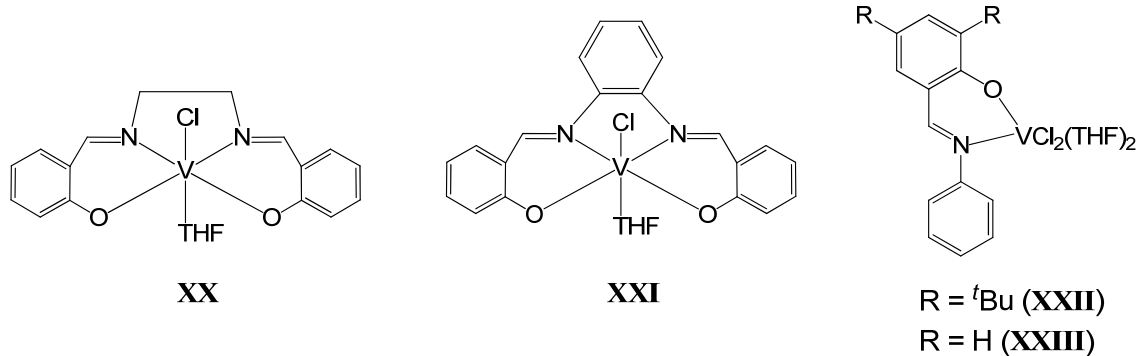


**Figure 34.** Literature examples of phenoxy-imines used within the study.

## 2.4 Ethylene polymerisation

### 2.4.1 Comparative studies

Complexes **7-14** and **XX-XXIII** were screened for their ability to polymerise ethylene in the presence of DMAC with the re-activating substance ETA. To enable comparisons to be made between the affect of the chelating ligands all pro-catalysts were screened under the same polymerisation conditions; 100 mL toluene, 30 min., 20 °C and 4000 equivalents of co-catalyst [Al]:[M].

Do to the formation of the dinuclear species (**11** and **12**) it was also possible to compare mono and dinuclear complexes to note if pro-catalysts **11** and **12** displayed a beneficial cooperative effect. As mentioned previously (Chapter 4, section 1.1) this ‘effect’ between two metal centres can result in improved activities in comparison to mono-nuclear counterparts (*i.e.* **1-10**, **12-14** and **XX-XXIII**).

**Table 13.** Results for ethylene polymerisation runs using pro-catalysts **7-14** and **XX-XXIII**.<sup>a</sup>

Run	Pro-catalyst	Yield PE (g)	Activity <sup>b</sup> ( $\times 10^3$ )	$M_w^c$	$M_n^d$	PDI <sup>e</sup>
1	<b>7</b>	2.10	8.4	217,000	49,300	4.4
2	<b>8</b>	0.64	2.6	-	-	-
3	<b>9</b>	0.34	1.4	536,000	136,000	3.9
4	<b>10</b>	0.42	1.7	404,000	28,800	1.4
5	<b>11</b>	2.38	9.5	445,000	181,000	2.5
6	<b>12</b>	1.20	4.8	170,000	30,500	5.6
7	<b>13</b>	2.41	9.6	-	-	-
8	<b>XX</b>	1.14	4.6	-	-	-
9	<b>14</b>	0.47	1.9	-	-	-
10	<b>XXI</b>	0.25	1.0	-	-	-
11	<b>XXII</b>	0.98	3.9	273,000	47,600	5.7
12	<b>XXIII</b>	1.31	5.2	168,000	39,200	4.3

<sup>a</sup>Conditions: 0.5  $\mu$ mol pro-cat., 1 bar ethylene; toluene (100 mL); ETA (0.1 mL); reaction quenched with dilute HCl, washed with methanol (20 mL) and dried for 12 h in a vacuum oven at 80 °C. <sup>b</sup> g/mmol.h.bar per V. <sup>c</sup> Weight average molecular weight. <sup>d</sup> Number average molecular weight. <sup>e</sup> Polydispersity index. All runs carried out at 25 °C, 30 min. and Al/V (Molar ratio) 4000.

In the presence of DMAC and ETA, all the complexes, **7-14** and **XX-XXIII**, can be considered to be highly active for the polymerisation of ethylene.<sup>23</sup> However, the activities ( $< 10,000$  g/mmol.h.bar) are disappointing in comparison to other V pro-catalyst/DMAC/ETA systems recently reported from the group.<sup>1, 24</sup> The general trend observed in Table 13 is that the 3,5-*tert*-butyl pro-catalysts (even numbers), show higher activities than their salicylaldehyde precursors (odd numbers), indicating the steric hindrance of the *tert*-butyl group does not seem to effect the approach of the monomer.

When comparing the chelating ligand backbone, it is evident that there is no significant difference in polymer molecular weight, polydispersity or activity values among these 12 pro-catalysts (*e.g.* run 8 vs. run 12). Also, when comparing the di-nuclear pro-catalysts (**11** and **12**, runs 5 and 6) to the mono-nuclear systems (**7-10**, **13**, **14**, **XX-XXIII**, runs 1-4 and 7-12), it is concluded that no beneficial cooperative effect occurs

between the vanadium metal centre's in the dinuclear species during the polymerisation of ethylene.

#### 2.4.2 Lifetime studies

Lifetime studies were also conducted on the dinuclear pro-catalysts **11** and **12**, and mono-nuclear species **XXII** and **XXIII**. Activities of the four pro-catalysts were observed over a 30 minute time period to observe the stability of each of the catalysts. It was hoped that comparisons could be made between the complexes to observe if the presence of a bridge on the phenoxy-imine ligand offered any stability during polymerisation. All the polymerisation runs were conducted in the presence of DMAC and the re-activator ETA, under the same conditions used for the pro-catalyst comparison runs.

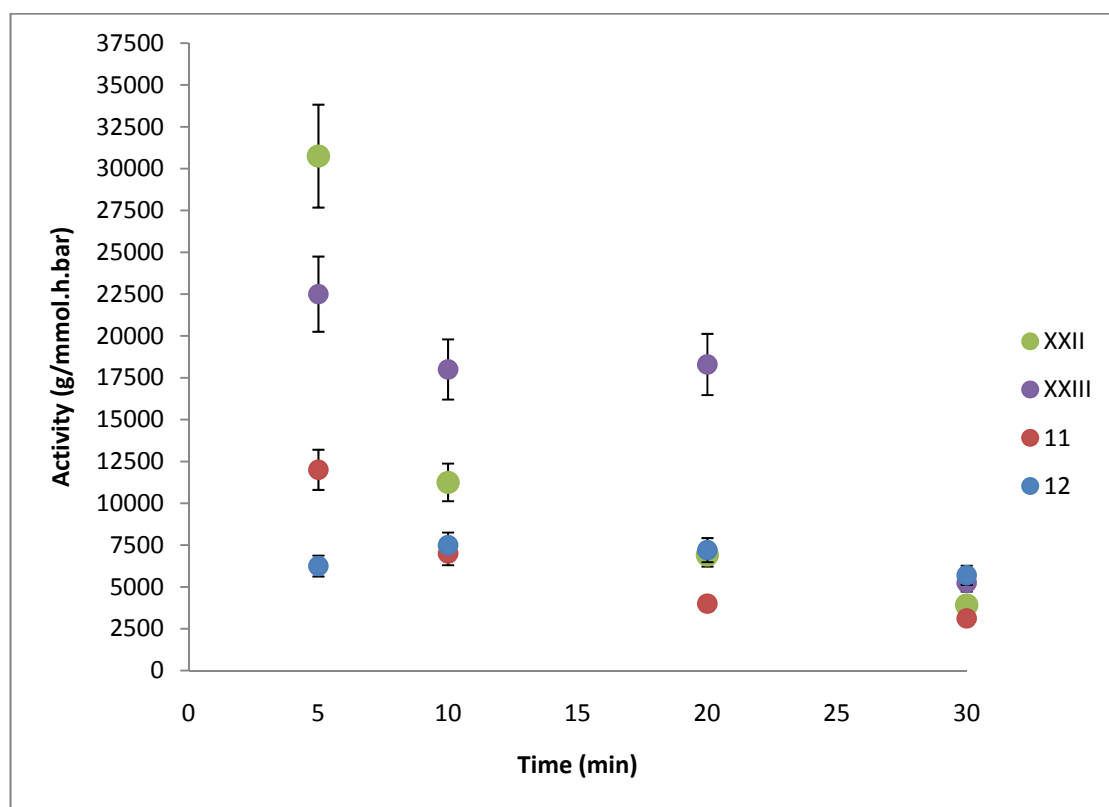


**Figure 35.** Lifetime studies comparing pro-catalysts **11**, **12**, **XXII** and **XXIII**.

The general observed trend for all the pro-catalysts was as the polymerisation time increased, the activities began to decrease. This appeared to be less dramatic for the dinuclear systems **11** and **12**. The mono-nuclear complexes **XXII** and **XXIII**, showed

higher initial activities (20,000-30,000 g/mmol.h.bar) however, over the observed 30 minute polymerisation time the activities decreased significantly.

It was noted that there appeared to be little difference in observed activities for pro-catalysts **7-14**, indicating that varying the bridged chelating ligand present in the systems has no beneficial impact on activity. However, when comparing the bridged systems to their Schiff base counterparts there appears to be an increased stability of the pro-catalysts during polymerisation (*e.g.* **11** vs. **XVII**, Figure 35).

### 2.5 $\epsilon$ -Caprolactone polymerisation

Complexes **7-14** and **XX-XXII** were also screened for their ability to polymerise  $\epsilon$ -caprolactone. Pro-catalyst **12** was subjected to temperature, time, monomer and co-initiator studies. No polymer was observed at 20-40 °C. The polymerisation results for these studies are shown in Table 14.

**Table 14.**  $\epsilon$ -Caprolactone polymerisation data for complex **12**.<sup>a</sup>

Run	Monomer / metal	Equiv BnOH	Time (h)	Temp (°C)	Conversion <sup>b</sup> (%)
1	400	1	72	60	10
2	400	1	72	80	70
3	200	1	72	80	47
4	600	1	72	80	-
5	400	0	72	80	51
6	400	5	72	80	-
7	400	1	12	80	9
8	400	1	24	80	11
9	400	1	48	80	20

<sup>a</sup>Conditions: 20 mL of toluene; 2 mL of  $\epsilon$ -caprolactone; benzyl alcohol taken from a 0.97 M solution in toluene; <sup>b</sup> calculated by <sup>1</sup>H NMR.

Complex **12** showed no observable activity at temperatures below 60 °C. At elevated temperatures (80 °C), there was a dramatic increase in conversion (run 2). This trend was mirrored in polymerisation time (runs 2 and 7-9). The longer the polymerisation time the higher the percentage conversion of  $\epsilon$ -caprolactone. Interestingly, polymer was

observed in runs where no initiator was used (run 5), however when initiator was added to the polymerisation solution the conversion rate almost doubled (run 2).

The conditions which produced the most poly( $\epsilon$ -caprolactone), *i.e.* 72 hours, 1 equivalent of benzyl alcohol, 80 °C and 400 equivalents of monomer (run 2), were then used for comparative studies for the 12 pro-catalysts.  $[\text{VCl}_3 \cdot 3\text{THF}]$  was also screened under the same conditions to enable comparisons to be made between the affect of the chelating ligand on conversion and polymer morphology.

**Table 15.**  $\epsilon$ -Caprolactone screening results for pro-catalysts **7-14** and **XX-XXII**.<sup>a</sup>

Run	Pro-catalyst	Conversion <sup>b</sup> (%)	$M_n$ calculated <sup>c</sup> (g/mol)	$M_n$ measured <sup>d</sup> (g/mmol)	PDI
1	<b>VCl<sub>3</sub>·3THF</b>	100	45.7	3.1	1.1
2	<b>7</b>	57	26.0	10.8	1.4
3	<b>8</b>	47	21.5	8.6	1.4
4	<b>9</b>	24	10.9	7.9	1.2
5	<b>10</b>	33	15.1	9.3	1.2
6	<b>11</b>	48	21.9	10.1	1.4
7	<b>12</b>	70	31.9	11.0	2.3
8	<b>13</b>	24	11.0	5.9	1.2
9	<b>XX</b>	94	42.9	4.8	1.1
10	<b>14</b>	15	6.9	2.4	1.1
11	<b>XXI</b>	3	1.4	4.6	1.4
12	<b>XXII</b>	72	32.9	5.0	1.2
13	<b>XXIII</b>	100	45.7	4.0	1.1

<sup>a</sup>Conditions: 20 mL of toluene; 2 mL of  $\epsilon$ -caprolactone; benzyl alcohol taken from a 0.97 M solution in toluene; <sup>b</sup> calculated by <sup>1</sup>H NMR; <sup>c</sup>  $\times 10^3$  <sup>d</sup> $M_n$  measured =  $0.58 \times M_n(\text{GPC} \times 10^3)$ .<sup>25</sup>

All complexes formed only oligomers with low polydispersity ( $\leq 2.3$ ), which suggests that these ‘polymerisations’ occurred without side reactions. Interestingly, only low molecular weight oligomers were obtained using these phenoxy-imine vanadium/benzyl alcohol systems.

The above results could possibly be described as disappointing, however they should be put into context by comparing them against recent work carried out by Mahha *et al.*<sup>26</sup> It was noted that the heteropolyacids had sufficiently lower activities under inert nitrogen atmosphere, this was attributed to the reduction of the metal centres to V(IV) and/or

Mo(V). However, when dioxygen was added, the reduced species were re-oxidised to the active vanadium(V) and Mo(VI). Unlike the heteropolyacid systems, the above phenoxy-imine systems show similar conversion rates without the need to re-oxidise the deactivated species.

Generally, the salicylaldiminato complexes **8**, **10**, **12**, **XX** and **XXIII** appear to out-perform their 3,5-*t*-butylated counterparts. However, it is pro-catalysts **XX** and **XXIII** that appear to excel in conversion rates in comparison to the other complexes, which is understandable in terms of the steric demands from the  $\epsilon$ -caprolactone monomer (the growing polymeric chain is bulkier than a *tert*-butyl group).

### 3. Conclusion

A new family of vanadium(III) diphenoxy-imine complexes have been synthesised and structurally characterised. All complexes were investigated for their effectiveness as ethylene polymerisation catalysts, in the presence of DMAC and ETA. All pro-catalysts were shown to be highly active for the polymerisation of ethylene under the utilised conditions.<sup>23</sup> When these results are put into context with recent findings for vanadium-based systems, they can be viewed as somewhat disappointing. There was no significant evidence that the presence of the bridged phenoxy-imine chelating ligand led to an increase in observed activities (**XX** 4,560 g/mmol.h.bar vs. **XXIII** 5,240 g/mmol.h.bar, Table 13). However, lifetime studies concluded that the bridged ligand systems did offer stability to the metal centre when compared to mono phenoxy-imine systems (Figure 35).

The vanadium(III) phenoxy-imine complexes were also screened for their ability to polymerise  $\epsilon$ -caprolactone. The conversion value was dictated by the steric hinderance on the vanadium(III) metal centre. The highest conversion (100 %) was observed for the vanadium(III) complex with the salicylaldehyde mono phenoxy-imine ligand. In general, the less sterically hindered salicylaldehyde complexes were able to produce higher conversion rates in comparison to the more sterically demanding *tert*-butyl complexes. All pro-catalysts produced oligomeric polymers with low polydispersity. However, the conditions required to achieve the obtained oligo( $\epsilon$ -caprolactone), *i.e.* 80 °C and 72 hours, can be viewed as robust when compared to literature examples.<sup>27</sup>

- 1 a) Y. Nakayama, H. Bando, Y. Sonobe, T. Fujita, *J. Mol. Catal. A: Chem.*, 2004, **213**, 141 b) Y. Nakayama, H. Bando, Y. Sonobe, Y. Suzuki, T. Fujita, *Chem. Lett.*, 2003, **32**, 766 c) Y. Nakayama, J. Saito, H. Bando, T. Fujita, *Chem. Eur. J.*, 2006, **12**, 7546
- 2 a) H. Makio, H. Terao, A. Iwashita, T. Fujita, *Chem. Rev.*, 2011, **111**, 2363 b) H. Makio, N. Kashiwa, T. Fujita, *Adv. Synth. Catal.*, 2002, **344**, 477 c) M. Mitani, T. T. Nakano, T. Fujita, *Chem. Eur. J.*, 2003, **9**, 2396 d) S. Matsui, T. Fujita, *Catal. Today.*, 2001, **66**, 63 e) T. Matsugi, T. Fujita, *Chem. Soc. Rev.*, 2008, **37**, 1264
- 3 a) S. Matsui, M. Mitani, J. Saito, Y. Tohi, H. Makio, H. Tanaka, T. Fujita, *Chem. Lett.*, 1999, 1263 b) S. Matsui, M. Mitani, J. Saito, N. Matsukawa, H. Tanaka, T. Fujita, *Chem. Lett.*, 2000, 554 c) S. Matsui, M. Mitani, J. Saito, Y. Tohi, H. Makio, N. Matsukawa, Y. Takagi, K. Tsuru, M. Nitabaru, T. Nakano, H. Tanaka, N. Kashiwa, T. Fujita, *J. Am. Chem. Soc.*, 2001, **123**, 6847
- 4 a) S. -I. Ishii, R. Furuyama, N. Matsukawa, J. Saito, M. Mitani, H. Tanaka, T. Fujita, *Macromol. Rapid Commun.*, 2003, **24**, 452 b) R. Furuyama, J. Saito, S. Ishii, H. Maiko, M. Mitani, H. Tanaka, T. Fujita, *J. Organomet. Chem.*, 2005, **690**, 4398 c) H. Terao, S. Ishii, M. Mitani, H. Tanaka, T. Fujita, *J. Am. Chem. Soc.*, 2008, **103**, 17636
- 5 Y. Nakayama, H. Bando, Y. Sonobe, T. Fujita, *Bull. Chem. Soc. Jpn.*, 2004, **77**, 617
- 6 a) S. Matsui, Y. Tohi, M. Mitani, J. Saito, H. Makio, H. Tanaka, M. Nitabaru, T. Nakano, T. Fujita, *Chem. Lett.*, 1999, 1065 b) J. Saito, M. Mitani, J. -I. Mohri, Y. Yoshida, S. Matsui, S. -I. Ishii, S. -I. Kojoh, N. Kashiwa, T. Fujita, *Angew. Chem. Int. Ed.*, 2001, **40**, 2918 c) M. Mitani, T. Nakano, T. Fujita, *Chem. Eur. J.*, 2003, **9**, 2396 d) R. Furuyama, J. Saito, S. -I. Ishii, M. Mitani, S. Matsui, Y. Tohi, H. Makio, N. Matsukawa, H. Tanaka, T. Fujita, *J. Mol. Catal. A: Chem.*, 2003, **200**, 31 e) Y. Suzuki, S. Kinoshita, A. Shibahara, S. Ishii, K. Kawamura, Y. Inoue, T. Fujita, *Organometallics*, 2010, **29**, 2394 f) N. I. Ivancheva, M. Y. Malinskaya, S. S. Ivanchev, I. I. Oleinik, A. I. Kochnev, G. A. Tolstikov, *Kinet. Catal.*, 2007, **48**, 829
- 7 a) K. V. Axenov, M. Klinga, O. Lehtonen, H. T. Koskela, M. Leskelä, T. Repo, *Organometallics*, 2007, **26**, 1444 b) H. Makio, Y. Tohi, J. Saito, M. Onda, T. Fujita, *Macromol. Rapid Commun.*, 2003, **24**, 894
- 8 B. A. Rodriguez, M. Delferro, T. J. Marks, *Organometallics*, 2008, **27**, 2166



- 9 a) Y. Onishi, S. katao, M. Fujiki, K. Nomura, *Organometallics*, 2008, **27**, 2590 b) European Patent, H. S. Zahalka., Patent No. EP 1 203 778 A1, 2001 c) J. –Q. Wu, L. Pan, N. –H. Hu, Y. –S. Li, *Organometallics*, 2008, **27**, 3840
- 10 a) H. Makio, T. Fujita, *Bull. Chem. Soc. Jpn.*, 2005, **78**, 52 b) M-S. Weiser, M. Wesolek, R. Mülhaupt, *J. Organometallic Chem.*, 2006, **691**, 2945 c) C. De Rosa, T. Circelli, F. Auriemma, R. T. Mathers, G. W. Coates, *Macromolecules*, 2004, **37**, 9034
- 11 a) B. A. Rodriguez, M. Delferro, T. J. Marks, *Organometallics*, 2008, **27**, 2166 b) M. R. Salata, T. J. Marks, *Macromolecules*, 2009, **142**, 1920
- 12 M. A. Murphy, M. R. Malachowski, US patent, US20050085555 A1, 2005
- 13 P. Hornmiron, E. L. Marshall, V. C. Gibson, R. I. Pugh, A. J. P. Andrews, *P. N. A. S. U. S. A.*, 2006, **103**, 15343
- 14 G. J. Clarkson, V. C. Gibson, P. K. Y. Goh, M. L. Hammond, P. D. Knight, P. Scott, T. M. Smit, A. J. P. White, D. J. Williams, *Dalton Trans.*, 2006, 5484
- 15 I. I. Oleinik, I. V. Oleinik, S. S. Ivanchev, G. A. Tolstikov, *Russian J. Org. Chem.*, 2009, **45**, 528
- 16 M. Bialek, K. Czaja, E. Syzdlo, *J. Polym. Sci: Part A: Polym. Chem.*, 2009, **47**, 565
- 17 M. Bialek, O. Liboska, *J. Polym. Sci: Part A: Polym. Chem.*, 2010, **48**, 471
- 18 D. Homden, C. Redshaw, J. A. Wright, D. L. Hughes, M. R. J. Elsegood, *Inorg. Chem.*, 2008, **47**, 5799
- 19 D. M. Homden, C. Redshaw, D. L. Hughes, *Inorg. Chem.*, 2007, **46**, 10827
- 20 S. Singh, H. W. Roesky, *Dalton Trans.*, 2007, 1360
- 21 R. J. Errington, *Advanced practical inorganic and metalorganic chemistry*, CRC press, 1<sup>st</sup> Edt, 1997
- 22 M. Mazzanti, S. Gamboratta, C. Floriana, A. Chiesi-Villa, C. Guastini, *Inorg. Chem.*, 1986, **25**, 2308
- 23 G. J. P. Britovsek, V. C. Gibson, D. F. Wass, *Angew. Chem. Int. Ed.*, 1999, **38**, 428
- 24 a) C. Redshaw, M. A. Rowan, D. M. Homden, S. H. Dale, M. R. J. Elsegood, S. Matsui, S. Matsuura, *Chem. Commun.*, 2006, 3329 b) C. Redshaw, M. A. Rowan, L. Warford, D. M. Homden, A. Arbaoui, M. R. J. Elsegood, S. H. Dale, T. Yamato, C. Pérez-Casas, S. Matsui, S. Matsuura, *Chem. Eur. J.*, 2007, **13**, 1090 c) C. Redshaw, L. Warford, S. H. Dale, M. R. J. Elsegood, *Chem. Commun.*, 2004, 1954
- 25 A. Kowalski, A. Duda, S. Penczek, *Macromolecules*, 1998, **31**, 2114

- 26 Y. Mahha, A. Atlamsani, J. –C. Blais, M. Tessier, J. –M. Brégeault, L. Salles, *J. Mol. Catal. A: Chem.*, 2005, **234**, 63
- 27 A. Arbaoui, C. Redshaw, *Polym. Chem.*, 2010, **1**, 801

## **Chapter 5**

### **Group V complexes bearing phenoxy-imine/imidazole and oxazole ligands**

## 1. Introduction

As mentioned previously in Chapter 4, section 1, non-metallocene-based pro-catalysts for the oligomerisation/polymerisation of  $\alpha$ -olefins continue to attract considerable academic and industrial interest.<sup>1</sup> Recent findings by Redshaw *et al.*<sup>2</sup> and Fujita *et al.*,<sup>3</sup> have shown that group V systems utilising various non-metallocene ligands can produce activities that can compete with the highly successful group IV metallocene complexes.

Phenoxy-imine systems have been proven to be highly efficient chelating ligands systems for the polymerisation of ethylene and other  $\alpha$ -olefins. These findings have been expanded upon by numerous successes with a variety of transition metals, and variations of substituents on the phenoxy-imine ligand backbone.<sup>4</sup>

### 1.1 Phenoxy-imine/imidazole and oxazole ligands

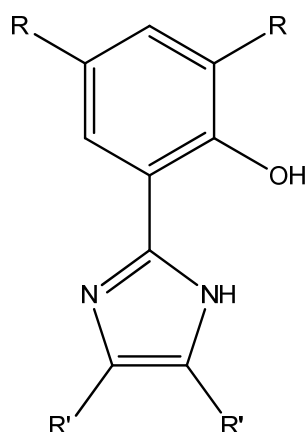


**Figure 36.** Phenoxy-imine/imidazole ligand. Typically, R = H, alkyl; R' = aryl.

Phenoxy-imine/imidazole and oxazole type ligands can be viewed as phenoxy-imine derivatives, as they contain the fundamental phenol ring bound directly to an imine. Imidazole phenol type of compounds have drawn considerable attention for their desirable properties when utilised in numerous fields, such as coordination chemistry,<sup>5</sup> photoluminescence/pH sensing studies,<sup>6</sup> biochemistry of metalloenzymes<sup>7</sup> and medicinal chemistry.<sup>8</sup>

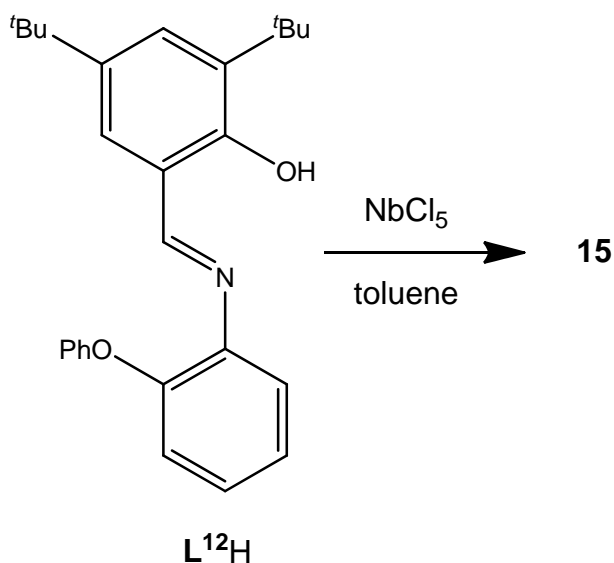
Sun and co-workers have reported the use of 2-(1*H*-imidazol-2-yl)phenol ligands and their neutral zinc(II) complexes for their fluorescent and luminescent properties.<sup>9, 10</sup> Whereas Benisvy *et al.* have used the ligand system complexed with copper(II) to form a phenoxyl radical copper(II) complex.<sup>11</sup> Sun *et al.* also used pyridine imidazole and

oxazole derivatives with nickel(II) to polymerise norbornene through predominately vinyl addition and minor ring-opening metathesis.<sup>12</sup> These ligands have been complexed with nickel(II) and palladium(II) to study their hemi-lability efficiency as transition metal complexes.<sup>13</sup> However, the use of such systems for the polymerisation of  $\alpha$ -olefins is limited to imine bridged imidazole systems complexed with group IV metals, zirconium and titanium, to co-polymerise 1-hexene and ethylene.<sup>14</sup> These pro-catalysts showed favourable results, with both high activities and high incorporation of the co-monomer. Due to the similarities in ligand structure when comparing phenoxy-imine/imidazole ligands to the 'classical' phenoxy-imine, and the great success of FI catalysts, it is surprising that there are few reports on phenoxy-imine/imidazole ligands used for polymerisation catalysis.

As mentioned previously phenoxy-imine ligands have been utilised with various transition metals, including the group V metal vanadium. However, there are no other reports in the literature regarding any of the other group V metals. Prior to Redshaw<sup>2</sup> and Fujita's<sup>3</sup> findings, vanadium systems were deemed to behave as catalysts with low activities when applied to the polymerisation of  $\alpha$ -olefins. We wish to duplicate this success by expanding upon Fujita and co-workers' research, by synthesising niobium and tantalum complexes bearing phenoxy-imine/imidazole and oxazole chelating ligands and screen them for their efficiency as ethylene polymerisation catalysts.

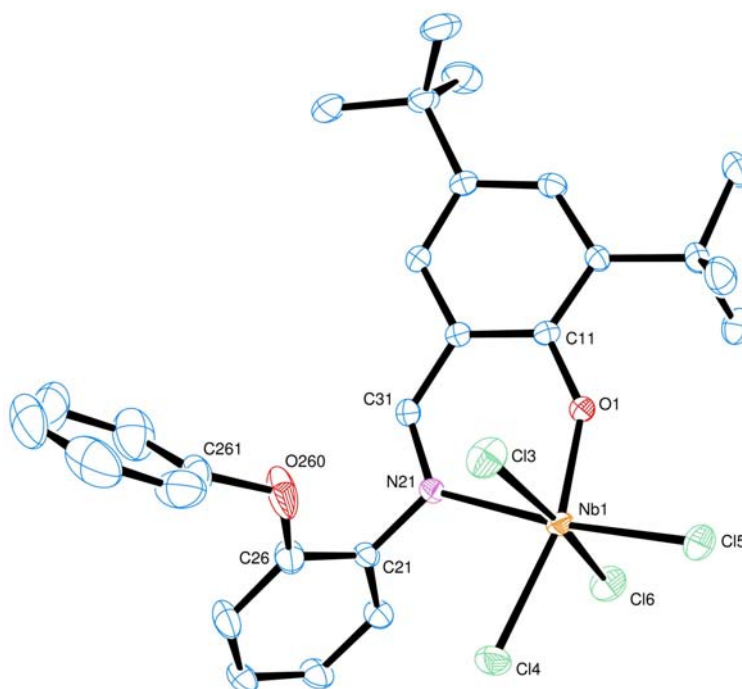
## 2. Results and Discussion

### 2.1 Niobium(V) complexes supported by phenoxy-imine ligands



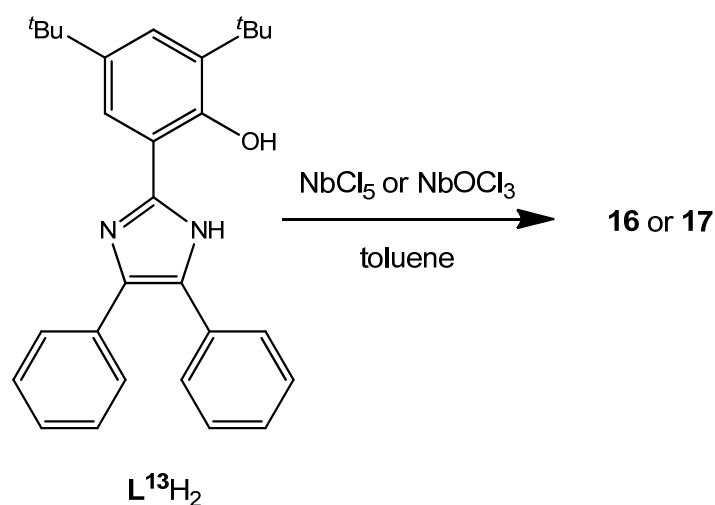
**Scheme 21.** Synthesis of niobium(V) complex **15**.

The phenoxy-imine ligand,  $L^{12}H$ , and 1.1 equivalents of  $[NbCl_5]$  were stirred in refluxing toluene overnight. The orange/red solution was cooled and once the volatile components were removed *in vacuo*, the residue was extracted in warm acetonitrile. After prolonged standing at ambient temperature, long yellow/brown needles were produced. The structure of complex **15** was determined by X-ray diffraction studies. A molecular structure of **15** is presented in Figure 37.



**Figure 37.** View of a molecule of  $[L^{12}NbCl_4]$  (**15**) indicating the atom numbering scheme. Thermal ellipsoids are drawn at the 50 % probability level. Selected bond lengths (Å) and angles ( $^\circ$ ): Nb(1)-O(1) 1.8746(13), Nb(1)-N(21) 2.2715(16), Nb(1)-Cl(3) 2.3640(6), Nb(1)-Cl(4) 2.3224(5), Nb(1)-Cl(5) 2.3143(6), Nb(1)-Cl(6) 2.3401(6); O(1)-Nb(1)-N(21) 78.90(6), O(1)-Nb(1)-Cl(4) 165.11(4), N(21)-Nb(1)-Cl(5) 173.60(4).

In **15** there are two independent molecules within the asymmetric unit, each niobium centre displaying a distorted octahedral environment, the main difference between the two molecules being in the rotation of the nitrogen-bonded phenyl ring of the diphenylether substituent  $-71.1^\circ$  about N(21)-O(21) *versus*  $-80.8^\circ$  about N(81)-C(81). The twist observed within the ether group is also significantly different between the two molecules; C(26)-O(260)-C(261)-C(262)  $68.0(3)^\circ$  and C(86)-O(860)-C(861)-C(862)  $45.8(5)$ . Neither molecule forms any close intermolecular interactions.

**2.2 Group V complexes supported by phenoxy-imine/imidazole ligands****Scheme 22.** Synthesis of complexes **16** and **17**.

Treatment of imidazole ligand,  $\text{L}^{13}\text{H}_2$ , with one equivalent of  $[\text{NbCl}_5]$  afforded, after work up, dark red plates of  $[\text{L}^{13}\text{HNbCl}_4]$  (**16**). The same method was used to produce  $[\text{L}^{13}\text{HNbOCl}_2(\text{MeCN})]$  (**17**) but using  $[\text{NbOCl}_3]$  instead of  $[\text{NbCl}_5]$ . Complex **17** was obtained as orange prisms. Crystals of **16** and **17** suitable for single crystal X-ray diffraction studies were grown from saturated acetonitrile solutions after prolonged standing at ambient temperature. Molecular structures of **16** and **17** are presented in Figures 38 and 39, respectively.

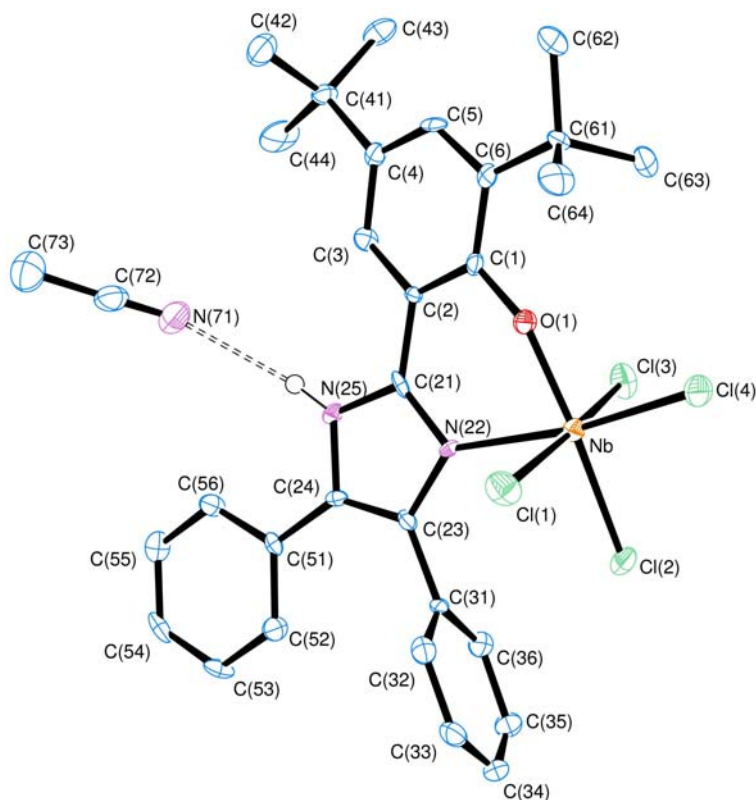


**Figure 38.** Molecular structure of  $[\text{L}^{13}\text{HNbCl}_4(\text{MeCN})]$  (**16**(MeCN)) and hydrogen-bonded acetonitrile molecule, indicating the atom numbering scheme. Thermal ellipsoids are drawn at the 50 % probability level. Hydrogen atoms have been omitted for clarity. Selected bond lengths (Å) and angles ( $^\circ$ ): Nb-O(1) 1.863(2), Nb-N(22) 2.267(3), Nb-Cl(1) 2.3576(9), Nb-Cl(2) 2.3092(8), Nb-Cl(3) 2.3843(9), Nb-Cl(4) 2.3083(9); O(1)-Nb-N(22) 79.09(9), Cl(1)-Nb-Cl(3) 172.09(4), Cl(4)-Nb-N(22) 171.36(7), O(1)-Nb-Cl(2) 169.31(7).



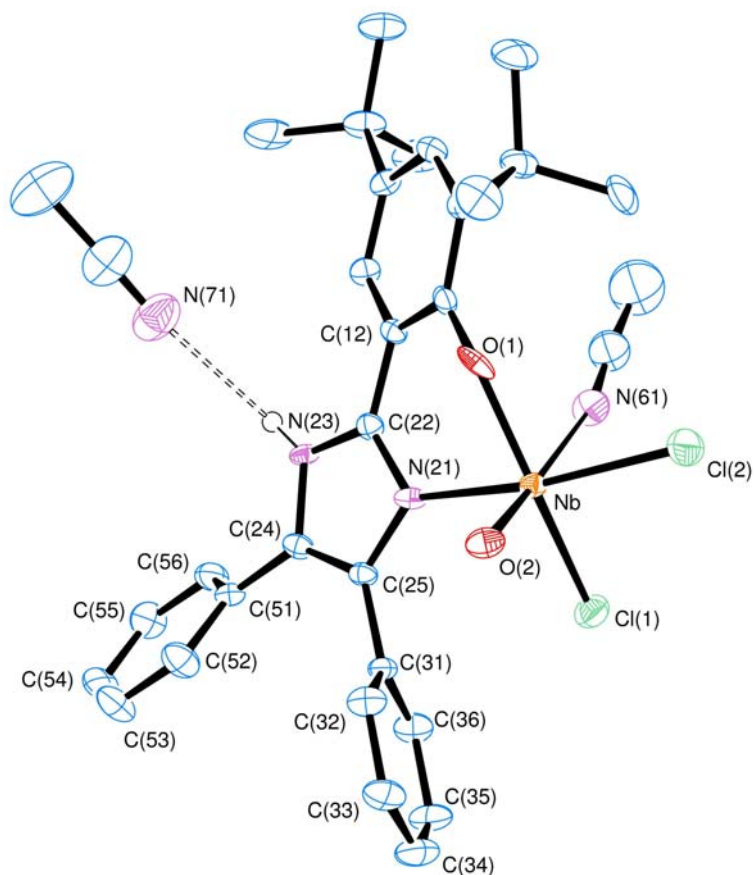
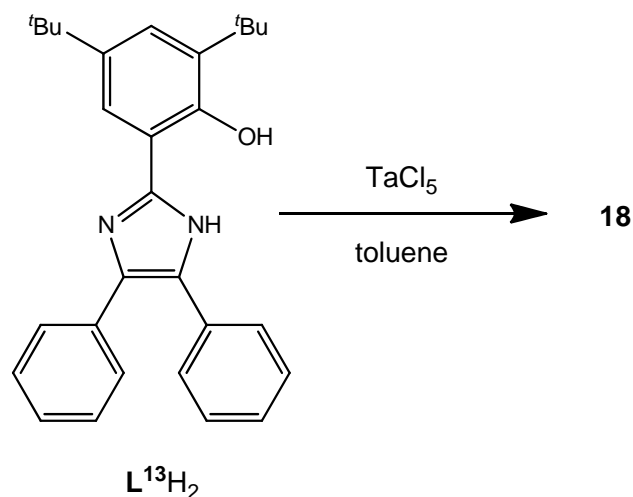


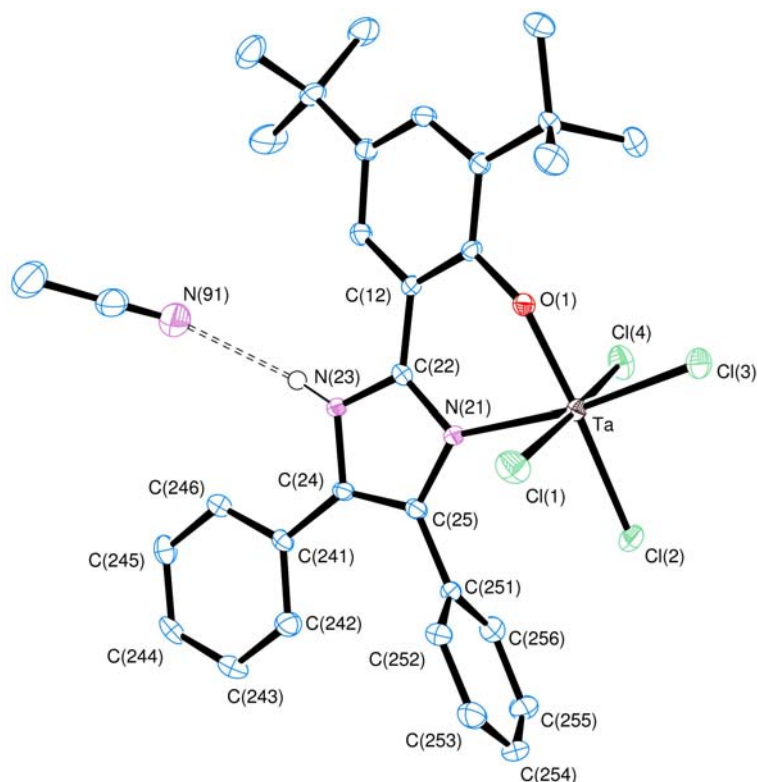
**Figure 39.** Molecular structure of  $[\text{L}^{13}\text{HNbOCl}_2(\text{MeCN})]$  (**17**(MeCN)) and hydrogen-bonded acetonitrile molecule, indicating the atom numbering scheme. Thermal ellipsoids are drawn at the 50 % probability level. Hydrogen atoms have been omitted for clarity. Selected bond lengths (Å) and angles ( $^\circ$ ): Nb-O(1) 1.951(6), N-O(2) 1.705(4), Nb-Cl(1) 2.3889(15), Nb-Cl(2) 2.3772(16), Nb-N(21) 2.234(4), Nb-N(61) 2.493(5); O(1)-Nb-Cl(1) 154.24(19), Cl(2)-Nb-N(21) 163.66(12), O(1)-Nb-O(2) 100.8(2), O(2)-Nb-N(21) 96.37(17), O(2)-Nb-N(61) 177.38(18).

In structures **16** and **17**, the niobium centre is present in a distorted octahedral environment. The phenyl rings are rotated  $83.2^\circ$  about C(23)-C(31) and  $2.9^\circ$  about C(24)-C(51) from the imidazole ring in complex **16**. The amino NH group is hydrogen bonded to an acetonitrile solvent molecule in both crystals. The rotation of rings in **17** are quite different, *viz*  $-19.2^\circ$  about C(12)-C(22),  $45.1^\circ$  about C(24)-C(56) and  $66.9^\circ$  about C(25)-C(31). The NH group here forms a hydrogen bond with O(2) of a neighbouring molecule, and an acetonitrile molecule in this crystal is coordinated to the niobium in one of two distinct orientations.



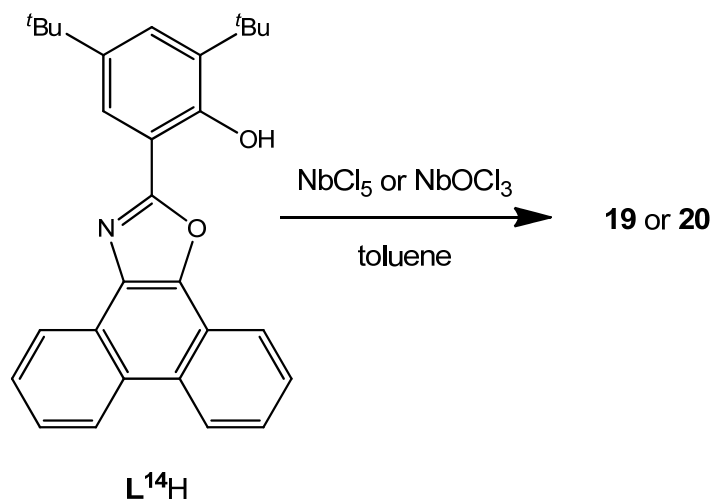
**Scheme 23.** Synthesis of tantalum(V) complex **18**

Following the complexation of the phenoxy-imine/imidazole ligand  $\text{L}^{13}\text{H}_2$  with niobium, tantalum pentachloride was reacted with  $\text{L}^{13}\text{H}_2$  using the same method described for the synthesis of pro-catalysts **16** and **17**. The reaction yielded dark red crystals, suitable for X-ray analysis. Like in its  $[\text{NbCl}_4]$  counterpart, complex **16**, there is no acetonitrile molecule coordinated to the metal centre in pro-catalyst **18**. However, there is an acetonitrile molecule linked to the NH of the imidazole ring through a hydrogen bond, which is also the case with complexes **16** and **17**.



**Figure 40.** Molecular structure of  $[\text{L}^{13}\text{HTaCl}_5(\text{MeCN})]$  (**18**(MeCN)) and hydrogen-bonded acetonitrile molecule, indicating the atom numbering scheme. Thermal ellipsoids are drawn at the 50 % probability level. Hydrogen atoms have been omitted for clarity. Selected bond lengths ( $\text{\AA}$ ) and angles ( $^\circ$ ): Ta-O(1) 1.8706(13), Ta-Cl(3) 2.3136(5), Ta-Cl(1) 2.3532(6), Ta-Cl(2) 2.3116(5), Ta-Cl(4) 2.3789(6), Ta-N(21) 2.2507(16); O(1)-Ta-Cl(1) 93.17(4), Cl(2)-Ta-N(21) 93.43(4), O(1)-Ta-N(21) 79.58(6), Cl(3)-Ta-Cl(4) 94.64(2), O(1)-Ta-Cl(2) 170.83(5), N(21)-Ta-Cl(3) 171.23(4), Cl(1)-Ta-Cl(4) 172.89(2).

Compounds **16** and **18** are isostructural, with similar coordination dimensions; the major difference in the imidazole ligand appears to be in the rotation about the C(2)-C(21) bond in **16**,  $-13.9^\circ$  versus  $1.4^\circ$  about C(12)-C(22) in **18**. The phenyl rings are rotated  $83.2^\circ$  about C(23)-C(31) and  $2.9^\circ$  about C(24)-C(51) from the imidazole ring in **16**; the corresponding angles in **18** are  $83.4$  and  $3.4^\circ$ .

**2.3 Niobium(V) complexes supported by phenoxy-imine/oxazole ligands****Scheme 24.** Synthesis of niobium(V) complexes **19** and **20**.

A similar procedure to that used to produce complexes **16** and **17** was utilised to synthesise pro-catalysts **19** and **20**. The oxazole ligand **L<sup>14</sup>H** was reacted with one equivalent of [NbCl<sub>5</sub>] or [NbOCl<sub>3</sub>] in toluene to produce **19** and **20**, respectively, in good yields. Extraction into warm acetonitrile and prolonged standing of the saturated solution at ambient temperature afforded red/orange crystals of **20** suitable for single crystal X-ray diffraction studies. The molecular structure of **20** is shown in Figure 41.

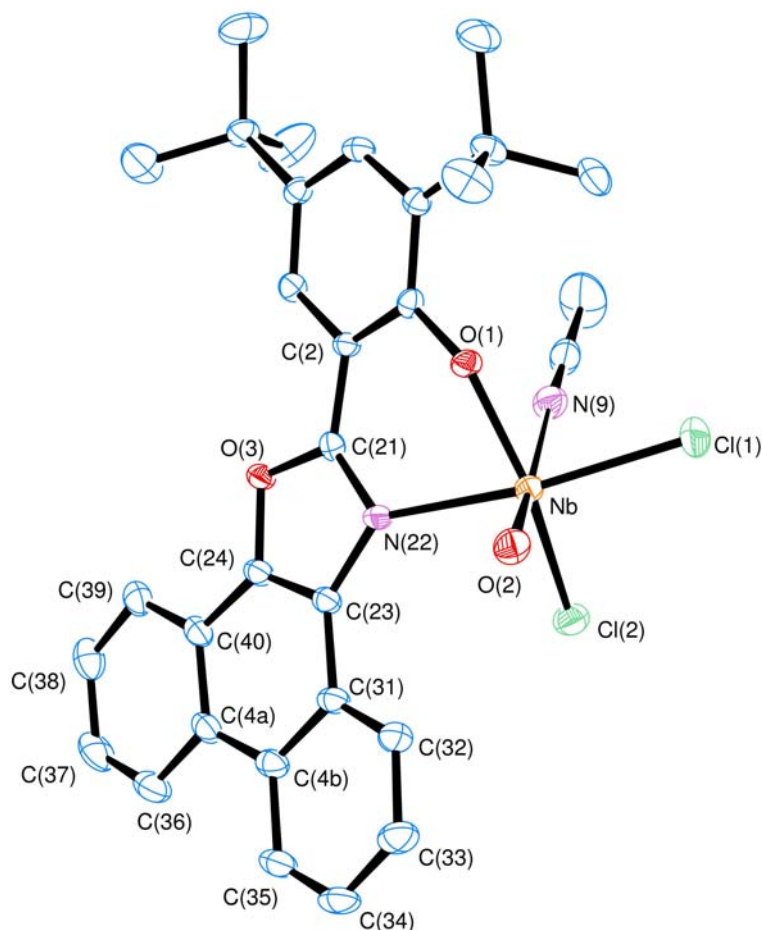


**Figure 41.** Molecular structure of  $[\text{L}^{14}\text{NbOCl}_2(\text{MeCN})]$  (**20**(MeCN)) and hydrogen-bonded acetonitrile molecule, indicating the atom numbering scheme. Thermal ellipsoids are drawn at the 50 % probability level. Hydrogen atoms have been omitted for clarity. Selected bond lengths (Å) and angles ( $^\circ$ ): Nb – O(1) 1.9319(16), Nb – O(2) 1.6899(16), Nb–N(22) 2.2727(18), Nb–Cl(1) 2.3741(6), Nb–Cl(2) 2.3696(7); O(1)–Nb–N(22) 78.78(7), O(1)–Nb–Cl(2) 152.50(5), N(22)–Nb–Cl(1) 166.02(5), O(2)–Nb–N(9) 177.79(8).

In complex **20** the structure is best described as square-based pyramidal with the acetonitrile molecule occupying a ‘second sphere’ position rather than the sixth coordination site *trans* to the oxo group [Nb – N(9) 2.558(2) Å]; the niobium centre lies 0.3540(6) Å out of the O(1), N(22), Cl(1), Cl(2) mean-plane. The fixed conformation of the phenanthrene group in compound **20** restrains rotation about the C(23)–C(31) and C(24)–C(40) bonds to 6.3 and 2.5 $^\circ$ , respectively; the phenolate ring is rotated -7.0 $^\circ$  from the oxazole ring, giving a much more planar ligand than in the other crystals. There is no hydrogen bonding in this crystal.

## 2.4 Ethylene polymerisation

The phenoxy-imine/imidazole and oxazole niobium and tantalum complexes **15–20** were screened for their ability to polymerise ethylene using DMAC in the presence of ETA as well as other co-catalysts such as, methylaluminium sesquichloride (MASC) and methylaluminium dichloride (MADC). Polymerisation runs were completed in the presence of the re-activating agent ETA. The effect of altering the quantity of ETA on pro-catalysts was also assessed. Runs were also conducted over a range of differing temperatures to assess the thermal stability of the six pro-catalysts.

### 2.4.1 Varying co-catalyst and concentration

The variation of the concentration of DMAC and MADC was investigated to try to obtain the optimum conditions for each pro-catalyst. To enable a fair comparison, all other conditions were kept constant, *e.g.* temperature, amount of solvent, time.

**Table 16.** Varying aluminium:metal ratio and co-catalyst using pro-catalyst **17**.<sup>a</sup>

Run	Co-catalyst	[Al]:[Nb]	Yield PE(g)	Activity <sup>b</sup> ( $\times 10^3$ )
1	DMAC	2000	0.070	0.56
2	DMAC	4000	0.089	0.71
3	DMAC	6000	0.090	0.72
4	DMAC	8000	0.130	1.04
5	MADC	2000	0.200	1.60
6	MADC	4000	0.379	3.03
7	MADC	6000	0.525	4.20
8	MADC	8000	0.695	5.60

<sup>a</sup>1 bar ethylene, 0.5  $\mu$ mol pro-catalyst, Schlenk tests carried out in toluene (150 mL), at room temperature, in the presence of ETA (0.1 mL) for 15 min. Reaction was quenched with dilute HCl. The resulting polymer was washed with methanol (50 mL) and dried for 12 h. at 80 °C. <sup>b</sup>g/mmol.h.bar.

Pro-catalysts, **15**, **16** and **18–20**, also showed very high activity in the presence of DMAC or MADC and ETA. The highest activities were observed when using MADC as co-catalyst, showing similar trends to that observed with pro-catalyst **17**. It is evident there exists a dependence of catalytic activity on the [Nb or Ta]:[Al] concentration, which is far more dramatic for MADC than for DMAC. 8000 equivalents of co-catalyst were used for screening the remaining pro-catalysts to maximise polymer yields.

From Figure 42, it is clear that 8000 equivalents of co-catalyst to pro-catalyst is the preferred molar ratio for all the tested pro-catalysts. It was also noted that even though DMAC produced exceptionally high results for these metals, these activities were overshadowed by the surprisingly, even higher activities observed when using MADC as co-catalyst. To fully investigate the effect of the choice of co-catalyst used, methylaluminium sesquichloride (MASC) was also used with pro-catalyst **20** under the same conditions as DMAC and MADC for comparison.

**Table 17.** Testing of equivalent of co-catalyst using pro-catalyst **15**, **16** and **18-20**.<sup>a</sup>

Run	Pro-catalyst	Co-catalyst	[Al]:[Nb or Ta]	Yield PE(g)	Activity <sup>b</sup> ( $\times 10^3$ )
1	<b>15</b>	DMAC	8000	0.085	1.40
2	<b>15</b>	MADC	8000	0.195	3.10
3	<b>16</b>	DMAC	8000	0.100	1.60
4	<b>16</b>	MADC	8000	0.307	4.90
5	<b>18</b>	DMAC	8000	0.072	1.20
6	<b>18</b>	MADC	8000	0.200	3.20
7	<b>19</b>	DMAC	8000	0.084	1.30
8	<b>19</b>	MADC	8000	0.521	8.30
9	<b>20</b>	DMAC	8000	0.089	1.40
10	<b>20</b>	MADC	8000	0.382	6.10

<sup>a</sup>1 bar ethylene, 0.25 $\mu$ mol pro-catalyst, Schlenk tests carried out in toluene (150 mL), at room temperature, in the presence of ETA (0.1 mL) for 15 min. Reaction was quenched with dilute HCl, washed with methanol (50 mL) and dried for 12 h at 20 °C. <sup>b</sup>g/mmol.h.bar.

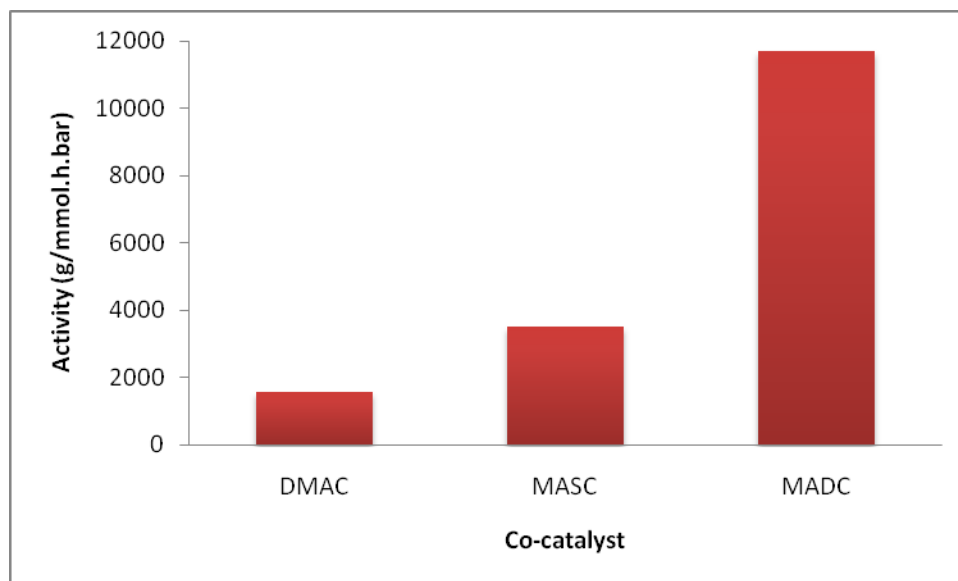


**Figure 42.** Activities of pro-catalyst **20** with varying type of co-catalyst (Conditions; 50 °C, 15 min., 0.25  $\mu$ mol pro-catalyst, 8000 eq. co-catalyst).

The obtained results were as expected. MASC can be viewed as essentially a mixture of DMAC and MADC, so the activities produced when using MASC should produce activities between that observed when DMAC and MADC are utilised. After this investigation on the nature and concentration of the co-catalyst, the impact of the re-activator, ETA, on polymerisation activity needed to be investigated. It has been noted by Gambarotta and co-workers that the use of re-activators does not always have a beneficial effect on catalytic activity.<sup>15</sup>

When no ETA was used, the yield of polymer produced was halved compared with when ETA was used. Altering the amount of ETA used, *i.e.* 700 equivalents of ETA to pro-catalyst rather than 1400 equivalents had little effect on the overall activity of the catalyst.

#### 2.4.2 Temperature screening

After screening pro-catalysts **15–20** for their behaviour towards co-catalyst variation, attention was then placed on investigating the influence of temperature on the activity of the six pro-catalysts.



**Table 18.** Testing of temperature using pro-catalyst **17**.<sup>a</sup>

Run	Co-catalyst	Temp (°C)	Yield PE(g)	Activity <sup>c</sup> (× 10 <sup>3</sup> )
1 <sup>a</sup>	DMAC	30	0.036	0.58
2 <sup>a</sup>	DMAC	40	0.067	1.07
3 <sup>a</sup>	DMAC	50	0.090	1.14
4 <sup>b</sup>	MADC	30	0.189	3.02
5 <sup>b</sup>	MADC	40	0.332	5.31
6 <sup>b</sup>	MADC	50	0.557	8.91

<sup>a</sup>0.5 μmol pro-catalyst, 0.1 mL ETA), <sup>b</sup>0.25 mmol pro-catalyst, 1 bar ethylene Schlenk tests carried out in toluene (150 mL), 8000 eq. co-catalyst, in the presence of ETA (0.05 mL) for 15 min. Reaction was quenched with dilute HCl. The polymer obtained was washed with methanol (50 mL) and dried for 12 h. at 80 °C. <sup>c</sup> g/mmol.h.bar.

As can be deduced from Table 18, there is a direct relationship between reaction temperature and polymerisation activity. As the temperature increases, the activity of pro-catalyst **17** also increases. This pattern was also noted for pro-catalysts **15**, **16** and **18-20**. (Table 19). The above table only shows initial results done in 10 °C increments, additional runs were completed in 20 °C increments up to 80 °C (Table 19, run 7). Interestingly, the systems employing MADC maintained their activity at elevated temperatures (80 °C). The trend for temperature is similar to that observed for co-catalyst concentration; when MADC is used, *i.e.* higher activities are achieved in comparison to when DMAC is used.

**Table 19.** Temperature runs using pro-catalysts **15**, **16** and **18-20**.<sup>a</sup>

Run	Pro-catalyst	Temp (°C)	Yield PE(g)	Activity <sup>b</sup> (× 10 <sup>3</sup> )
1	<b>15</b>	40	0.074	1.18
2	<b>15</b>	50	0.213	3.41
3	<b>16</b>	40	0.119	1.90
4	<b>16</b>	50	0.350	5.60
5	<b>17</b>	80	0.557	8.91
6	<b>18</b>	40	0.206	3.30
7	<b>18</b>	50	0.309	4.94
8	<b>19</b>	40	0.215	3.18
9	<b>19</b>	50	0.284	4.54
10	<b>20</b>	40	0.436	6.98
11	<b>20</b>	50	0.741	11.86

<sup>a</sup>0.25 μmol pro-catalyst, 1 bar ethylene Schlenk tests carried out in toluene (150 mL), 8000 eq. MADC, in the presence of ETA (0.05 mL) for 15 min. Reaction was quenched with dilute HCl, washed with methanol (50 mL) and dried for 12 h. <sup>b</sup> g/mmol.h.bar.

At elevated temperatures, the oxydichloride based systems (*e.g.* **20**, run 11) appear to out-perform their tetrachloride counterparts (*e.g.* **19**, run 9). From these activities pro-catalysts **15-20** can be classed as very highly active systems in the rating of catalyst efficiency (Chapter 1, section 1.5).<sup>16</sup>

### 2.4.3 Lifetime studies

Lifetime studies were carried out on pro-catalyst **17**, using both DMAC and MADC, over extended periods of time (maximum 30 minutes). The aim was to establish the lifetime of the pro-catalysts using **17** as a reference point for the related complexes.

**Table 20.** Lifetime studies using pro-catalyst **17**.<sup>a</sup>

Run	Co-catalyst	Temp. (°C)	Time (min)	Yield PE(g)	Activity <sup>b</sup> (× 10 <sup>3</sup> )	<i>M<sub>w</sub></i> <sup>c</sup>	<i>M<sub>n</sub></i> <sup>d</sup>	PDI <sup>e</sup>
1	DMAC	40	5	0.067	1.61	1030000	371000	2.8
2	DMAC	40	20	0.172	1.03	775000	228000	3.4
3	DMAC	40	30	0.386	1.54	764000	164000	4.6
4	MADC	60	5	0.228	5.47	555000	146000	3.8
5	MADC	60	10	0.202	2.42	490000	200000	2.5
6	MADC	60	30	0.615	2.46	496000	109000	4.6

<sup>a</sup>0.5 μmol pro-catalyst, 1 bar ethylene Schlenk tests carried out in toluene (150 mL), 8000 eq. co-catalyst, in the presence of ETA (0.1 mL). Reaction was quenched with dilute HCl. The resulting polymer was washed with methanol (50 mL) and dried for 12 h. <sup>b</sup> g/mmol.h.bar. <sup>c</sup> Weight average molecular weight. <sup>d</sup> Number average molecular weight. <sup>e</sup> Polydispersity index.

In the case of DMAC, there was no appreciable drop in activity over 15 min., whereas for MADC, the activity dropped by 50 % within 10 mins. In both cases, the polyethylene produced exhibited high molecular weights in the range of 490,000–1,000,000 g/mol. Generally, the DMAC runs produced higher molecular weights than the MADC runs. However, the molecular weight distributions were quite broad (2.5–4.6), indicating a lack of control over the polymerisation process. All the catalysts produced essentially linear high molecular weight polyethylene (melting points by DSC: 142 °C). Polymer samples from runs utilising DMAC contained some insoluble gel, whilst a number of the samples resulting from the use of MADC also proved too insoluble for GPC analysis. <sup>1</sup>H NMR and IR spectroscopic end group analysis of the polymer showed no vinylic groups, rather data that were consistent with the polymer containing only saturated end groups.<sup>17</sup>

### 3. Conclusion

A series of group V systems bearing phenoxy-imine/imidazole and oxazole chelating ligands have been synthesised and structurally analysed. All pro-catalysts were investigated for their efficiency as ethylene polymerisation catalysts. The choice of co-catalyst, either DMAC or MADC, was shown to have a dramatic effect on the activity of the screened pro-catalysts, as did the concentration of the chosen co-catalyst. In general, the highest activities were observed when the concentration of the co-catalyst MADC were increased. Although DMAC produced lower activities compared to when

MADC was employed, the molecular weights of the produced polymers were significantly greater.

The complexes bearing either the phenoxy-imine/imidazole or oxazole ligands showed greater thermal stability in comparison to the more ‘classical’ phenoxy-imine niobium(V) pro-catalyst. All pro-catalysts were shown to be very highly active for the polymerisation of ethylene under the utilised conditions<sup>16</sup> with activities exceeding those previously reported for known niobium  $\alpha$ -olefin polymerisation catalysts.<sup>18</sup>

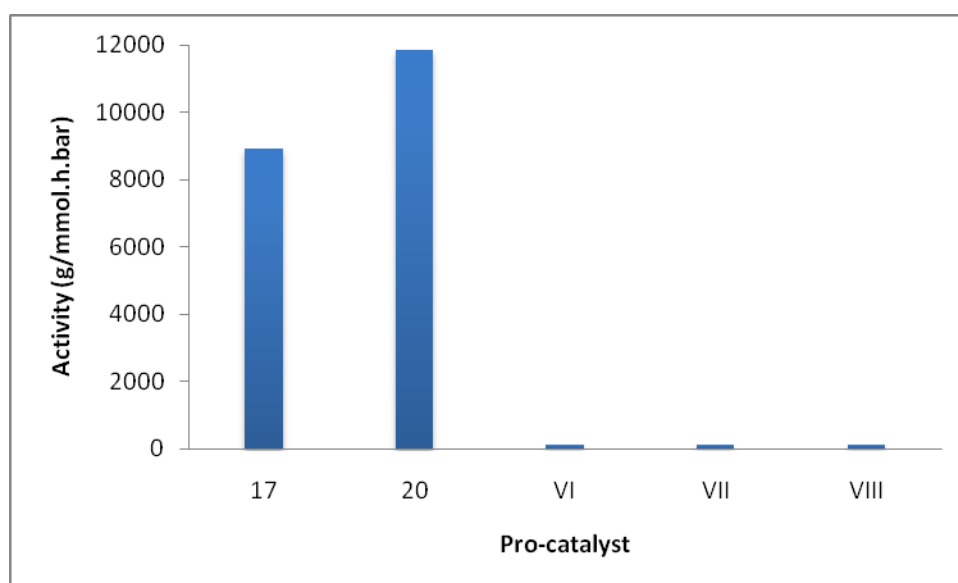


**Figure 43.** Comparing niobium pro-catalysts **17** and **20** with known literature examples of niobium-based pro-catalysts (**VI**, **VII** and **VIII**, Chapter 1, section 1.7)

- 
- 1 V. Busico, *Dalton Trans.*, 2009, 8794
  - 2 a) C. Redshaw, M. A. Rowan, D. M. Homden, S. H. Dale, M. R. J. Elsegood, S. Matsui, S. Matsuura, *Chem. Commun.*, 2006, 3329 b) C. Redshaw, M. A. Rowan, L. Warford, D. M. Homden, A. Arbaoui, M. R. J. Elsegood, S. H. Dale, T. Yamato, C. Pérez-Casas, S. Matsui, S. Matsuura, *Chem. Eur. J.*, 2007, **13**, 1090 c) C. Redshaw, L. Warford, S. H. Dale, M. R. J. Elsegood, *Chem. Commun.*, 2004, 1954
  - 3 a) Y. Nakayama, H. Bando, Y. Sonobe, T. Fujita, *J. Mol. Catal. A: Chem.*, 2004, **213**, 141 b) Y. Nakayama, H. Bando, Y. Sonobe, Y. Suzuki, T. Fujita, *Chem. Lett.*, 2003, **32**, 766 c) Y. Nakayama, J. Saito, H. Bando, T. Fujita, *Chem. Eur. J.*, 2006, **12**, 7546
  - 4 a) Makio, H. Terao, A. Iwashita, T. Fujita, *Chem. Rev.*, 2011, **111**, 2363 b) H. Makio, N. Kashiwa, T. Fujita, *Adv. Synth. Catal.*, 2002, **344**, 477 c) M. Mitani, T. T. Nakano, T. Fujita, *Chem. Eur. J.*, 2003, **9**, 2396 d) S. Matsui, T. Fujita, *Catal. Today.*, 2001, **66**, 63 e) T. Matsugi, T. Fujita, *Chem. Soc. Rev.*, 2008, **37**, 1264
  - 5 a) A. W. Kleij, *Eur. J. Inorg. Chem.*, 2009, 193 b) Y. –P. Tong, S. –L. Zheng, X. –M. Chen, *Eur. J. Inorg. Chem.*, 2005, **18**, 3734
  - 6 a) C. Foulon, C. Danel, C. Vaccher, S. Yous, J. –P. Bonte, J. –F. Goossens, *J. Chromatogr. A*, 2004, **131**, 1035 b) W. Lin, L. Long, L. Yuan, Z. Cao, B. Chen, W. Tan, *Org. Lett.*, 2008, **10**, 5577 c) L. Bu, T. Sawada, Y. Kuwahara, H. Shosenji, K. Yishida, *Dyes Pigments*, 2003, **57**, 43
  - 7 W. N. Lipscomb, N. Sträter, *Chem. Rev.*, 1996, **96**, 2375
  - 8 Y. Sato, Y. Onozaki, T. Sugimoto, H. Kurihara, K. Kamijo, C. Kadowaki, T. Tsujino, A. Watanabe, S. Otsuki, M. Mitsuya, M. Iida, K. Haze, T. Machida, Y. Nakatsuru, H. Komatani, H. Kotani, Y. Iwasawa, *Bioorg. Med. Chem. Lett.*, 2009, **19**, 4673
  - 9 A. O. Eseola, W. Li, R. Gao, M. Zhang, X. Hao, T. Liang, N. O. Obi-Egbedi, W-H. Sun, *Inorg. Chem.*, 2009, **48**, 9133
  - 10 A. O. Eseola, W. Li, W. –H. Sun, M. Zhang, L. Xiao, J. A. O. Woods, *Dyes Pigments*, 2011, **88**, 262
  - 11 a) L. Benisvy, A. J. Blake, D. Collison, E. S. Davies, C. D. Garner, E. J. L. McInnes, J. McMaster, G. Whittaker, C. Wilson, *Chem. Commun.*, 2001, 1824 b) L. Benisvy, E. Bill, A. J. Blake, D. Collison, E. S. Davies, C. D. Garner, C. I.

- Guindy, E. J. L. McInnes, G. McArdle, J. McMaster, C. Wilson, J. Wolowska, *Dalton Trans.*, 2004, 3647
- 12 A. O. Eseola, M. Zhang, J-F. Xiang, W. Zuo, Y. Li, J. A. O. Woods, W-H. Sun, *Inorg. Chim. Acta.*, 2010, 1970
- 13 A. O. Eseola, W. Li, O. G. Adeyemi, N. Obi-Egbedi, J. A. O. Woods, *Polyhedron*, 2010, **29**, 1891
- 14 L. Ma, H. Wang, J. Yi, Q. Huang, K. Gao, W. Yang, *J. Polym. Sci: Part A.*, 2010, **48**, 417
- 15 D. Reardon, J. Guan, S. Gambarotta, G. P. A. Yap, D. R. Wilson, *Organometallics*, 2002, **21**, 4390
- 16 G. J. P. Britovesk, V. C. Gibson, D. F. Wass, *Angew. Chem. Int. Ed.*, 1999, **38**, 428
- 17 J. F. O'Keefe, *Rubber World*, 2004, **230**, 27
- 18 A. M. Raspolli Galletti, G. Pampaloni, *Coord. Chem. Rev.*, 2010, **254**, 525

## Overview

It is evident from previously reported works that group V based systems for  $\alpha$ -olefin polymerisation can potentially compete with the more well established metallocene-based systems.<sup>1,2</sup> However, there are areas of group V metal catalysis which remain to be investigated, for instance the potential of group V metals for the application of ring opening polymerisation of lactones. More fundamentally to the progression of group V based polymerisation chemistry, is the exact identification of the active species in such systems. The identification of active species will lead to more specific catalyst design for both  $\alpha$ -olefin and lactone polymerisation, which in-turn could potentially lead to even greater catalytic activities.

The study herein has also shown the importance in using the appropriate ancillary ligand and the impact the use of a chelating ligand can have on the overall activity of the metal-based catalytic system. Studies similar to this have been able to provide researchers with the knowledge to design structural features to obtain higher catalytic activities and desirable polymer properties. For example, Redshaw *et al.* noted that the use of oxacalix[3]arene ligands produced highly active vanadium(V) pro-catalysts for the polymerisation of ethylene.<sup>1</sup> This led to depleted calix[4]arenes (Chapter 2) and various sulfur bridged calix[4]arene ligands (Chapter 3) to be investigated for their potential as polymerisation catalysts. All these new vanadium-based systems showed high catalytic activities when used for ethylene polymerisation. Although these results did not surpass those previously reported by Redshaw's oxacalix[3]arene vanadium system, they did highlight the importance of the linker group between the phenolic units of the calixarene. For example, the sulfonyl systems showed higher activities than their thia- and sulfinyl- calix[4]arenes counterparts (**6>III>5>XVIII**), which as for the oxacalixarene ligand set, was thought to be due donation from the oxygens of the -SO<sub>2</sub>- linkage.

Due to the impressive results achieved by phenoxy-imine based pro-catalysts<sup>2</sup> it was assumed that the vanadium systems (**7-14**) discussed in Chapter 4 would also exhibit high activities for ethylene polymerisation. However, although they can still be classified as 'highly' active systems,<sup>3</sup> they were disappointing when compared to previously reported pro-catalysts.<sup>1-4</sup> When phenoxy-imine type ligands were applied to

other group V based systems, such as niobium (Chapter 5), the resulting pro-catalysts proved to be highly active catalysts for the polymerisation of ethylene. Indeed, the results for niobium greatly surpassed those previously reported by other groups.<sup>5</sup> Although the observed activities ( $< 11,860$  g/mmol.h.bar) do not alter the overall activity trend for group V metal-based catalysts ( $V \gg Ta > Nb$ ), it does show that with the use of an appropriate ancillary ligand set and under the right polymerisation conditions, group V-based systems based on either niobium or tantalum can also compete with those of vanadium.

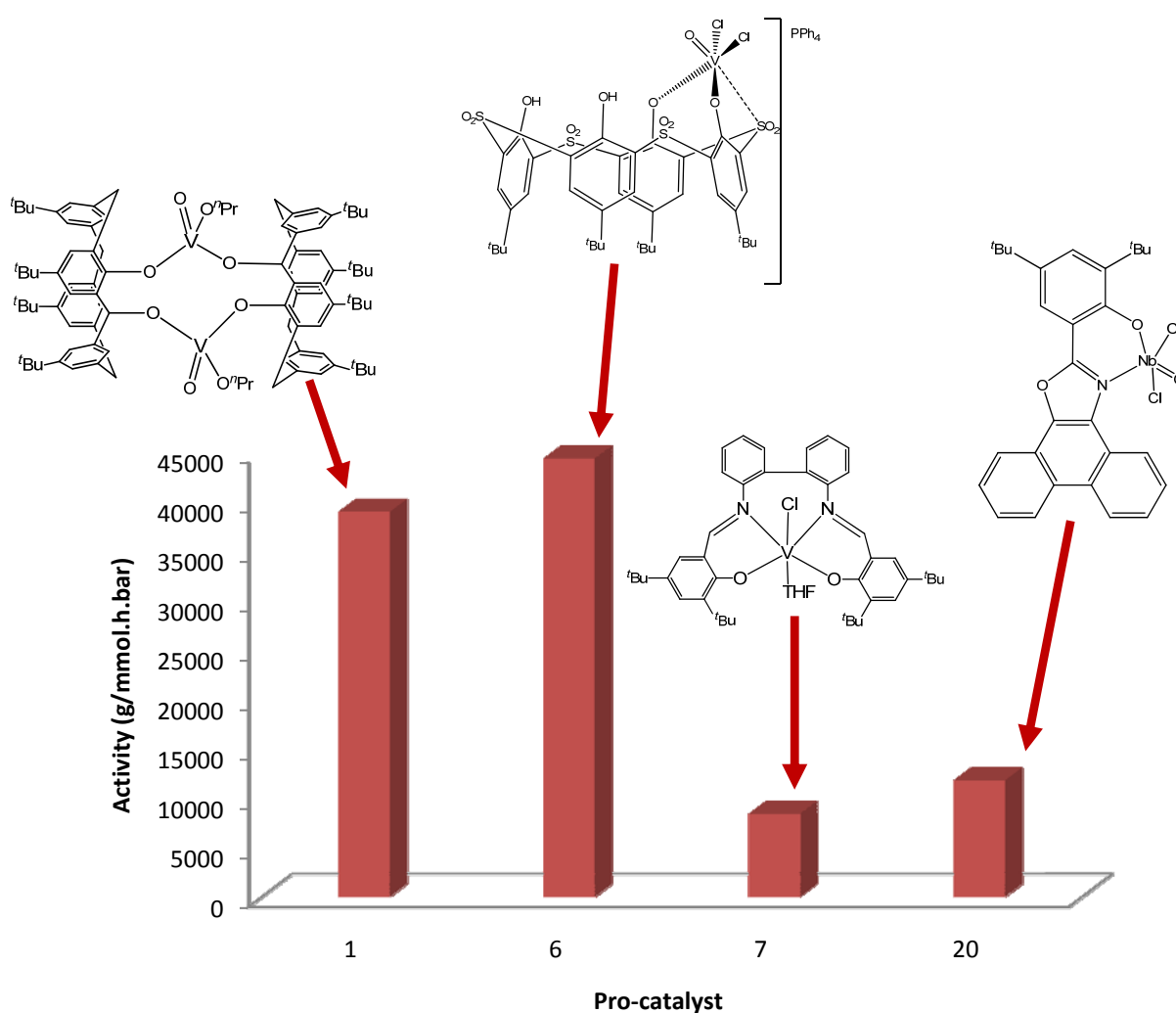


**Figure 44.** Observed catalytic activities for pro-catalysts investigated within this study.



- 
- 1 C. Redshaw, M. A. Rowan, L. Warford, D. M. Homden, A. Arbaoui, M. R. J. Elsegood, S. H. Dale, T. Yamato, C. Pérez-Casas, S. Matsui, S. Matsuura, *Chem. Eur. J.*, 2007, **13**, 1090
  - 2 a) H. Makio, H. Terao, A. Iwashita, T. Fujita, *Chem. Rev.*, 2011, **111**, 2363 b) H. Makio, N. Kashiwa, T. Fujita, *Adv. Synth. Catal.*, 2002, **344**, 477 c) M. Mitani, T. T. Nakano, T. Fujita. *Chem. Eur. J.*, 2003, **9**, 2396 d) S. Matsui, T. Fujita, *Catal. Today.*, 2001, **66**, 63 e) T. Matsugi, T. Fujita, *Chem. Soc. Rev.*, 2008, **37**, 1264
  - 3 G. J. P. Britovsek, V. C. Gibson, D. F. Wass, *Angew. Chem. Int. Ed.*, 1999, **38**, 428
  - 4 a) Y. Nakayama, H. Bando, Y. Sonobe, T. Fujita, *J. Mol. Catal. A: Chem.*, 2004, **213**, 141 b) Y. Nakayama, H. Bando, Y. Sonobe, Y. Suzuki, T. Fujita, *Chem. Lett.*, 2003, **32**, 766 c) Y. Nakayama, J. Saito, H. Bando, T. Fujita, *Chem. Eur. J.*, 2006, **12**, 7546 d) C. Redshaw, M. A. Rowan, D. M. Homden, S. H. Dale, M. R. J. Elsegood, S. Matsui, S. Matsuura, *Chem. Commun.*, 2006, 3329 e) C. Redshaw, L. Warford, S. H. Dale, M. R. J. Elsegood, *Chem. Commun.*, 2004, 1954
  - 5 A. M. Raspolli Galletti, G. Pampaloni, *Coord. Chem. Rev.*, 2010, **254**, 525

## **Chapter 6**

### **Experimental section**

## 1. General considerations

All manipulations, unless otherwise stated, were carried out under an atmosphere of dry nitrogen using conventional Schlenk and cannula techniques or in a conventional nitrogen-filled glove box. Hexane, diethyl ether and tetrahydrofuran were heated at reflux over sodium and benzophenone. Toluene was heated at reflux over sodium. Dichloromethane and acetonitrile were heated at reflux over calcium hydride. All solvents were distilled and degassed prior to use.  $\epsilon$ -Caprolactone was dried over calcium hydride, vacuum distilled and degassed prior to use. Deuterated solvents were dried over molecular sieves (4Å) ( $C_6D_6$ ,  $CD_3CN$ ,  $(CD_3)_2CO$ ) or phosphorous pentoxide ( $CDCl_3$ ) and were stored in young tap ampoules under an atmosphere of nitrogen and over activated molecular sieves (4Å) and degassed *via* several freeze-thaw cycles. IR spectra (Nujol mulls, KBr windows) were recorded on a Nicolet Avatar 360 FT IR spectrometer. Mass spectrometry data were recorded by the EPSRC National Mass Spectrometry Service Centre at Swansea University. Elemental analyses were performed by the elemental analysis service at London Metropolitan University. NMR spectra were performed at room temperature on a Varian VXR 400 S spectrometer at 400 MHz ( $^1H$ ) and 105.1 MHz ( $^{51}V$ ) NMR, a Gemini 300 NMR spectrometer at 300 MHz ( $^1H$ ) or a Bruker Avance DPX-300 spectrometer at 300 MHz. The  $^1H$  NMR spectra were calibrated against the residual protio impurity of the deuterated solvent. The  $^{51}V$  NMR spectra were calibrated against an external  $VOCl_3/CDCl_3$  reference. Solution state magnetic susceptibility was measured by Evans' method on a Varian VXR 400 S spectrometer instrument using a 5%  $d_{12}$ -cyclohexane/95%  $d_2$ -dichloromethane solution.<sup>1</sup>

Ethylene was passed over phosphorous pentoxide, 4Å molecular sieves and through a triethyl aluminium silicone oil suspension.

X-Ray crystallography was conducted by D. L. Hughes or A. -M. Fuller (complex **15**) on an Oxford Diffraction Xcalibur-3 CCD diffractometer equipped with a Mo-K $\alpha$  radiation and graphite monochromator. Intensity data were measured by thin-slice  $\omega$ - and  $\phi$ -scans. Data were processed using the CrysAlis-CCD and -RED programs.<sup>2</sup> Structures were determined by the direct methods, on  $F^2$ , in SHELXL.<sup>3</sup> Alternatively X-ray crystallography was conducted by M. R. J. Elsegood on a Bruker SMART 1000 CCD diffractometer using narrow slice 0.38  $\omega$ -scans (data collection), SAINT (integration and cell refinement), and SHELXTL (solution, refinement and graphics) at

the Chemistry Department at Loughborough University, or on the synchrotron source at Daresbury Laboratory SRS Station 9.8 or 16.2 SMX using silicon 111 monochromated X-radiation.

Gel permeation chromatography (GPC) measurements were performed at RAPRA Technology Ltd. Polymer melting points were determined using a TA Instruments DSC Q1000 using TA Universal Analysis software. Number and weight average molecular weights ( $M_n$  and  $M_w$ ) for poly( $\epsilon$ -caprolactone) samples were measured on a Polymer Laboratories PL GPC 220 instrument equipped with PLgel 5 Å mixed C column eluted with tetrahydrofuran at 1.0 mL/min at 40 °C and calibrated using nine monodisperse polystyrene standards in the range 580–1 233 000 Da.

## 2. Synthesis of known compounds

*p*-*tert*-Butylcalix[4]arene, 1,3 depleted *p*-*tert*-butylcalix[4]arene ( $L^1H_2$ ) and *p*-*tert*-butylhexahomotrioxacalix[3]arene were synthesised according to reported literature procedures.<sup>4, 5, 6</sup>

*p*-*tert*-Butylthiacalix[4]arene, *p*-*tert*-butylsulfinylcalix[4]arene ( $L^2H_4$ ) and *p*-*tert*-butylsulfonylcalix[4]arene ( $L^3H_4$ ) were gifts from Dr Hitoshi Kumagaya of the Cosmo oil company.

Schiff base ligands  $L^4H_2$  –  $L^9H_2$  were prepared using the same method as Gibson and co-workers.<sup>7</sup> Ligands  $L^{10}H_2$  and  $L^{11}H_2$  were made using the method stated by Oleinik *et al.*<sup>8</sup> Phenoxy-imine ( $L^{12}H$ ) and phenoxy-imine/imidazole-type and oxazole ligands ( $L^{13}H_2$  and  $L^{14}H$ ) were all prepared following literature procedures.<sup>9, 10</sup>

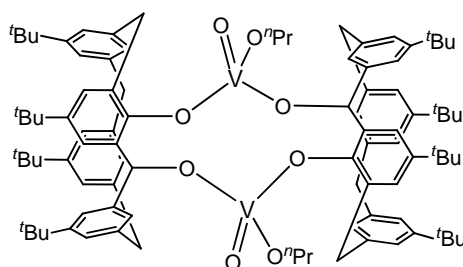
The known complex [V(O)*p*-*tert*-butylhexahomotrioxacalix[3]arene] (**III**) was prepared using the same procedure as Redshaw *et al.*<sup>11</sup> The anion [VOCl<sub>2</sub>(*p*-*tert*-butylcalix[4,S]areneH<sub>2</sub>)]<sup>−</sup> (**XVIII**) was synthesised using the same method as Limberg *et al.*<sup>12</sup> The vanadium(III) schiff base complexes [V(N,N'-ethylenebis(salicylaldiminato))Cl(THF)] (**XX**) and [V(N,N'-*o*-phenylenebis(salicylaldiminato))Cl(THF)] (**XXI**) were prepared using Gambarotta and co-workers method.<sup>13</sup>

[V(*Np*-tolyl)(OR)<sub>3</sub>] (R = <sup>t</sup>Bu or <sup>n</sup>Pr) complexes were synthesised using slight variations of reported literature procedures.<sup>14</sup> NbOCl<sub>3</sub> was prepared according to a literature procedure by Gibson and co-workers.<sup>15</sup>

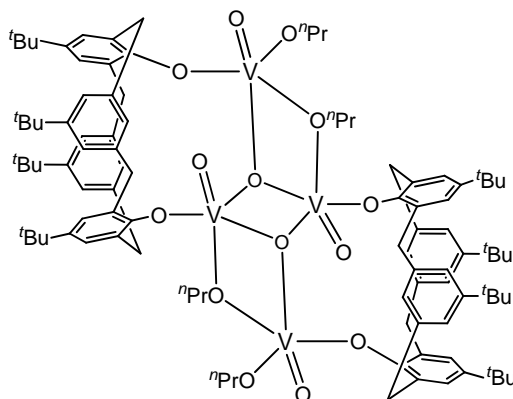
All other chemicals were obtained commercially and used as received.

### 3. Vanadium(V) complexes bearing 1,3-depleted calix[4]arenes

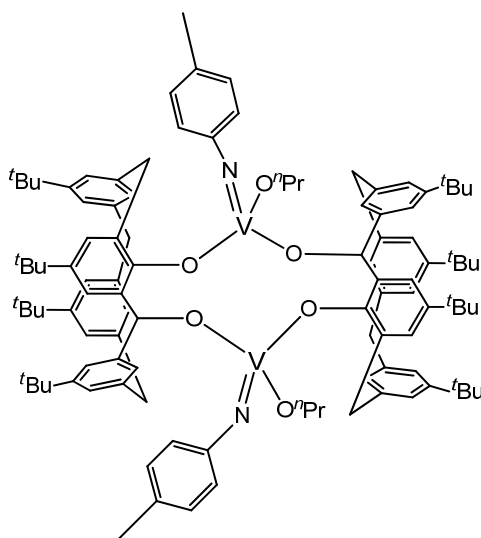
#### 3.1 Synthesis of $[\text{VO}(\text{O}^i\text{Pr})\text{L}^1]_2$ (**1**)



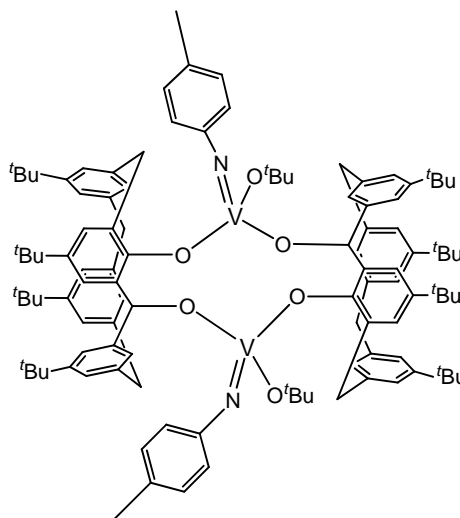
A solution of 1,3-depleted calix[4]arene,  $\text{L}^1\text{H}_2$  (0.5g, 0.81 mmol) and  $[\text{VO}(\text{O}^i\text{Pr})_3]$  (1.1 *eq.*, 0.22 g, 0.90 mmol) was added to a solution of ligand  $\text{L}^1\text{H}_2$  in 30 mL toluene. The reaction mixture was stirred at reflux for 12 hours. The reaction solution was cooled to room temperature and volatile components removed under *vacuo*. The solid residue was extracted into hot acetonitrile and after prolonged standing **1** obtained as dark red plates. Yield: 0.47 g, 39 %. Elemental analysis calcd (%) for  $\text{V}_2\text{C}_{94}\text{H}_{122}\text{O}_8$ : C 76.18, H 8.30; found C 76.03, H 8.21. MS (E.S.):  $m/z$ : 1379  $[\text{M}-\text{O}-2^i\text{Pr}]^+$ , 1297  $[\text{M}^+-\text{VO}]^+$ , 1280  $[\text{M}^+-\text{O}2\text{H}]^+$ . IR (Nujol mull, KBr): 1596(m), 1364(m), 1261(s), 1203(m), 1096(s), 1016(s), 977(w), 936(w), 891(w), 869(w), 799(s), 707(w), 626(m).  $^1\text{H}$  NMR ( $\text{CDCl}_3$ ):  $\delta$  = 7.11 (s, 1H, ArH), 7.06 (s, 3H, ArH), 6.95 (s, 9H, ArH), 6.93 (s, 4H, ArH), 5.01–4.9 (m, 4H,  $\text{OCH}_2\text{CH}_2\text{CH}_3$ ), 4.60 (dd, 8H,  $^1J = 5.5$ ,  $^2J = 13.7$ , Ar $\text{CH}_2\text{Ar}$ ), 3.60 (d, 4H,  $J = 14.1$ , Ar $\text{CH}_2\text{Ar}$ ), 3.30 (d, 4H,  $J = 13.7$ , Ar $\text{CH}_2\text{Ar}$ ), 1.90 (s, 3H,  $\text{CH}_3\text{CN}$ ), 1.70 (m, 4H,  $\text{OCH}_2\text{CH}_2\text{CH}_3$ ), 1.32 (s, 36H,  $\text{C}(\text{CH}_3)_3$ ), 1.22 (s, 18H,  $\text{C}(\text{CH}_3)_3$ ), 1.10 (s, 18H,  $\text{C}(\text{CH}_3)_3$ ), 0.80 (t, 6H,  $J = 7.4$ ,  $\text{OCH}_2\text{CH}_2\text{CH}_3$ ).  $^{51}\text{V}$  NMR ( $\text{CDCl}_3$ ):  $\delta$  = -533.32 ( $\omega_{1/2}$  140 Hz).

3.2 Synthesis of  $\{[\text{VO}(\text{O}^n\text{Pr})]_2(\mu\text{-O})\text{L}^1\}_2$  (**2**)

The minor hydrolysed product of **1** was obtained as dark red clusters. Yield: 0.39g, 27 %. Elemental analysis calcd (%) for  $\text{V}_4\text{C}_{100}\text{H}_{136}\text{O}_{14}$ : C 68.01, H 7.76; found C 68.12, H 7.60. MS (E.S.):  $m/z$ : 1765  $[\text{M}]^+$ , 1722  $[\text{M}^+ - n\text{Pr}]^+$ . IR (Nujol mull, KBr): 2248(w), 1592(s), 1363(m), 1261(s), 1201(s), 1101(s), 1056(s), 1033(s), 1001(s), 973(s), 937(w), 893(m), 869(m), 841(m), 799(s), 774(m), 709(w), 625(s).  $^1\text{H}$  NMR ( $\text{CDCl}_3$ ):  $\delta$  = 7.25 – 7.22 (m, 1H, ArH), 7.17-7.10 (m, 8H, ArH), 7.0-6.90 (m, 8H, Ar-H), 6.19 (s, 2H, ArH), 6.05(s, 1H, ArH), 5.47–5.14 (overlapping m, 8H,  $\text{OCH}_2\text{CH}_2\text{CH}_3$ ), 4.78 (dd, 4H,  $^1J = 15.9$ ,  $^2J = 22.3$ ,  $\text{ArCH}_2\text{Ar}$ ), 4.10 (dd, 4H,  $^1J = 15.6$ ,  $^2J = 25.5$ ,  $\text{ArCH}_2\text{Ar}$ ), 3.75 (t, 4H,  $J = 14.6$ ,  $\text{ArCH}_2\text{Ar}$ ), 3.60 (d, 4H,  $J = 14.8$ ,  $\text{ArCH}_2\text{Ar}$ ), 1.95 (s, 3H,  $\text{CH}_3\text{CN}$ ), 1.80 (m, 8H,  $\text{OCH}_2\text{CH}_2\text{CH}_3$ ), 1.32 (s, 25H,  $\text{C}(\text{CH}_3)_3$ ), 1.22 (s, 46H,  $\text{C}(\text{CH}_3)_3$ ), 1.00 (t, 12H,  $J = 7.4$ ,  $\text{OCH}_2\text{CH}_2\text{CH}_3$ ).  $^{51}\text{V}$  NMR ( $\text{CDCl}_3$ ):  $\delta$  = -625.71 ( $\omega_{1/2}$  160 Hz).

3.3 Synthesis of  $[V(Np\text{-tolyl})(O^iPr)L^1]_2$  (**3**)

As described for **1** but using  $[V(Np\text{-tolyl})(O^iPr)_3]$  (1.1 eq., 0.3 g, 0.90 mmol) and  $L^1H_2$  (0.50 g, 0.81 mmol) afforded yellow blocks. Yield: 0.57 g, 43 %. Elemental analysis calcd (%) for  $V_2C_{108}H_{136}N_2O_6$ : C 78.14, H 8.26, N 1.69; found C 77.93, H 8.13, N 1.78. MS (E.S.):  $m/z$ : 1660  $[M]^+$ , 1600  $[M^+ - O^iPr]$ . IR (Nujol mull, KBr): 1595(s), 1363(w), 1261(s), 1199(m), 1097(s), 1071(s), 1021(s), 959(w), 888(w), 868(w), 800(s), 772(s), 649(w), 623(w).  $^1H$  NMR ( $CDCl_3$ ):  $\delta$  = 7.79 (s, 2H, ArH), 7.71 (s, 1H, ArH), 7.10-7.05 (overlapping m, 10H, ArH), 6.90 (d, 4H, ArH), 6.74 (s, 4H, ArH), 6.70 (d, 3H,  $J$  = 8.2, ArH), 6.10 (d, 4H,  $J$  = 8.2, ArH), 5.00 (m, 4H,  $OCH_2CH_2CH_3$ ), 4.76 (dd, 8H,  $^1J$  = 13.1,  $^2J$  = 22.5,  $ArCH_2Ar$ ), 3.50 (d, 4H,  $J$  = 12.2,  $ArCH_2Ar$ ), 3.10 (d, 4H,  $J$  = 12.9,  $ArCH_2Ar$ ), 2.22 (s, 6H,  $Np\text{-tolyl}CH_3$ ), 1.96 (s, 3H,  $CH_3CN$ ), 1.85 (m, 4H,  $OCH_2CH_2CH_3$ ), 1.27 (s, 18H,  $C(CH_3)_3$ ), 1.19 (s, 36H,  $C(CH_3)_3$ ), 1.16 (s, 18H,  $C(CH_3)_3$ ), 0.80 (t, 6H,  $J$  = 7.4,  $OCH_2CH_2CH_3$ ).  $^{51}V$  NMR ( $CDCl_3$ ):  $\delta$  = -486.89 ( $\omega_{1/2}$  335 Hz).

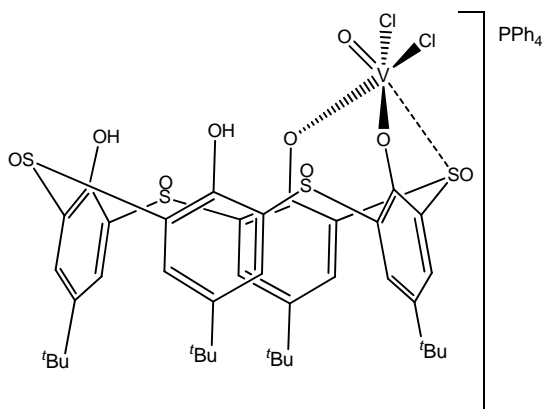
3.4 Synthesis of  $[V(Np\text{-toly})_2(O^tBu)_2]_2$  (**4**)

As described for **1** but using  $[V(Np\text{-toly})(O^tBu)_3]$  (1.1 eq., 0.34 g, 0.90 mmol) and  $L^1H_2$  (0.50 g, 0.81 mmol) afforded yellow laths. Yield: 0.53 g, 40 %. Elemental analysis calcd (%) for  $V_2C_{110}H_{140}N_2O_6$ : C 78.26, H 8.36, N 1.66 ; found C 78.17, H 8.26, N 1.76. MS (E.S.):  $m/z$ : 1688  $[M]^+$ , 1632  $[M-tBu]^+$ , 1558  $[M-O^tBu]^+$ . IR (Nujol mull, KBr): 1596(m), 1361(m), 1316(w), 1260(s), 1170(s), 1093(s), 1014(s), 966(s), 868(w), 838(w), 814(m), 796(s), 774(w).  $^1H$  NMR ( $CDCl_3$ ):  $\delta$  = 7.65 (s, 1H, ArH), 7.56 (s, 1H, ArH), 7.15 (s, 2H, ArH), 7.05-6.82 (overlapping m, 10H, ArH), 6.68 (s, 4H, ArH), 6.52 (d, 4H,  $J$  = 8.1, ArH), 6.40 (d, 6H,  $J$  = 8.3, ArH), 4.70 (d, 4H,  $J$  = 15.3, ArCH<sub>2</sub>Ar), 4.55 (d, 4H,  $J$  = 14.1, ArCH<sub>2</sub>Ar), 3.70 (overlapping m, 8H, ArCH<sub>2</sub>Ar), 2.38 (s, 6H, Np-tolylCH<sub>3</sub>), 2.00 (s, 3H, CH<sub>3</sub>CN), 1.58–1.44 (overlapping m, 81H, C(CH<sub>3</sub>)<sub>3</sub>), 1.33 (s, 9H, C(CH<sub>3</sub>)<sub>3</sub>).  $^{51}V$  NMR ( $CDCl_3$ ):  $\delta$  = -602.19 ( $\omega_{1/2}$  400 Hz), -608.08 ( $\omega_{1/2}$  400 Hz).

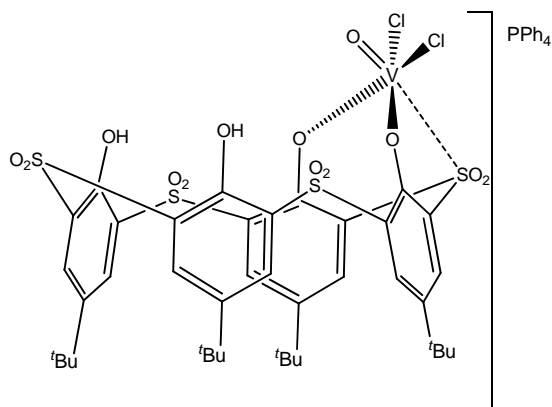


## 4. Oxovanadium(V) complexes bearing sulfur-bridged calix[4]arenes

### 4.1 Synthesis of anion $[\text{VOCl}_2(\text{L}^2\text{H}_2)]^-$ (**5**)



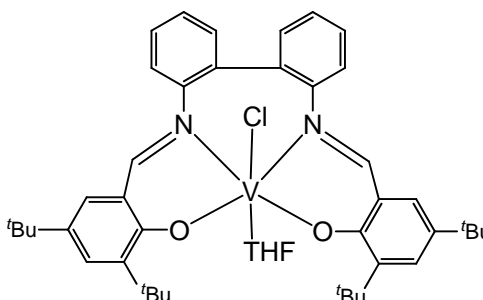
Complex **5** was synthesized using the method of Limberg *et al.*<sup>12</sup> employed for the anion  $[\text{VOCl}_2(\text{p-tert-butylcalix}[4,\text{S}]\text{areneH}_2)]^-$  (**XVIII**) using *p-tert-butylcalix*[4,SO]areneH<sub>2</sub>, L<sup>2</sup>H<sub>4</sub> (1.0 g, 1.27 mmol) with [PPh<sub>4</sub>][VO<sub>2</sub>Cl<sub>2</sub>] (0.70 g, 1.4 mmol), affording blue crystals. Yield: 0.62 g, 77 %. Elemental analysis calcd (%) for C<sub>64.5</sub>H<sub>67</sub>Cl<sub>8</sub>O<sub>13</sub>PS<sub>4</sub>V (sample dried in *vacuo* for 12 h, - 2CH<sub>2</sub>Cl<sub>2</sub>): C 60.99, H 5.28; found C 60.78, H 5.19. MS (E.S.): *m/z*: 1259 [M]<sup>+</sup>, 1242 [M<sup>+</sup>-O]<sup>+</sup>, 1211 [M<sup>+</sup>-2OH]<sup>+</sup>. IR (Nujol mull, KBr): 1586 (w), 1261 (s), 1095(s), 1019(s), 966(m), 864(m), 800(s), 725(w). <sup>1</sup>H NMR (CDCl<sub>3</sub>, 300 MHz, 254 K) δ = 8.81 (bs, 2H, OH), 8.16 (m, 4H, PPh<sub>4</sub>), 8.13 (m, 4H, PPh<sub>4</sub>), 7.96–7.30 (b overlapping m, 12H, PPh<sub>4</sub> + 8H, arylH), 1.26–1.19 (3 × overlapping s, 36H, C(CH<sub>3</sub>)<sub>3</sub>). On cooling to 254 K, the *tert*-butyl region changed to two singlets δ: 1.28 (s, 18H, C(CH<sub>3</sub>)<sub>3</sub>), 1.22 (s, 18H, C(CH<sub>3</sub>)<sub>3</sub>). <sup>51</sup>V NMR (CDCl<sub>3</sub>): δ = -364.36 ppm (w<sub>1/2</sub> 60 Hz).

4.2 Synthesis of anion  $[\text{VOCl}_2(\text{L}^3\text{H}_2)]^-$  (**6**)

*p*-*tert*-Butylsulfonylcalix[4]arene,  $\text{L}^3\text{H}_4$  (0.85 g, 1.0 mmol) with  $[\text{PPh}_4][\text{VO}_2\text{Cl}_2]$  (0.54 g, 1.1 mmol) were dissolved in 40 mL tetrahydrofuran and the reaction mixture was stirred for 48 h under nitrogen. The solvent was removed under reduced pressure, and the residue extracted into dichloromethane. Slow addition of a hexane layer and diffusion over 7 days produced prismatic purple crystals. Yield: 1.02 g, 65 %. Elemental analysis calcd (%) for  $\text{C}_{64}\text{H}_{66}\text{Cl}_2\text{O}_{13}\text{PS}_4\text{V}$  (sample dried in *vacuo* for 24 h): C 58.05, H 5.02; found C 57.85, H 4.96. Mass Spec (CI negative mode): 1253 ( $\text{M}^+-2\text{Cl}$ ); (EI) : 1186 ( $\text{M}^+-2\text{Cl}-\text{VO}$ ). IR (Nujol mull, KBr): 2360(w), 1738(w), 1261(s), 1091(bs), 1020(bs), 800(s), 723(w).  $^1\text{H}$  NMR ( $\text{CDCl}_3$ , 300 MHz, 254 K)  $\delta$  = 8.81 (bs, 2H, OH), 8.16 (m, 4H,  $\text{PPh}_4$ ), 8.13 (m, 4H,  $\text{PPh}_4$ ), 7.96–7.30 (b overlapping m, 12H,  $\text{PPh}_4$  + 8H, arylH), 1.26–1.19 (3  $\times$  overlapping s, 36H,  $\text{C}(\text{CH}_3)_3$ ). On cooling to 254 K, the *tert*-butyl region changed to two singlets  $\delta$ : 1.28 (s, 18H,  $\text{C}(\text{CH}_3)_3$ ), 1.22 (s, 18H,  $\text{C}(\text{CH}_3)_3$ ).  $^{51}\text{V}$  ( $\text{CDCl}_3$ ):  $\delta$  = -193.3 ppm ( $w_{1/2}$  835 Hz).

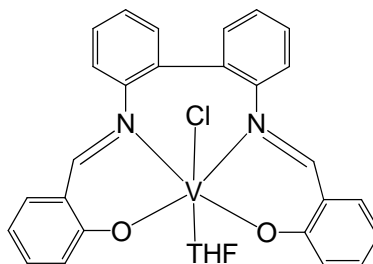
## 5. Vanadium(III) complexes bearing phenoxy-imine ligands

### 5.1 Synthesis of $L^4VCl(THF)$ (**7**)

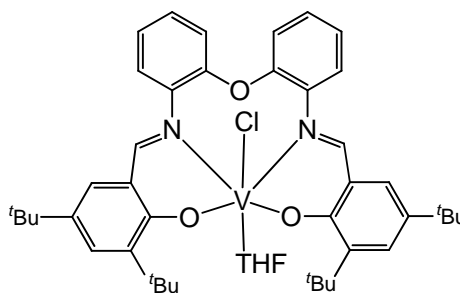


To a solution of  $L^4H_2$  (0.5 g, 0.8 mmol) in THF (20 mL),  $[VCl_3 \cdot 3THF]$  (0.67 g, 1.8 mmol) was added and this solution stirred for 10 minutes before adding  $Et_3N$  (0.25 mL, 1.8 mmol). The solution was stirred at room temperature for 4 hours and then concentrated to approximately 15 mL. The mixture was filtered and recrystallised by diffusion of hexane (10 mL) to yield complex **7** as a brown powder. Yield: 0.42 g, 47 %. Elemental analysis calcd (%) for  $VC_{46}H_{58}ClN_2O_3$ : C 71.44, H 7.56, N 3.62; found C 71.42, H 7.39, N 3.53. MS (EI,  $m/z$ ): 700  $[M-THF]^+$ , 666  $[M-Cl]^+$ . IR (Nujol mull, KBr): 1946(w), 1808(w), 1741(w), 1610(s), 1589(s), 1553(m), 1535(s), 1303(m), 1254(s), 1199(s), 1173(s), 917(w), 874(m), 843(s), 750(m), 661(w), 641(w). Magnetic moment  $\mu = 2.70\mu_B$ .

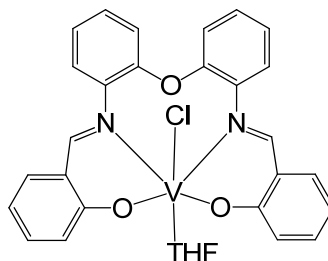
### 5.2 Synthesis of $L^5VCl(THF)$ (**8**)



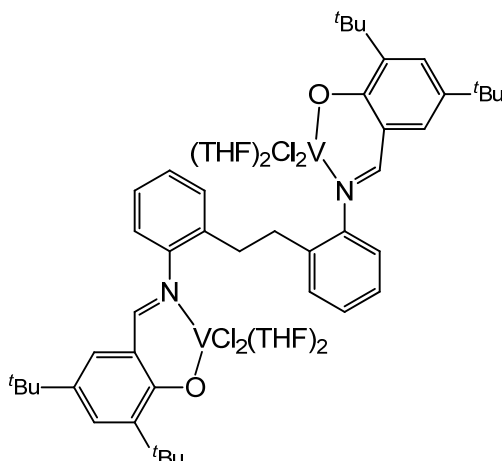
Procedure as described for complex **7** using  $L^5H_2$  (0.5 g, 1.2 mmol),  $[VCl_3 \cdot 3THF]$  (0.97 g, 2.6 mmol) and  $Et_3N$  (0.36 mL, 2.6 mmol). Complex **8** was obtained maroon crystals. Yield: 0.56 g, 51 %. Elemental analysis calcd (%) for  $VC_{26}H_{18}ClN_2O_2$  (baked dried under *vacuo* for 24 h – THF): C 65.49, H 3.80, N 5.87; found C 65.40, H 3.87, N 5.78. MS (EI,  $m/z$ ): 476  $[M-THF]^+$ , 441  $[M-Cl]^+$ . IR (Nujol mull, KBr): 1605(s), 1537(s), 1297(m), 1188(m), 1148(m), 924(w), 853(m), 757(m), 737(w), 722(w). Magnetic moment  $\mu = 2.23\mu_B$ .

5.3 Synthesis of **L<sup>6</sup>VCl(THF) (9)**

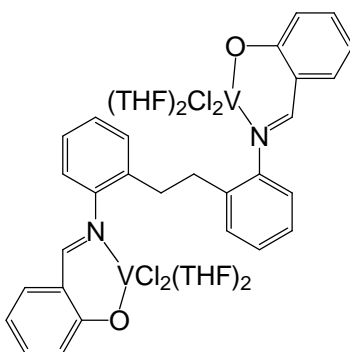
Procedure as described for complex **7** using **L<sup>6</sup>H<sub>2</sub>** (0.5 g, 0.8 mmol), [VCl<sub>3</sub>.3THF] (0.34 g, 0.9 mmol) and Et<sub>3</sub>N (0.13 mL, 0.9 mmol). Complex **9** was obtained as a dark brown powder. Yield: 0.34 g, 54 %. Elemental analysis calcd (%) for VC<sub>46</sub>H<sub>58</sub>ClN<sub>2</sub>O<sub>4</sub>: C 69.99, H 7.41, N 3.55; found C 69.81, H 7.55, N 3.35. MS (EI, *m/z*): 716 [M-THF]<sup>+</sup>, 682 [M-Cl]<sup>+</sup>. IR (Nujol mull, KBr): 1769(w), 1609(s), 1574(s), 1552(m), 1534(s), 1487(s), 1304(s), 1201(s), 1168(s), 940(m), 872(s), 754(s), 703(w), 647(w). Magnetic moment  $\mu = 1.91\mu_B$ .

5.4 Synthesis of **L<sup>7</sup>VCl(THF) (10)**

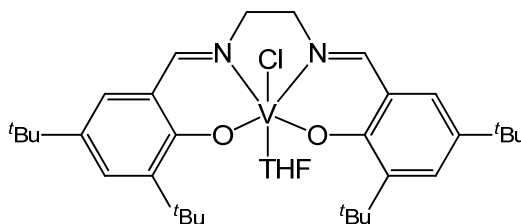
Procedure as described for complex **7** using **L<sup>7</sup>H<sub>2</sub>** (0.5 g, 1.2 mmol), [VCl<sub>3</sub>.3THF] (0.97 g, 2.6 mmol) and Et<sub>3</sub>N (0.36 mL, 2.6 mmol). Complex **10** was obtained as a dark brown powder. Yield: 0.43 g, 63 %. Elemental analysis calcd (%) for VC<sub>30</sub>H<sub>26</sub>ClN<sub>2</sub>O<sub>4</sub>: C 63.78, H 4.64, N 4.96; found C 63.37, H 4.85, N 4.83. MS (EI, *m/z*): 492 [M-THF]<sup>+</sup>, 457 [M-Cl]<sup>+</sup>. IR (Nujol mull, KBr): 1946(w), 1631(m), 1606(s), 1537(s), 861(s), 726(w), 704(m), 659(m), 621(m). Magnetic moment  $\mu = 1.78\mu_B$ .

5.5 Synthesis of  $L^8[VCl_2(THF)_2]_2$  (**11**)

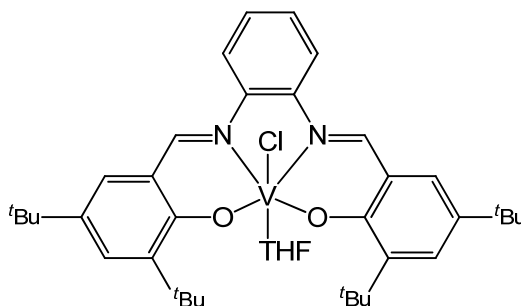
Procedure as described for complex **7** using  $L^8H_2$  (0.25 g, 0.6 mmol),  $[VCl_3 \cdot 3THF]$  (0.33 g, 0.9 mmol) and  $Et_3N$  (0.12 mL, 0.9 mmol). Complex **11** was obtained dark red plates. Yield: 0.57 g, 65 %. Mp: 110 °C. Elemental analysis calcd (%) for  $V_2C_{60}H_{86}Cl_4N_2O_6$ : C 61.33, H 7.38, N 2.38; found C 61.24, H 7.28, N 2.45. MS (EI,  $m/z$ ): 693  $[M-V-4Cl-4THF]^+$ . IR (Nujol mull, KBr): 1609(m), 1598(w), 1539(m), 1410(w), 705(m), 687(w), 665(w). Magnetic moment  $\mu = 1.90\mu_B$ .

5.6 Synthesis of  $L^9[VCl_2(THF)_2]_2$  (**12**)

Procedure as described for complex **7** using  $L^9H_2$  (0.25 g, 0.6 mmol),  $[VCl_3 \cdot 3THF]$  (0.49 g, 1.3 mmol) and  $Et_3N$  (0.18 ml, 1.3 mmol). Complex **12** was obtained as a red powder. Yield: 0.34 g, 61 %. Elemental analysis calcd (%) for  $V_2C_{44}H_{54}Cl_4N_2O_6$ : C 55.59, H 5.73, N 2.95; found C 55.65, H 5.6, N 3.07. MS (EI,  $m/z$ ): 468  $[M-V-4Cl-4THF]^+$ . IR (Nujol mull, KBr): 1608(s), 1542(m), 1300(m), 926(w), 862(m), 756(m), 739(m), 705(w), 664(w), 637(m). Magnetic moment  $\mu = 2.18\mu_B$ .

5.7 Synthesis of  $L^{10}VCl(THF)$  (**13**)

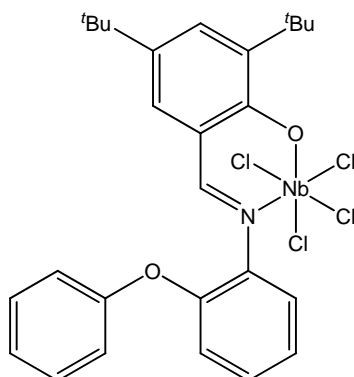
Using the literature procedure as described for Complex **XX**<sup>13</sup> using  $L^{10}H_2$  (0.5 g, 1.0 mmol),  $[VCl_3 \cdot 3THF]$  (0.41 g, 1.1 mmol) and  $Et_3N$  (0.15 mL, 1.1 mmol). Complex **13** was obtained as a dark brown/red powder. Yield: 0.37 g, 64 %. MS (EI,  $m/z$ ): 576  $[M-THF]^+$ . IR (Nujol mull, KBr): 2730(w), 1943(w), 1804(w), 1744(w), 1610(s), 1538(s), 1412(m), 1363(m), 1336(m), 1303(m), 1200(m), 1173(s), 916(m), 750(s), 685(w), 661(w). Magnetic moment  $\mu = 1.83\mu_B$ .

5.8 Synthesis of  $L^{11}VCl(THF)$  (**14**)

Using the literature procedure as described for Complex **XXI**<sup>13</sup> using  $L^{11}H_2$  (0.5 g, 0.9 mmol),  $[VCl_3 \cdot 3THF]$  (0.37 g, 1.0 mmol) and  $Et_3N$  (0.14 mL, 1.0 mmol). Complex **14** was obtained as a dark brown/red powder. Yield: 0.24 g, 43 %. MS (EI,  $m/z$ ): 624  $[M-THF]^+$ , 590  $[M-Cl]^+$ . IR (Nujol mull, KBr): 1943(w), 1801(w), 1649(s), 1599(s), 1580(s), 1532(s), 1427(m), 1383(s), 1362(s), 1311(m), 1198(m), 1171(s), 919(m), 833(w), 754(s), 711(w), 642(w), 581(s). Magnetic moment  $\mu = 1.91\mu_B$ .

## 6. Niobium(V) complex bearing a phenoxy-imine ligand

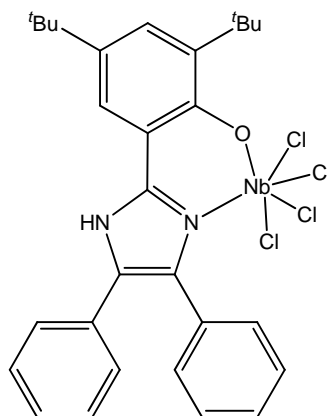
### 6.1 Synthesis of $L^{12}NbCl_4$ (**15**)



A solution of  $L^{12}H$  (0.50 g, 1.25 mmol) and  $[NbCl_5]$  (1.1 eq., 0.37 g, 1.38 mmol) in 30 mL toluene were refluxed for 12 hours. The reaction mixture was cooled to room temperature and volatiles removed in *vacuo*. The solid residue was extracted into hot acetonitrile, after prolonged standing at ambient temperature dark yellow/brown plates of **15** were formed. Yield: 0.42 g, 53 %. Elemental analysis calcd (%) for  $NbC_{27}H_{30}Cl_4NO_2$ : C 51.05, H 4.76, N 2.20; found C 50.92, H 4.74, N 2.18. MS (E.S.):  $m/z$ : 600  $[M-Cl]^+$ , 528  $[M^+-2Cl]^+$ , IR (Nujol mull, KBr): 1585(m), 1552(m), 1483(s), 1365(s), 1329(w), 1202(w), 1175(w), 1157(w), 1104(s), 982(w), 923(w), 891(w), 874(m), 846(w), 762(w), 752(m), 736(w), 688(m), 619(w).  $^1H$  NMR ( $CDCl_3$ ):  $\delta$  = 8.44 (s, 1H,  $CH=N$ ), 7.80 (d, 1H,  $J=2.2$ ,  $ArH$ ), 7.50 (dd, 1H,  $^1J=2.2$ ,  $^2J=7.9$ ,  $ArH$ ), 7.36–7.30 (overlapping m, 3H,  $ArH$ ), 7.25–7.18 (overlapping m, 1H,  $ArH$ ), 7.13–7.06 (overlapping m, 4H,  $ArH$ ), 6.90 (dd, 1H,  $^1J=1.3$ ,  $^2J=8.3$ ,  $ArH$ ), 1.52 (s, 9 H,  $C(CH_3)_3$ ), 1.34 (s, 9 H,  $C(CH_3)_3$ ).

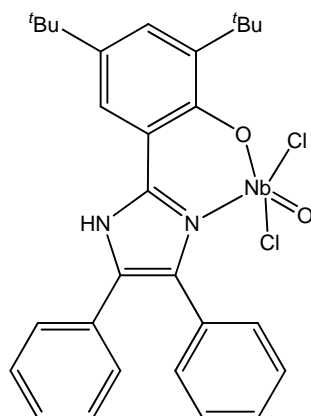
## 7. Group V complexes bearing phenoxyimine/imidazole-type ligands

### 7.1 Synthesis of $L^{13}HNbCl_4$ (**16**)

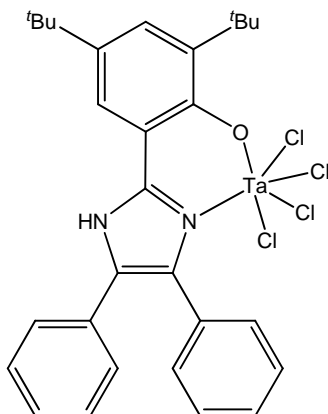


As described for **15** but using 2,4-di-*tert*-butyl-6-(4,5-diphenyl-imidazol-2-yl)phenol,  $L^{13}H_2$  (1.0 g, 2.36 mmol) and  $[NbCl_5]$  (1.1 eq., 0.69 g, 2.60 mmol). After prolonged standing at room temperature, deep red plates of **16** formed. Yield: 0.82 g, 56 %. Elemental analysis calcd (%) for  $NbC_{29}H_{31}Cl_4N_2O$ : C 52.91, H 4.75, N 4.26; found C 53.00, H 4.62, N 4.34. MS (E.S.):  $m/z$ : 658  $[M]^+$ , 587  $[M^+-2Cl]^+$ , 851  $[M^+-3Cl]^+$ . IR (Nujol mull, KBr): 3279(m), 2289(w), 2257(w), 1587(m), 1568(w), 1508(m), 1444(s), 1419(m), 1402(s), 1365(m), 1325(w), 1146(s), 924(m), 906(w), 877(s), 845(m), 766(m), 732(w), 712(m), 698(s), 670(m)  $cm^{-1}$ .  $^1H$  NMR ( $C_6D_6$ ):  $\delta$  = 9.87 (s, 1H, NH), 7.60 (dd, 2H,  $^1J = 2.0$ ,  $^2J = 15.7$ , ArH), 7.47 (m, 1H, ArH), 7.45 (d, 1H,  $J = 1.7$ , ArH), 7.39-7.35 (overlapping m, 3H, ArH), 7.30 (m, 3H, ArH), 7.17 (m, 2H, ArH), 2.00 (s, 3H,  $CH_3CN$ ), 1.56 (s, 9 H,  $C(CH_3)_3$ ), 1.43 (s, 9 H,  $C(CH_3)_3$ ).



7.2 Synthesis of  $L^{13}HNbOCl_2$  (**17**)

As described for **15** but using  $[NbOCl_3]$  (1.1 eq., 0.28 g, 1.30 mmol) and  $L^{13}H_2$  (0.50 g, 1.18 mmol) afforded orange prisms of **17**. Yield: 0.41 g, 54 %. Elemental analysis calcd (%) for  $NbC_{31}H_{34}Cl_2N_3O_2$ : C 57.78, H 5.32, N 6.52; found C 57.67, H 5.30, N 6.50. MS (E.S.):  $m/z$ : 602  $[M-CH_3CN+H]^+$ , 551  $[M^+-Cl-O+H]^+$ . IR (Nujol mull, KBr): 3572(w), 3405(w), 3195(m), 2307(m), 2278(m), 1950(w), 1883(w), 1810(w), 1617(s), 1604(s), 1589(s), 1575(m), 1523(m), 1500(m), 1404(s), 1364(s), 1326(m), 1201(m), 1184(m), 1150(m), 1126(s), 1072(s), 975(m), 910(s), 890(m), 846(s), 769(m), 697(s), 668(m)  $cm^{-1}$ .  $^1H$  NMR ( $(CD_3)_2CO$ ):  $\delta$  = 7.88 (d, 1H,  $J$  = 2.4, ArH), 7.57 (d, 4H,  $J$  = 7.0, ArH), 7.40 (overlapping m, 7H, ArH), 2.68 (s, 3H,  $CH_3CN$ ), 1.49 (s, 9H,  $C(CH_3)_3$ ), 1.33 (s, 9 H,  $C(CH_3)_3$ ).

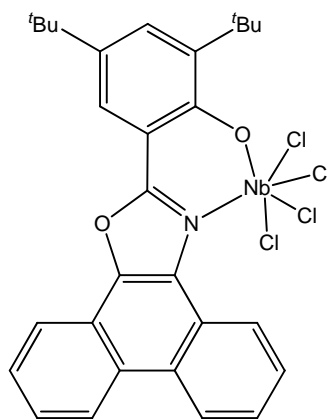
7.3 Synthesis of  $L^{13}HTaCl_4$  (**18**)

As described for **15** but using  $[TaCl_5]$  (1.1 eq., 0.47 g, 1.30 mmol) and  $L^{13}H_2$  (0.50 g, 1.18 mmol) afforded dark red plates of **18**. Yield: 0.50 g, 57 %. Elemental analysis

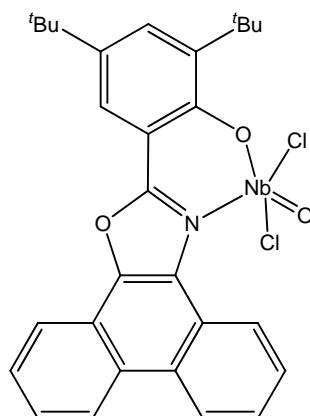
calcd (%) for  $\text{TaC}_{29}\text{H}_{31}\text{Cl}_4\text{N}_2\text{O}$ : C 46.67, H 4.19, N 3.75; found C 46.78, H 4.07, N 3.81. MS (E.S.):  $m/z$ : 746.1  $[\text{M}]^+$ , 675.1  $[\text{M}^+-2\text{Cl}]$ . IR (Nujol mull, KBr): 3283(s), 2291(w), 2259(w), 1597(m), 1509(s), 1403(s), 1326(m), 1286(s), 1177(s), 1147(s), 1128(s), 971(m), 928(s), 906(m), 881(s), 846(s), 771(s), 734(m), 698(s)  $\text{cm}^{-1}$ .  $^1\text{H}$  NMR ( $\text{C}_6\text{D}_6$ ):  $\delta$  = 8.517 (s, 1H, NH), 7.67-7.65 (overlapping m, 2H, ArH), 7.23-7.15 (overlapping m, 7H, ArH), 7.04 (s, 1H, ArH), 6.80 (m, 1H, ArH), 6.67 (m, 1H, ArH), 1.67 (s, 9 H,  $\text{C}(\text{CH}_3)_3$ ), 1.23 (s, 9 H,  $\text{C}(\text{CH}_3)_3$ ), 0.56 (s, 3H,  $\text{CH}_3\text{CN}$ ).

## 8. Niobium(V) complexes bearing oxazole ligands

### 8.1 Synthesis of $\text{L}^{14}\text{NbCl}_4$ (**19**)



As described for **15** but using  $[\text{NbCl}_5]$  (1.11 eq., 0.35 g, 1.30 mmol) and 2,4-di-*tert*-butyl-6-(phenanthro[9,10]oxazole-2-yl)phenol,  $\text{L}^{14}\text{H}$  (0.50 g, 1.18 mmol) afforded red/orange crystals of **19**. Yield: 0.56g, 72 %. Elemental analysis calcd (%) for  $\text{NbC}_{29}\text{H}_{28}\text{Cl}_4\text{NO}_2$ : C 53.03, H 4.31, N 2.33; found C 53.12, H 4.22, N 2.24. MS (E.S.):  $m/z$ : 657  $[\text{M}]^+$ , 622  $[\text{M}^+-\text{Cl}]^+$ , 550  $[\text{M}^+-3\text{Cl}]^+$ . IR (Nujol mull, KBr): 2297(w), 2271(w), 1601(w), 1572(w), 1515(m), 1364(m), 1316(w), 1291(w), 1035(s), 996(m), 958(s), 922(m), 885(m), 851(m), 774(m), 752(s), 731(m), 686(m).  $^1\text{H}$  NMR ( $(\text{CD}_3)_2\text{CO}$ ):  $\delta$  = 8.90 (t, 2H,  $J$  = 8.4, ArH), 8.6–8.54 (overlapping m, 1H, ArH), 8.47-8.46 (overlapping m, 1H, ArH), 8.20 (d, 1H,  $J$  = 2.5, ArH), 8.10 (d, 1H,  $J$  = 2.5, ArH), 7.84-7.68 (overlapping m, 3H, ArH), 7.50 (d, 1H,  $J$  = 2.5, ArH), 3.68 (s, 3H,  $\text{CH}_3\text{CN}$ ), 1.46 (s, 9H,  $\text{C}(\text{CH}_3)_3$ ), 1.35 (s, 9 H,  $\text{C}(\text{CH}_3)_3$ ).

8.2 Synthesis of  $L^{14}NbOCl_2$  (**20**)

As described for **15** but using  $[NbOCl_3]$  (1.1 eq., 0.20 g, 0.91 mmol) and  $L^{14}H$  (0.35 g, 0.83 mmol) afforded orange/yellow wedge crystals. Yield: 0.34g, 64 %. Elemental analysis calcd (%) for  $NbC_{31}H_{31}Cl_2N_2O_3$  (sample dried in *vacuo* for 12 h, **20** - MeCN): C 57.83, H 4.69 N 2.33; found C 57.91, H 4.58, N 2.51. MS (E.S.):  $m/z$ : 603  $[M-CH_3CN+H]^+$ , 566  $[M^+-CH_3CN-Cl]^+$ . IR (Nujol mull, KBr): 22969(w), 2270(w), 1601(w), 1571(w), 1515(m), 1315(w), 1291(w), 1201(m), 1157(m), 958(s), 922(m), 885(m), 851(m), 751(s), 731(s).  $^1H$  NMR ( $(CD_3)_2CO$ ):  $\delta$  = 9.0 (t, 2H,  $J$  = 8.1, ArH), 8.6 (d, 1H,  $J$  = 7.8, ArH), 8.54-8.49 (overlapping m, 1H, ArH), 8.20 (dd, 1H,  $^1J$  = 0.5,  $^2J$  = 2.5, ArH), 7.95-7.73 (overlapping m, 4H, ArH), 7.62 (d, 1H,  $J$  = 2.4, ArH), 2.68 (s, 6H, 2 $CH_3CN$ ), 1.54 (s, 9H,  $C(CH_3)_3$ ), 1.44 (s, 9 H,  $C(CH_3)_3$ ).

## 9. Polymerisation Procedure

### 9.1 Ethylene polymerisation

*9.1.1 Schlenk line procedure* - Ethylene polymerisations were carried out in flame dried glass 500 mL flasks with mechanical stirrer and temperature controller. The flask was evacuated and filled with ethylene gas at 1 bar pressure, which was maintained throughout the polymerisation. Then pre-dried and degassed toluene, required amount of co-catalyst and re-activating agent (ETA) were added *via* glass syringe. The solution was allowed to stir for approximately 10 min to allow ethylene saturation and the correct temperature to be acquired using a water bath. The pro-catalyst was injected as a toluene solution (prepared immediately prior to use). The polymerisation was quenched by acidified methanol. The polymer was collected by filtration and dried overnight at 80 °C.

*9.1.2 Silica supported procedure* – using method referred to as pore-filling or incipient wetness to produce free flowing powders that are easy to test.<sup>16</sup> The powders consist of a known quantity of pro-catalyst mixed with silica to produce the silica-catalyst. 1g of the supported catalyst was used in the test. The slurry polymerisation tests using the silica-catalyst were carried out at 70 °C for 1 h, at 15.2 bar ethylene pressure and used TiBAL as a scavenger.

### 9.2 $\epsilon$ -Caprolactone procedure

$\epsilon$ -Caprolactone polymerisations were carried out in Schlenk tubes, equipped with magnetic stirrer bars, previously dried in an oven at 170 °C for 12 h. and flamed dried under vacuum immediately before use. In a typical polymerisation run, 20 mL of dry toluene was transferred into the Schlenk tube with the required amount of pro-catalyst. The solution was stirred and maintained at the desired temperature by the aid of an oil bath. Benzyl alcohol was then added from a 0.97 M solution in toluene. After approximately five minutes the polymerisation was started by the addition of the required equivalent of  $\epsilon$ -caprolactone.

The polymerisation was quenched by precipitating the polymer in methanol. The polymer was then collected *via* filtration and dried under *vacuo*.

- 1 R. J. Errington, *Advanced practical inorganic and metalorganic chemistry*, CRC press, 1<sup>st</sup> Ed, 1997
- 2 *Programs CrysAlis-CCD and –RED*, Oxford Diffraction Ltd., Abington, UK (2005)
- 3 G. M. Sheldrick, *SHELX-97 – Programs for crystal structure determination (SHELXS) and refinement (SHELXL)*, University of Gottingen, Germany (1997)
- 4 J. Espinas, U. Darbost, J. Pelletier, E. Jeanneau, C. Duchamp, F. Bayard, O. Boyron, J. Thivolle-Cazart, J. M. Basset, M. Taoufik, I. Bonnamour, *Eur. J. Inorg. Chem.*, 2010, **9**, 1349
- 5 A. Arduini and A. Casnati, *Macrocyclic Synthesis*, Oxford University Press, 1996, 145 - 174
- 6 B. Dhawan, C. D. Gutsche, *J. Org. Chem.*, 1983, **48**, 1536
- 7 P. Hormnirum, E. L. Marshall, V. C. Gibson, R. I. Pugh, A. J. P. White, *Proc. Nat. Acad. Sci. USA*, Oct. 17 2006, **103**, 15343
- 8 I. I. Oleinik, I. V. Oleinik, S. S. Ivanchev, G. A. Tolstikov, *Russian J. Org. Chem.*, 2009, **45**, 528
- 9 M. B. Abrams, B. L. Scott, R. T. Baker, *Organometallics*, 2000, **19**, 4944
- 10 A. O. Eseola, W. Li, R. Gao, M. Zhang, X. Hao, t. Liang, N. O. Obi-Egbedi, W. H. Sun, *Inorg. Chem.*, 2009, **48**, 9133
- 11 C. Redshaw, M. A. Rowan, L. Warford, D. M. Homden, A. Arbaoui, M. R. J. Elsegood, S. H. Dale, T. Yamato, C. P. Casas, S. Matsui, *S. Chem. Eur. J.*, 2007, **13**, 1090
- 12 E. Hoppe, C. Limberg, *Chem. Eur. J.*, 2007, **13**, 7006
- 13 M. Mazzanti, S. Gambarotta, C. Floriani, A. Chiesi-Villa, C. Guastini, *Inorg. Chem.*, 1986, **25**, 2308
- 14 M. Lutz, H. Hagen, A. M. M. Schreurs, A. L. Spek and G. Van Koten, *Acta Cryst.*, 1999, **C55**, 1636
- 15 V. C. Gibson, T. P. Kee and A. Shaw, *Polyhedron*, 1988, **7**, 2217
- 16 S. Nagy (Lyondell Chemical Company), Personnel Communication

## **Chapter 7**

## **Appendix**

**Table 21.** Crystallographic data for complexes **1-4**

Compound	<b>1</b>	<b>2</b>	<b>3</b>	<b>4</b>
Formula	C <sub>94</sub> H <sub>118</sub> O <sub>8</sub> V <sub>2</sub> , 4(C <sub>2</sub> H <sub>3</sub> N)	C <sub>100</sub> H <sub>136</sub> O <sub>14</sub> V <sub>4</sub> , 2(C <sub>2</sub> H <sub>3</sub> N)	C <sub>108</sub> H <sub>136</sub> N <sub>2</sub> O <sub>6</sub> V <sub>2</sub> , 6(C <sub>2</sub> H <sub>3</sub> N)	3(C <sub>110</sub> H <sub>140</sub> N <sub>2</sub> O <sub>6</sub> V <sub>2</sub> ), 11(C <sub>2</sub> H <sub>3</sub> N)
Formula weight (g/mol)	1642.0	1848.0	1906.39	5515.95
Crystal system	Triclinic	Monoclinic	Triclinic	Triclinic
Space group	P-1	P2 <sub>1</sub> /n	P-1	P-1
Unit cell dimensions				
<i>a</i> (Å)	12.5484(4)	12.3632(7)	12.0454(3)	12.1955(8)
<i>b</i> (Å)	19.6001(6)	21.7638(10)	13.2444(2)	27.1953(19)
<i>c</i> (Å)	20.2006(9)	19.9295(12)	19.3366(4)	50.486(4)
<i>α</i> (°)	86.074(3)	90	101.5039(12)	78.5872(14)
<i>β</i> (°)	77.914(3)	106.105(6)	103.0898(9)	83.260(2)
<i>γ</i> (°)	80.074(3)	90	102.2226(11)	81.467(2)
<i>V</i> (Å <sup>3</sup> )	4782.8(3)	5152.0(5)	2835.69(10)	16164.4(19)
<i>Z</i>	2	2	1	2
Calculated density (Mg.m <sup>3</sup> )	1.140	1.191	1.116	1.133
Absorption coefficient (mm <sup>-1</sup> )	0.251	0.411	0.220	0.228
Transmission factors (max., min.)	1.034 and 0.976	1.024 and 0.966	1.00 and 0.882	1.00 and 0.811
Crystal size (mm)	0.23 × 0.20 × 0.05	0.20 × 0.17 × 0.05	0.19 x 0.15 x 0.1	0.18 x 0.09 x 0.03
2θ <sub>max</sub> (°)	22.5	22.5	25.0	20.00
Reflections measured	50213	58567	9970	74299
Unique reflections, R <sub>int</sub>	12464, 0.100	6711, 0.180	9970, -	25893, 0.131
Reflections with <i>F</i> <sup>2</sup> > 2σ( <i>F</i> <sup>2</sup> )	5860	3440	9355	12761
Number of parameters	1064	560	1284	1789
R <sub>1</sub> , wR <sub>2</sub> [ <i>F</i> <sup>2</sup> > 2σ( <i>F</i> <sup>2</sup> )]	0.047, 0.079	0.066, 0.139	0.068, 0.147	0.168, 0.389
R <sub>1</sub> , wR <sub>2</sub> (all data)	0.122, 0.087	0.141, 0.156	0.078, 0.154	0.300, 0.342
GOOF	0.755	0.921	1.136	1.023
Largest difference peak and hole (e Å <sup>-3</sup> )	0.51 and -0.28	0.55 and -0.38	0.40 and -0.40	0.77 and -0.50

**Table 22.** Crystallographic data for complexes **5**, **6**, **L<sup>8</sup>H<sub>2</sub>** and **8**

Compound	<b>5</b>	<b>6</b>	<b>L<sup>8</sup>H<sub>2</sub></b>	<b>8</b>
Formula	C <sub>64</sub> H <sub>66</sub> Cl <sub>2</sub> O <sub>9</sub> PS <sub>4</sub> V·2CH <sub>2</sub> Cl <sub>2</sub>	C <sub>64</sub> H <sub>66</sub> Cl <sub>2</sub> O <sub>13</sub> PS <sub>4</sub> V·3CH <sub>2</sub> Cl <sub>2</sub>	C <sub>44</sub> H <sub>56</sub> N <sub>2</sub> O <sub>2</sub>	2(C <sub>30</sub> H <sub>26</sub> ClN <sub>2</sub> O <sub>3</sub> V),1.5(C <sub>4</sub> H <sub>8</sub> O)
Formula weight (g/mol)	1429.0	1578.0	644.9	1205.99
Crystal system	Triclinic	Triclinic	Monoclinic	Monoclinic
Space group	<i>P</i> $\bar{1}$	<i>P</i> $\bar{1}$	P2 <sub>1</sub> /a	P2 <sub>1</sub> /a
Unit cell dimensions				
<i>a</i> (Å)	11.7107(2)	13.7043(16)	9.6297(3)	17.8598(14)
<i>b</i> (Å)	14.4377(4)	16.4065(19)	12.1792(4)	10.7750(8)
<i>c</i> (Å)	22.2159(5)	17.809(2)	16.2276(6)	31.054(2)
$\alpha$ (°)	89.098(2)	85.5859(16)	90	90
$\beta$ (°)	77.160(2)	76.1046(16)	100.851(4)	101.730(4)
$\gamma$ (°)	75.928(2)	74.8501(16)	90	90
<i>V</i> (Å <sup>3</sup> )	3549.43(14)	3751.5(7)	1869.18(11)	5881.2(7)
<i>Z</i>	2	2	2	4
Calculated density (Mg.m <sup>3</sup> )			1.146	1.369
Absorption coefficient (mm <sup>-1</sup> )	0.558	0.608	0.069	0.47
Transmission factors (max., min.)			1.118 and 0.904	0.7456 and 0.6039
Crystal size (mm)			0.41 x 0.30 x 0.09	0.2 x 0.16 x 0.08
2 $\theta$ <sub>max</sub> (°)	22.5	26.42	25.0	20.00
Reflections measured	39262	31727	19826	27495
Unique reflections, R <sub>int</sub>	9273, 0.086	15209, 0.029	3295, 0.106	5438, 0.111
Reflections with $F^2 > 2\sigma(F^2)$	5434	1093	19826	
Number of parameters			221	737
R <sub>1</sub> , wR <sub>2</sub> [ $F^2 > 2\sigma(F^2)$ ]	0.065	0.068	0.5	0.065
R <sub>1</sub> , wR <sub>2</sub> (all data)	0.174	0.219	0.096	0.127
GOOF			0.926	1.037
Largest difference peak and hole (e Å <sup>-3</sup> )			0.16 and -0.15	0.39 and -0.30



**Table 23.** Crystallographic data for complexes **11** and **15-17**

Compound	<b>11</b>	<b>15</b>	<b>16</b>	<b>17</b>
Formula	C <sub>60</sub> H <sub>86</sub> Cl <sub>4</sub> N <sub>2</sub> O <sub>6</sub> V <sub>2</sub>	NbCl <sub>4</sub> N(C <sub>6</sub> H <sub>4</sub> OC <sub>6</sub> H <sub>5</sub> )(CHC <sub>6</sub> H <sub>2</sub> O(C <sub>4</sub> H <sub>9</sub> ) <sub>2</sub> )	C <sub>29</sub> H <sub>31</sub> Cl <sub>4</sub> N <sub>2</sub> NbO.C <sub>2</sub> H <sub>3</sub> N	C <sub>31</sub> H <sub>34</sub> Cl <sub>2</sub> N <sub>3</sub> NbO <sub>2</sub> .3(C <sub>2</sub> H <sub>3</sub> N)
Formula weight (g/mol)	1175.0	635.23	699.3	767.6
Crystal system	Orthorhombic	Triclinic	Orthorhombic	Orthorhombic
Space group	Pbca	P-1	Pbca	Pbca
Unit cell dimensions				
<i>a</i> (Å)	15.4851(3)	12.1954(2)	12.1825(3)	26.4887(6)
<i>b</i> (Å)	12.3449(2)	12.6842(2)	19.4186(5)	14.1088(2)
<i>c</i> (Å)	33.0323(6)	18.5633(4)	26.5342(5)	20.7568(5)
$\alpha$ (°)	90	89.5122(14)	90	90
$\beta$ (°)	90	86.343(2)	90	90
$\gamma$ (°)	90	86.3393(14)	90	90
<i>V</i> (Å <sup>3</sup> )	6314.5(2)	2859.81(9)	6277.1(3)	7757.3(3)
<i>Z</i>	4	4	8	8
Calculated density (Mg.m <sup>3</sup> )	1.236	1.475	1.480	1.314
Absorption coefficient (mm <sup>-1</sup> )	0.512	0.819	0.753	0.487
Transmission factors (max., min.)	1.020 and 0.982	1.000 and 0.853	1.081 and 0.912	
Crystal size (mm)	0.43 x 0.41 x 0.09	0.31 x 0.22 x 0.15	0.24 x 0.15 x 0.015	0.33 x 0.18 x 0.18
$2\theta_{\max}$ (°)	25	30°	25.0	25.0
Reflections measured	104961	56330	79369	104864
Unique reflections, <i>R</i> <sub>int</sub>	5557, 0.072	16648 (0.0472)	5518, 0.143	6819, 0.076
Reflections with $F^2 > 2\sigma(F^2)$	4572	13655	3062	5021
Number of parameters	339	631	362	441
<i>R</i> <sub>1</sub> , <i>wR</i> <sub>2</sub> [ $F^2 > 2\sigma(F^2)$ ]	0.061		0.034, 0.041	0.064, 0.135
<i>R</i> <sub>1</sub> , <i>wR</i> <sub>2</sub> (all data)	0.113		0.099, 0.047	0.089, 0.141
GOOF			0.743	1.193
Largest difference peak and hole (e Å <sup>3</sup> )	0.39 and -0.31		0.90 and -0.58	0.83 and -1.26

**Table 24.** Crystallographic data for complexes **18** and **20**

Compound	<b>18</b>	<b>20</b>
Formula	C <sub>29</sub> H <sub>31</sub> Cl <sub>4</sub> N <sub>2</sub> TaO <sub>3</sub> ·C <sub>2</sub> H <sub>3</sub> N	C <sub>31</sub> H <sub>31</sub> Cl <sub>2</sub> N <sub>2</sub> NbO <sub>3</sub>
Formula weight (g/mol)	787.4	643.4
Crystal system	Orthorhombic	Triclinic
Space group	Pbca	P-1
Unit cell dimensions		
<i>a</i> (Å)	12.20751(12)	9.2530(3)
<i>b</i> (Å)	19.4381(2)	9.6926(3)
<i>c</i> (Å)	26.55212(3)	16.9423(4)
<i>α</i> (°)	90	91.042(2)
<i>β</i> (°)	90	102.538(2)
<i>γ</i> (°)	90	100.719(2)
<i>V</i> (Å <sup>3</sup> )	6300.55(11)	1454.64(7)
<i>Z</i>	8	2
Calculated density (Mg.m <sup>3</sup> )	1.660	1.469
Absorption coefficient (mm <sup>-1</sup> )	3.858	0.632
Transmission factors (max., min.)	1.204 and 0.650	1.087 and 0.896
Crystal size (mm)	0.42 x 0.22 x 0.06	0.30 x 0.18 x 0.12
2 $\theta_{\max}$ (°)	30.0	27.5
Reflections measured	119629	24291
Unique reflections, R <sub>int</sub>	9179, 0.058	6659, 0.053
Reflections with $F^2 > 2\sigma(F^2)$	6566	5231
Number of parameters	362	353
R <sub>1</sub> , wR <sub>2</sub> [ $F^2 > 2\sigma(F^2)$ ]	0.021, 0.037	0.032, 0.080
R <sub>1</sub> , wR <sub>2</sub> (all data)	0.040, 0.039	0.046, 0.082
GOOF	0.893	0.983
Largest difference peak and hole (e Å <sup>-3</sup> )	0.70 and -0.56	0.73 and -0.55

